

# **An Evaluation of Granular Overlays in Washington State**

WA-RD 226.1

Final Technical Report  
May 1991



**Washington State Department of Transportation**

Planning, Research and Public Transportation Division

in cooperation with the  
United States Department of Transportation  
Federal Highway Administration

## TECHNICAL REPORT STANDARD TITLE PAGE

1. REPORT NO. WA-RD 226.1	2. GOVERNMENT ACCESSION NO.	3. RECIPIENT'S CATALOG NO.	
4. TITLE AND SUBTITLE AN EVALUATION OF GRANULAR OVERLAYS IN WASHINGTON STATE		5. REPORT DATE May 1991	
		6. PERFORMING ORGANIZATION CODE	
7. AUTHOR(S) Daniel J. O'Neil, Joe P. Mahoney, Newton C. Jackson		8. PERFORMING ORGANIZATION REPORT NO.	
9. PERFORMING ORGANIZATION NAME AND ADDRESS Washington State Transportation Center (TRAC) University of Washington, JE-10 The Corbet Building, Suite 204; 4507 University Way N.E. Seattle, Washington 98105		10. WORK UNIT NO.	
		11. CONTRACT OR GRANT NO. GC8719, Task 31	
12. SPONSORING AGENCY NAME AND ADDRESS Washington State Department of Transportation Transportation Building, KF-01 Olympia, Washington 98504		13. TYPE OF REPORT AND PERIOD COVERED Final technical report	
		14. SPONSORING AGENCY CODE	
15. SUPPLEMENTARY NOTES This study was conducted in cooperation with the U.S. Department of Transportation, Federal Highway Administration.			
16. ABSTRACT  <p style="text-indent: 40px;">Granular overlays have been used by the Washington State Department of Transportation (WSDOT) for about 30 years. Since the mid-1980s and along with the full implementation of the WSDOT Pavement Management System (WSPMS), WSDOT has been interested in examining the performance of granular overlays. It is felt by WSDOT that the performance of this rehabilitation treatment is better than one might reasonably expect. Further, past practice in Washington state occasionally required that the preexisting surfacing (often several bituminous surface treatment (BST) layers) be scarified prior to placement of the crushed rock layer. As will be shown in this report, this practice is not supported by this research.</p> <p style="text-indent: 40px;">This study examined granular overlays by using three different techniques. First, previous research on the behavior of confined crushed rock layers was studied. Through these studies, information was sought concerning the stiffnesses that have been found in crushed rock layers, what can be done to improve the crushed rock layer, and the problems that have been encountered in working with confined crushed rock layers. Next, the usable life of the granular overlay was compared with that of other types of pavement resurfacing, including asphalt concrete (AC) overlays and BST. Finally, the granular overlays were tested to determine their properties and to measure the effect of different designs on their performance.</p>			
17. KEY WORDS Granular overlay		18. DISTRIBUTION STATEMENT No restrictions. This document is available to the public through the National Technical Information Service, Springfield, VA 22616	
19. SECURITY CLASSIF. (of this report)  None	20. SECURITY CLASSIF. (of this page)  None	21. NO. OF PAGES  143	22. PRICE

**Final Technical Report**

Research Project GC 8719, Task 31  
Granular Overlay (Cushion Course)

**AN EVALUATION OF GRANULAR OVERLAYS  
IN WASHINGTON STATE**

by

Daniel J. O'Neil  
Graduate Civil Engineer  
University of Washington

Joe P. Mahoney  
Professor, Civil Engineering  
University of Washington

Newton C. Jackson  
Pavement and Soils Engineer  
Washington State Department  
of Transportation

**Washington State Transportation Center (TRAC)**  
University of Washington, JE-10  
The Corbet Building, Suite 204  
4507 University Way N.E.  
Seattle, Washington 98105

Washington State Department of Transportation  
Technical Monitor  
Newton C. Jackson  
Pavement and Soils Engineer

Prepared for

**Washington State Transportation Commission**  
Department of Transportation  
and in cooperation with  
**U.S. Department of Transportation**  
Federal Highway Administration

May 1991

## **DISCLAIMER**

The contents of this report reflect the views of the authors, who are responsible for the facts and the accuracy of the data presented herein. The contents do not necessarily reflect the official views or policies of the Washington State Transportation Commission, Department of Transportation, or the Federal Highway Administration. This report does not constitute a standard, specification, or regulation.

## TABLE OF CONTENTS

<u>Chapter</u>	<u>Page</u>
<b>1. Introduction.....</b>	<b>1</b>
<b>2. Methodology .....</b>	<b>5</b>
2.1 Literature Review .....	5
2.2 Survival Life and Performance Estimates .....	6
2.3 Field Testing.....	6
2.4 Elastic Layer Analysis.....	6
2.5 Study Conclusions.....	6
<b>3. Literature Review and Background.....</b>	<b>7</b>
3.1 Overview of Overlays .....	7
3.1.1 Bituminous Surface Treatments .....	7
3.1.2 Asphalt Concrete Overlays.....	9
3.1.3 Reflection Cracking.....	9
3.2 Granular Overlays .....	9
3.3 Equivalency Factors .....	10
3.4 South African Studies.....	14
3.4.1 Effective Moduli and Stress Dependence of Granular Layers.	20
3.4.2 Moisture Content.....	26
3.4.3 Gradation.....	33
3.4.4 Reflection Cracking.....	35
3.5 Construction of the Crushed Rock Layer.....	38
3.6 The Surface Layer .....	39
3.6.1 Surface Layer Options.....	39
3.6.2 Improvement in BST Construction .....	39
3.7 Existing pavement.....	40
3.8 Other Advantages and Limitations.....	41
3.8.1 Insulation .....	41
3.8.2 Increased Frost Resistance .....	41
3.8.3 Change in Road Geometry .....	42
3.8.4 Resistance to Shear.....	42
3.9 Design of Granular Overlays.....	45
3.9.1 Mechanistic Design .....	45
3.9.2 One Thickness Approach .....	46
3.10 Overlay Costs .....	47
<b>4. Survival Lives and Performance Periods .....</b>	<b>57</b>
4.1 Introduction .....	57
4.2 Source of Data.....	59
4.3 Bituminous Surface Treatments.....	64
4.4 Asphalt Concrete Overlay .....	64
4.5 Granular Overlay.....	68
4.6 Chapter Summary.....	72

## TABLE OF CONTENTS (Continued)

<u>Chapter</u>		<u>Page</u>
<b>5.</b>	<b>Initial Analysis of Nondestructive Testing Data .....</b>	<b>75</b>
5.1	Introduction .....	75
5.2	Testing Apparatus Description and Testing Procedure .....	75
5.3	Selection of Test Sections .....	78
	5.3.1 Overlay Analysis Methods .....	80
	5.3.2 Test Section Pavement Cross-Sections .....	82
5.4	Deflection Basins .....	93
5.5	Analysis of the Subgrade .....	94
5.6	Analysis of $D_0$ .....	95
5.7	Analysis of the Area Parameter .....	98
5.8	Comparisons of $D_0$ and the Area Parameter .....	100
5.9	Variable Crushed Rock Thickness .....	106
5.10	Chapter Summary .....	106
<b>6.</b>	<b>Elastic Layer Analysis .....</b>	<b>109</b>
6.1	Introduction .....	109
6.2	EVERCALC .....	110
	6.2.1 Layer Thicknesses .....	110
	6.2.2 Poisson's Ratio .....	111
	6.2.3 Modeling .....	111
	6.2.4 Outputs .....	111
6.3	Analysis .....	112
	6.3.1 Sections with Poor Results .....	113
	6.3.2 Backcalculation Results for SR28B .....	114
	6.3.3 Backcalculation Results for SR17 .....	116
6.4	Chapter Summary .....	118
<b>7.</b>	<b>Summary and Conclusions .....</b>	<b>123</b>
7.1	Introduction .....	123
7.2	Background Information .....	123
7.3	Survival Life Calculations .....	125
7.4	Nondestructive Testing .....	126
7.5	Elastic Layer Analysis .....	126
7.6	Summary .....	127
7.7	Conclusions .....	127
	<b>Acknowledgments .....</b>	<b>131</b>
	<b>References .....</b>	<b>133</b>

## LIST OF FIGURES

<b>Figure</b>		<b>Page</b>
1.1	Typical Granular Overlain Pavement.....	2
1.2	Typical AC Overlain Pavement .....	2
2.1	Typical Inverted Pavement Structure.....	5
3.1	The Deterioration of Pavement Condition Over Time due to Traffic Loads and Environmental Effects (AASHTO [1]).....	8
3.2	Pavement Structures Modelled by Sibal [26] Using ELSYM5.....	12
3.3	Pavement Structures Modelled by Sibal [26] Using Nonlinear Model for Crushed Rock Layers .....	13
3.4	The Equivalency Factors versus the Modulus of Elasticity for the Crushed Rock Layer Based on Sibal's Calculations [26].....	17
3.5	South African Pavement Material Classifications (from Maree, et al. [16] and Maree, et al. [17]).....	19
3.6	Light Pavements, Road P 6/1 and Road P 123/1, Tested by the Heavy Vehicle Simulator (after Maree et al. [16]).....	21
3.7	Inverted Pavements, Road P157/1 and P157/2, Tested with the Heavy Vehicle Simulator (after Maree et al. [16]).....	22
3.8	Map of South Africa Showing the Average Annual Precipitation (Jackson [11] Location of Five Test Sites (Maree et al. [17])..	23
3.9	Inverted Pavements, Road P205/1 and Road P157/1, Tested with the Heavy-Vehicle Simulator (Maree et al. [17]).....	27
3.10	Inverted Pavements, Road P157/2 and N3, Tested with the Heavy-Vehicle Simulator (Maree et al. [17]).....	28
3.11	Light Pavement, Road TR 77/1, Tested with the Heavy-Vehicle Simulator (Maree et al. [17]).....	29
3.12	The Rutting of the Five Different Pavement Structures Against the Number of 18 kip (80 kN) ESALs .....	29
3.13	The Rebuilt Section of Road P175/2.....	31
3.14	The Stress-Stiffening Behavior of the Crushed Stone Base in Road P157/2 .....	32
3.15	Relative Time to First Reflection Crack .....	37
3.16	Relative Construction Costs for the Different Sources of Overlays ....	37
3.17	Safety Factors for Shear Stress (after Freeme et al. [4]) .....	43
3.18	Comparison of the Cost of the Different Layers in a Granular Overlay Based on WSDOT Cost Estimates .....	54
4.1	Plot of Regression Equation for SR21A Milepost 44.73 to 46.95 .....	62
4.2	Map of the Granular Overlay Study Area and WSDOT District Boundaries.....	62
4.3	Survival Times for BSTs in Districts 2 and 6 .....	65
4.4	The Predicted Amount of Time for BSTs to Reach a PCR of 40, Based on Project Specific Regression Equation .....	66
4.5	The Predicted Amount of Time for BSTs to Reach a PCR of 20, Based on Project Specific Regression Equations .....	66
4.6	The Predicted Amount of Time for BSTs to Reach a PCR of 0, Based on Project Specific Regression Equations .....	66
4.7	Survival Times for AC Overlays in Districts 2 and 6 .....	69
4.8	Predicted Amount of Time for AC Overlays to Reach a PCR of 40, Based on Project Specific Regression Equations (Districts 2 and 6 .....	70

## LIST OF FIGURES (Continued)

<b>Figure</b>		<b>Page</b>
4.9	Predicted Amount of Time for AC Overlays to Reach a PCR of 20, Based on Project Specific Regression Equations (Districts 2 and 6).....	70
4.10	Predicted Amount of Time for AC Overlays to Reach a PCR of 0, Based on Project Specific Regression Equations (Districts 2 and 6).....	70
4.11	Predicted Amount of Time for Granular Overlays to Reach a PCR of 40, Based on Project Specific Regression Equations.....	71
4.12	Predicted Amount of Time for Granular Overlays to Reach a PCR of 20, Based on Project Specific Regression Equations.....	71
4.13	Predicted Amount of Time for Granular Overlays to Reach a PCR of 0, Based on Project Specific Regression Equations.....	71
5.1	Profile of the FWD Sensors and Weights (SR28B at Milepost 57.0)..	76
5.2	Deflection Basins for SR28B, Mileposts 56.8, 56.9, and 57.0.....	77
5.3	Sections of Roads Tested During the Granular Overlay Study.....	79
5.4	Cross-Section of SR17, Mileposts 120 to 128 .....	82
5.5	Cross-Section of SR 24, Milepost 49 to 60.....	84
5.6	SR28 Section A Milepost 31.7 to 36.5 (with Granular Overlay).....	84
5.7	SR28 Section A, Mileposts 36.5 to 37.5 (without Granular Overlay)..	86
5.8	SR28 Section B, Mileposts 55 to 60 .....	86
5.9	Cross-Section of SR21 Section A, Milepost 40 to 45.....	87
5.10	Cross-Section of SR21 Section B, Milepost 70 to 75 .....	90
5.11	Cross-Section of SR231 Section A, Milepost 0.0 to 2.7 (without Granular Overlay).....	90
5.12	Cross-Section of SR231 Section A, Milepost 2.7 to 7.3 (with Granular Overlay) .....	91
5.13	Cross-Section of SR231 Section B, Milepost 22.0 to 27.0 .....	91
5.14	Comparison of the Asphalt Institute Effective Thicknesses (Right Hand Scale), Area Parameters (Left Hand Scale), and $D_0$ 's (left Hand Scale) for the Typical Pavements .....	101
5.15	Comparison of the Asphalt Institute Effective Thicknesses (Right Hand Scale), Area Parameters (Left Hand Scale), and $D_0$ 's (left Hand Scale) for the Tested Roads .....	102
5.16	Plot of SR17 Showing the Variation in $D_0$ with the Thickness of the Crushed Rock Layer in the Granular Overlay.....	107
6.1	Plot of the Thickness of the Crushed Rock Layer in the Granular Overlay on SR17 Against Backcalculated Moduli for this Layer.....	117
6.2	Bulk Stress for the Crushed Rock Layer in SR17 Assuming that the Modulus of Elasticity is Constant .....	119
6.3	Shear Stress for the Crushed Rock Layer in SR17 Assuming that the Modulus of Elasticity is Constant .....	120



## LIST OF TABLES

<b>Table</b>		<b>Page</b>
3.1	"Typical" Values for the Constants $K_1$ and $K_2$ Based on a Laboratory Analysis (Mahoney [12]) Compared with AASHTO Values [2]	10
3.2	Equivalent Thicknesses and Equivalency Factors Based on Most Critical Failure Mode Using Linear Elastic Moduli for Crushed Rock Layers (after Sibal [26]).....	15
3.3	Equivalent Thicknesses and Equivalency Factors Based on Most Critical Failure Mode Using Nonlinear Moduli for Crushed Rock Layers (after Sibal [26]).....	16
3.4	The Moduli of Elasticity of the Base Course (G5) in a Light Pavement (Road P6/1) Tested with a Heavy-Vehicle Simulator.....	24
3.5	The Moduli of Elasticity of the Base Course (G5) in a Light Pavement (Road P123/1) Tested with a Heavy-Vehicle Simulator.....	24
3.6	The Moduli of Elasticity of the Base Course (G2) in an Inverted Pavement (Road P157/1) Tested with a Heavy-Vehicle Simulator.....	24
3.7	The Moduli of Elasticity of the Base Course (G1A) in an Inverted Pavement (Road P157/2) Tested with a Heavy-Vehicle Simulator.....	24
3.8	Comparison of WSDOT and South African Granular Layer Moduli ..	25
3.9	Results of Increasing Load Repetitions on Road P157/1 .....	25
3.10	Results of Increasing Load Repetitions on Road P157/2.....	25
3.11	Resilient Moduli for the Crushed Rock Base in P157/2 .....	32
3.12	Gradation Bands for Various Crushed Rock Specifications .....	34
3.13	Description of the Reflection Crack Test Sections .....	36
3.14	Typical Granular Material Shear Properties (after Freeme et al. [4]) ..	43
3.15	Material and Construction Costs for AC and BST Wearing Course Surfaces Based on Means Construction Data (1989). Costs Reflect Haul Distances of 30 Miles or Less.....	48
3.16	Material and Construction Costs for Pavement Base Courses with a Maximum Aggregate Size of 3/4 in. (19 mm) Based on Means Construction Data [18] .....	48
3.17	Comparison of Costs for AC Overlays and Granular Overlays with a BST Surfacing Based upon an Equivalency Factor of 2.0.....	48
3.18	WSDOT Construction Costs for AC and BST Surfaces on Granular Overlays .....	50
3.19	Quantity and Costs of AC Estimated for the AC Surface Granular Overlays (Based on WSDOT Estimates) .....	50
3.20	Bituminous Surface Treatment Details Which Influence Costs.....	50
3.21	Quantities and Costs of Crushed Rock Layer in Granular Overlays (Based on WSDOT Estimates).....	51
3.22	Summary of Total Construction Cost of Granular Overlays Based on WSDOT Projects.....	53
4.1	WSPMS Construction Data for SR21, Milepost 46.95 to 50.50.....	59
4.2	Typical PCR Survey Data as Reported in WSPMS (Data from the 1989 Survey of SR231).....	61
4.3	Performance Periods for SR21A Milepost 44.73 to 46.95.....	63
4.4	Basic Statistics for the Performance Periods of BSTs (Based on 21 Data Points).....	67
4.5	Basic Statistics for the Survival Times of AC Overlays in Districts 2 and 6.....	67

## LIST OF TABLES (Continued)

<b>Table</b>		<b>Page</b>
4.6	Basic Statistics for the Performance Periods for AC Overlays in Districts 2 and 6 (Statistics Based on 29 Data Points).....	67
4.7	Basic Statistics for the Performance Periods of Granular Overlays (Based on 17 Data Points).....	72
4.8	Mean Survival Times and Predicted Performance Periods for the Resurfacings.....	72
5.1	Road Sections Tested with the FWD.....	79
5.2	Test Sections Surface Thicknesses and Temperatures Taken During FWD Testing.....	80
5.3	AASHTO Factors Used in Overlay Design Calculations.....	81
5.4	Asphalt Institute Equivalency Factors Used in Overlay Design Calculations.....	81
5.5	Average PCR Survey Results for SR17 Milepost 120 to 128.....	83
5.6	Overlay Calculations Based on AASHTO and Asphalt Institute Design Procedures for SR17 Milepost 120 to 128.....	83
5.7	Average PCR Survey Results for SR24 Milepost 49 to 60.....	83
5.8	Overlay Calculations Based on AASHTO and Asphalt Institute Design Procedures for SR24 Milepost 49 to 60.....	83
5.9	Average PCR Survey Results for SR28A Milepost 31.7 to 37.5.....	85
5.10	Overlay Analysis for SR28A Milepost 31.7 to 37.5.....	85
5.11	Average PCR Survey Results for SR28B Milepost 55 to 60.....	85
5.12	Overlay Analysis for SR28B Milepost 55 to 60.....	88
5.13	Average PCR Survey Results for SR21A Milepost 40 to 45.....	88
5.14	Overlay Analysis for SR21A Milepost 40 to 45.....	88
5.15	Average PCR Survey Results for SR21B Milepost 70 to 75.....	88
5.16	Overlay Analyses for SR21B Milepost 70 to 75.....	88
5.17	Average PCR Survey Results for SR231A, Milepost 0.0 to 7.3.....	92
5.18	Overlay Analysis for SR231A, Milepost 0.0 to 7.3.....	92
5.19	Average PCR Survey Results for SR231B, Milepost 22 to 27.....	92
5.20	Overlay Analysis for SR231B, Milepost 22 to 27.....	92
5.21	Calculated Subgrade Moduli for the Test Sections.....	94
5.22	Summary of D <sub>0</sub> Values Normalized to a 9000 lb (40.0 kN) Load and 77°F (25°C).....	95
5.23	Layer Properties in the Typical Pavement Sections.....	96
5.23	Asphalt Institute Equivalent Thicknesses for the Typical Pavements.....	96
5.25	D <sub>0</sub> Values for the Typical Pavement Sections.....	97
5.26	Comparison of the Area Parameters for the Tested Roads.....	99
5.27	Area Parameters for the Typical Pavement Sections.....	99
5.28	Summary of the Comparisons Between the Asphalt Institute Effective Thicknesses and the Equivalent Pavement Thicknesses.....	105
6.1	EVERCALC Results for SR28A without the Granular Overlay.....	114
6.2	EVERCALC Results for SR28A with the Granular Overlay.....	115
6.3	EVERCALC Results for SR17 with the Granular Overlay.....	116
6.4	Typical Elastic Moduli and Bulk Stresses from Inverted Pavements (Maree et al. [16]).....	121
7.1	Survival Times and Predicted Performance Periods for the Overlays.....	130
7.2	Moduli Calculated for Confined Crushed Rock Layers in Granular Overlays (WSDOT) and Inverted Pavements (South Africa).....	130

# CHAPTER 1

## INTRODUCTION

The granular overlay system (hereafter referred to as "granular overlay") is an alternative type of overlay for rehabilitating mostly low volume, rural roads. The overlay consists of a layer of densely compacted, crushed rock overlain by a generally thin surface layer. Figures 1.1 and 1.2 show typical granular and asphalt concrete (AC) overlays.

Granular overlays have been used throughout the world as a pavement rehabilitation treatment. The justification for such use appears to fall into four primary categories:

1. reduce reflective cracking from preexisting pavement structure,
2. add extra pavement structure thickness to combat frost related effects,
3. improve cross-slope, road profile (and ride in general), and
4. strengthen the pavement structure.

This last category will be the primary focus of this report.

Granular overlays have been used by the Washington State Department of Transportation (WSDOT) for about 30 years. Since the mid-1980s and along with the full implementation of the WSDOT Pavement Management System (WSPMS), WSDOT has been interested in examining the performance of granular overlays. It is felt by WSDOT that the performance of this rehabilitation treatment is better than one might reasonably expect. Further, past practice in Washington state occasionally required that the preexisting surfacing (often several bituminous surface treatment (BST) layers) be scarified prior to placement of the crushed rock layer. As will be shown in this report, this practice is not supported by this research.

One view of why the granular overlays had worked well structurally was that they took advantage of the stress stiffening behavior of granular materials. When a crushed rock layer is subjected to a confining pressure, it stiffens because of the friction between the grains. Since the old pavement surface and the new surfacing confine the crushed rock

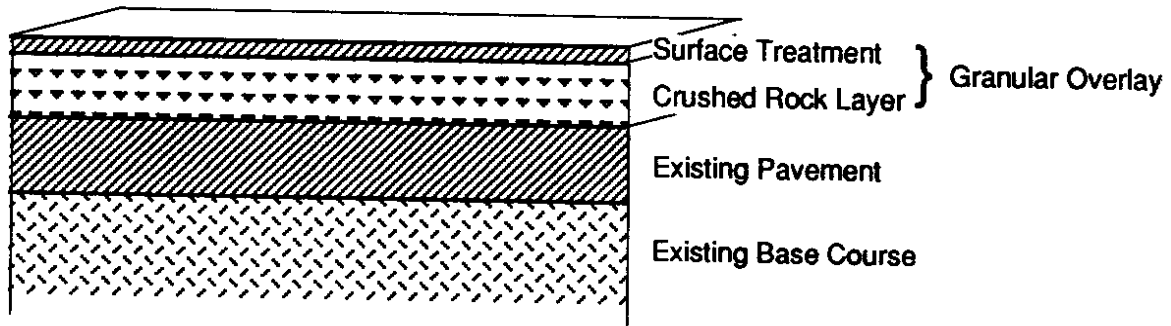


Figure 1.1 Typical Granular Overlay Pavement

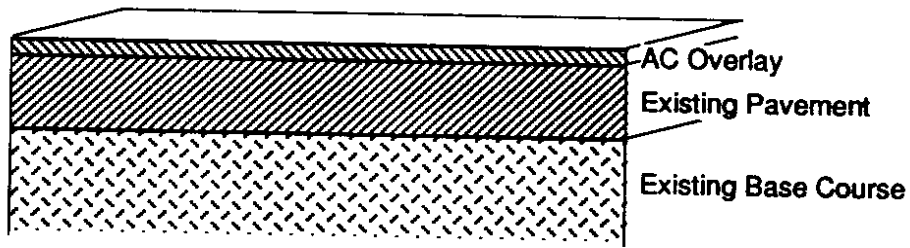


Figure 1.2. Typical AC Overlay Pavement

layer in a granular overlay, traffic loads can provide high confining stresses which, in effect, increase the stiffness of the crushed rock layer.

As the use of the granular overlay increased in Washington State, WSDOT realized that to improve and continue to use granular overlays, it needed to better understand how they worked, where they were appropriate, and how best to design and build them.

In cooperation with WSDOT, two initial studies were undertaken at the University of Washington (Deoja [3], Sibal [26]). The results of these graduate student studies were encouraging. This led WSDOT and its associated Washington State Transportation Center (TRAC) at the University of Washington to enter into an agreement with the Federal Highway Administration to prepare a report overviewing this topic, hence this report.

This study examined granular overlays by using three different techniques. First, previous research on the behavior of confined crushed rock layers was studied. Through these studies, information was sought concerning the stiffnesses that have been found in crushed rock layers, what can be done to improve the crushed rock layer and the problems that have been encountered in working with confined crushed rock layers. Next, the useable life of the granular overlay was compared with that of other types of pavement resurfacing, including asphalt concrete (AC) overlays and BST. Finally, the granular overlays were field tested to determine their properties and to measure the effect of different designs on their performance .



## CHAPTER 2

### METHODOLOGY

#### 2.1 LITERATURE REVIEW

The first stage of this study was a review of research done on granular overlays and related topics. This literature review was conducted through searches of the National Technological Information Service (NTIS), the WSDOT information service (DIALOG), the U. S. government information service, and the University of Washington information service, as well as extensive manual searches of the University of Washington Library. Although a wide variety of information was found on the behavior of different pavements, little was found on the behavior of confined crushed rock layers. The most valuable source of information was on "inverted" pavements. These are pavements that have uncemented bases and cemented subbases (Figure 2.1). Studies on these types of pavements showed that crushed rock layers can have moduli in excess of 100 ksi (690 MPa) (Maree et al. [16]). Additional studies on the behavior of thin flexible pavement surfaces helped define the behavior of granular overlays as a system. The results of this literature review are presented in Chapter 3.

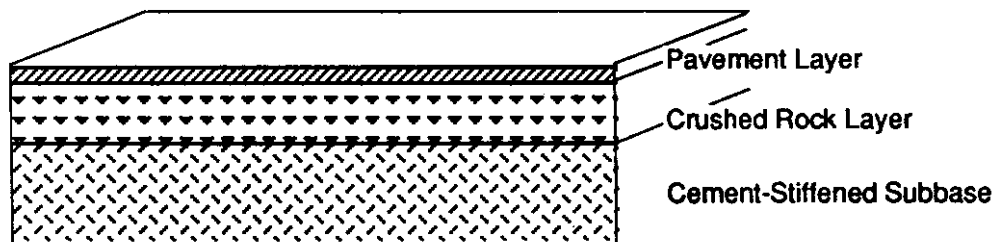


Figure 2.1. Typical Inverted Pavement Structure

## **2.2 SURVIVAL LIFE AND PERFORMANCE ESTIMATES**

The second stage of the research attempted to determine how long granular overlays last in relation to other overlays. Data were obtained from the WSPMS and WSDOT construction records concerning the length of time the overlays had lasted and the rate at which they had deteriorated. A comparison of the survival lives and performance estimates of the different overlay techniques allowed an estimate of the relative "longevity" of granular overlays to be calculated. The procedure, sources of data and results from these estimates are presented in Chapter 4.

## **2.3 FIELD TESTING**

The final stage of the study was to nondestructively test roads with granular overlays and interpret the deflection results. Over 50 centerline miles of road were tested with a falling weight deflectometer. Several techniques were used to analyze the data. The results of these analyses were compared among each other and to expected results to indicate the effects of the different pavement structures. This analysis is presented in Chapter 5.

## **2.4 ELASTIC LAYER ANALYSIS**

In addition to analyzing the data with the techniques listed in Chapter 5, the data was analyzed using elastic layer analysis. The purpose of this technique was to estimate the moduli of the crushed rock layer in the granular overlay. The results of this analysis are presented in Chapter 6.

## **2.5 STUDY CONCLUSIONS**

Finally in Chapter 7, the analyses from the previous chapters are discussed and conclusions are listed as to design and construction of granular overlays.



## **CHAPTER 3**

### **LITERATURE REVIEW AND BACKGROUND**

#### **3.1 OVERVIEW OF OVERLAYS**

Flexible pavements deteriorate because of traffic loads and environmental effects. This deterioration can result in the formation of cracks and ruts in the pavement. The gradual decline in the condition of a pavement is shown in Figure 3.1. Once the pavement has deteriorated below a minimally acceptable level, it must be repaired. Although there are a variety of types of repairs ranging from sealing cracks, patching, and reconstruction, this study concentrated on techniques for resurfacing the existing pavement. The resurfacing serves to reduce moisture infiltration and, in some cases, strengthen the pavement structure.

The two types of resurfacings generally used to seal and/or strengthen flexible pavements are BST and AC overlays. Since BST and AC Surfacing will be discussed throughout this report, a clear statement of those terms follows.

##### **3.1.1 Bituminous Surface Treatments**

A BST is composed of alternating layers of asphalt emulsion or cut-back asphalt and rock. The asphalt is sprayed onto the road and the stone is spread across and compacted into it. These layers are repeated as often as required. WSDOT generally uses two- or three-layer BSTs. Since the BST is a thin layer and somewhat flexible, it does not add much strength to the pavement. It serves instead to seal the road and add a new wearing surface. Additionally BSTs are relatively inexpensive to construct (Section 3.10). Since the construction technique does not require a nearby processing plant and the construction costs are low, this type of resurfacing is frequently used on low volume rural roads.

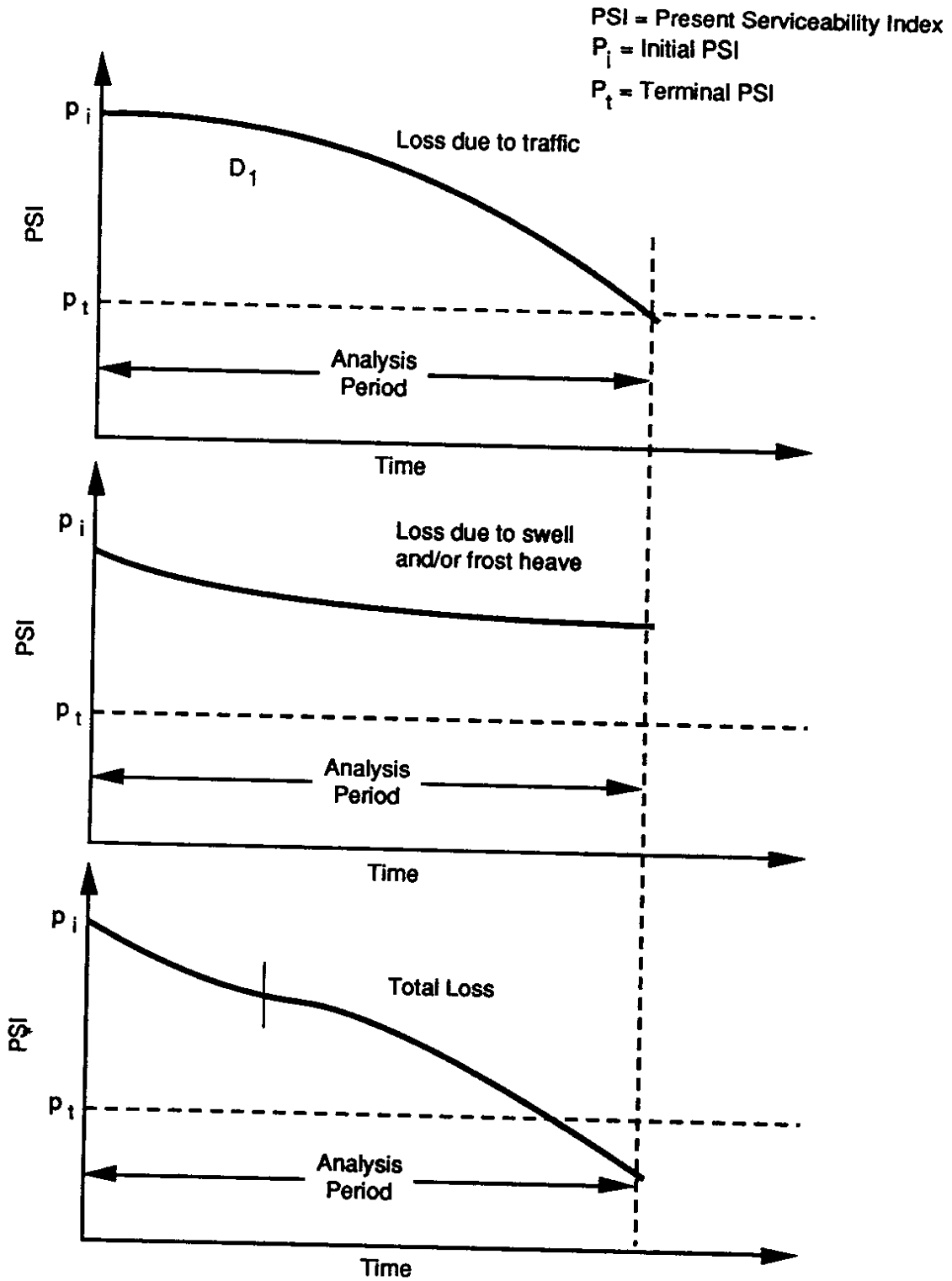


Figure 3.1. The Deterioration of Pavement Condition Over Time due to Traffic Loads and Environmental Effects (AASHTO [1])

### **3.1.2 Asphalt Concrete Overlays**

An AC overlay consists of a mixture of asphalt cement and stone. The ingredients are heated, then mixed together in a batch plant and trucked to the project. The AC is then spread across the road and compacted into place.

Once the AC has cooled, it provides a relatively stiff, new wearing surface to the road. Although this technique is effective in strengthening the pavement system, it is also expensive (Section 3.10).

### **3.1.3 Reflection Cracking**

A recurrent problem with any resurfacing is reflection cracking. If the new overlay binds to the old surface, cracks in the old surface often will, in time, reflect through the new overlay. Several methods have been suggested for reducing reflection cracking, including using low viscosity asphalt cement, heater scarifying the old surface, placing an interlayer fabric between the old surface and the overlay and using thick AC overlays (Monismith [20]). All of these techniques have had some degree of success, but all increase the cost of the overlay.

## **3.2 GRANULAR OVERLAYS**

The behavior of granular overlays depends upon the condition of the crushed rock layer. Both the surface and the old pavement serve to protect this layer and to confine it. The crushed rock layer can provide much of the "strength" of the overlay. When crushed rock is used as a base course it generally has a modulus of elasticity of about 15 to 30 ksi (100 to 200 MPa) (AASHTO [1]), when it is subjected to a confining pressure of 125 psi (0.9 MPa), its modulus of elasticity can exceed 100 ksi (690 MPa) (Maree et al. [16]) or more.

When a granular material is subjected to a confining pressure, interparticle friction causes the material to behave in a stiffer manner. The degree of this stress sensitivity

depends on the roughness of the particles, the percentage of fine particles, and the moisture content of the material. In general the stress stiffening will follow Equation 3.1:

$$E = K_1 \theta^{K_2} \quad \text{(Equation 3.1)}$$

where  $E$  = modulus of elasticity (psi),  
 $K_1, K_2$  = constants,  
 $\theta$  =  $\sigma_1 + \sigma_2 + \sigma_3$  = bulk stress, and  
 $\sigma_1, \sigma_2, \sigma_3$  = principal stresses.

A study done by the University of Washington and WSDOT (Mahoney [12]) found that the crushed rock used by WSDOT (crushed surfacing top and base course) has "typical" values for the constants, as shown in Table 3.1. The WSDOT laboratory tests were conducted at a variety of bulk stresses ranging from 4 to 28 psi.

In a traditional pavement system, the confining stresses on the crushed rock base depends on a number of factors including the stiffness of the subgrade. Since the granular overlay is sandwiched between two "stiff" pavement layers, it will be subjected to higher confining pressures.

### **3.3 EQUIVALENCY FACTORS**

The stiffness of a granular overlay is provided largely by the crushed rock layer (assuming that the surfacing is relatively thin). One method for comparing granular overlays and AC overlays is to determine the thickness of a granular overlay that would provide the same "life" as a thickness of AC overlay. This is the technique used by Sibal [26] and Deoja [3] in their studies of granular overlays.

Table 3.1. "Typical" Values for the Constants  $K_1$  and  $K_2$  Based on a Laboratory Analysis (Mahoney [12]) Compared with AASHTO Values [1]

Constants	Mean (WSDOT)	Standard Deviation (WSDOT)	AASHTO Range
$K_1$	8500	2300	2000 - 4000
$K_2$	0.375	0.067	0.5 - 0.7

Sibal [26] used two elastic layer programs to model the behaviors of AC and granular overlays: ELSYM5 and EVERSTR. The ELSYM5 program treats all layers as linearly elastic. EVERSTR treats the granular layers as nonlinear. Sibal determined the thicknesses of the crushed rock layer in a granular overlay that would provide the same pavement performance as different thicknesses of AC. In both the granular and AC overlay analyses, he varied the moduli of the subgrade and the granular overlay crushed rock layer.

Using these modeling techniques (Figures 3.2 and 3.3), Sibal used ELSYM5 and EVERSTR to calculate the strains at critical locations in the pavement system. Equations 3.2 and 3.3 were used to estimate the performance of the pavement:

Fatigue  
Cracking  
Failure:

$$\log(N_f) = 15.947 - 3.29 \log \left[ \frac{\epsilon_t}{10^{-6}} \right] - 0.845 \log \left[ \frac{E_R}{10^3} \right] \quad (\text{Equation 3.2})$$

$N_f$  = number of loads to failure

$\epsilon_t$  = horizontal tensile strain at the bottom of the AC (in/in x  $10^{-6}$ )

$E_R$  = the resilient modulus of the AC (psi)

Rutting  
Failure:

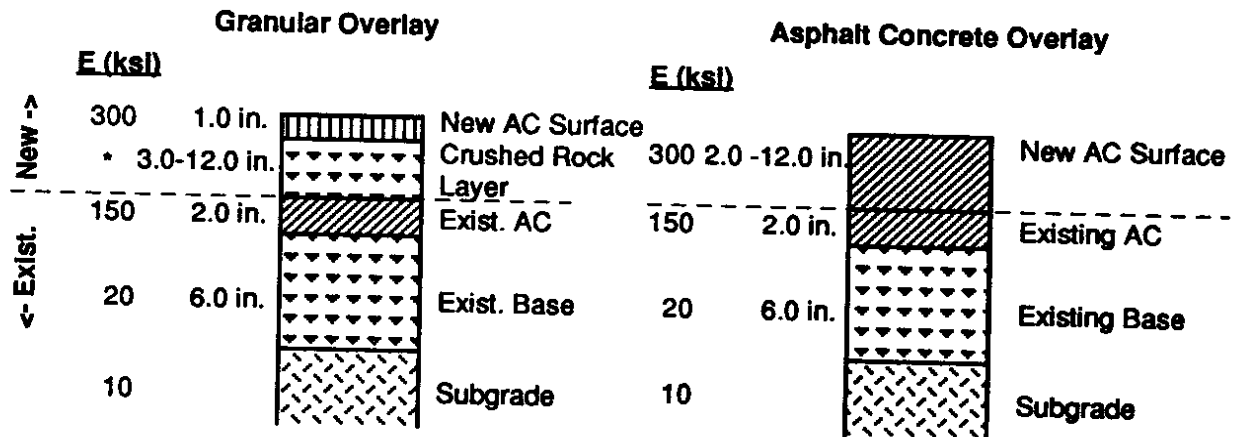
$$N_f = 1.077 \times 10^{18} \left[ \frac{10^{-6}}{\epsilon_{vs}} \right]^{4.4843} \quad (\text{Equation 3.3})$$

$N_f$  = number of loads to cause a 0.75 in. (19 mm) rut

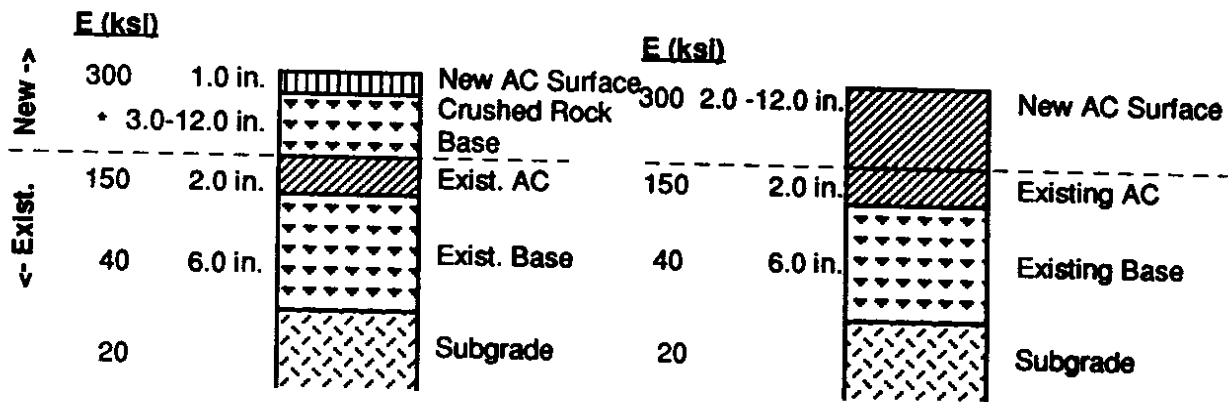
$\epsilon_{vs}$  = vertical compressive strain at the top of the subgrade (in/in x  $10^{-6}$ )

Sibal considered three modes of failure: fatigue cracking of the surface, fatigue cracking of the preexisting pavement surface layer, and rutting. He determined which of the three modes of failure was critical for each model and used the corresponding number as the number of loads to failure for the pavement. Finally, he compared the number of loads to failure for each of the models to determine the equivalent thicknesses of granular overlays and AC overlays. The 1.0 in. of AC on top of the crushed rock layer was not calculated in the equivalency factor. For example, if a 4 in. AC overlay was to be

### Case 1 – Weak Subgrade



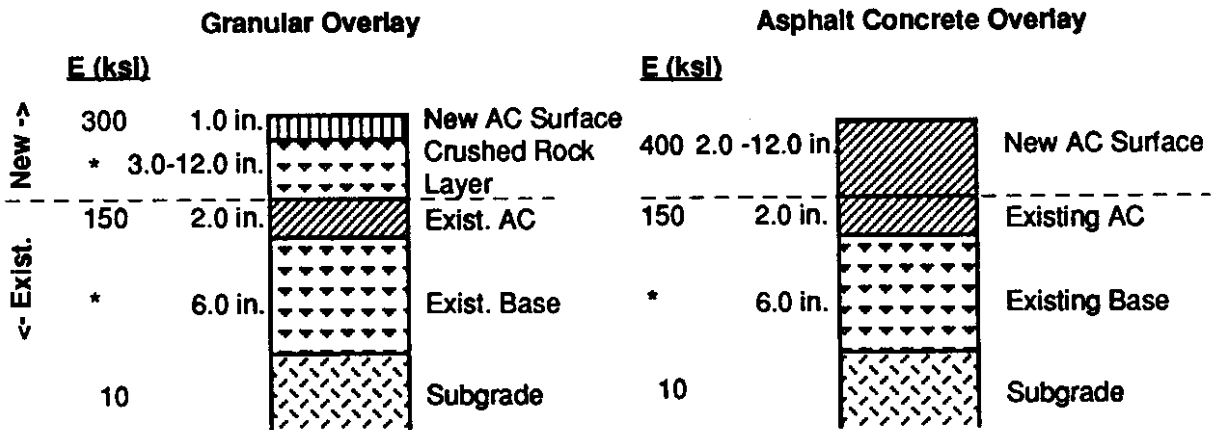
### Case 2 – Strong Subgrade



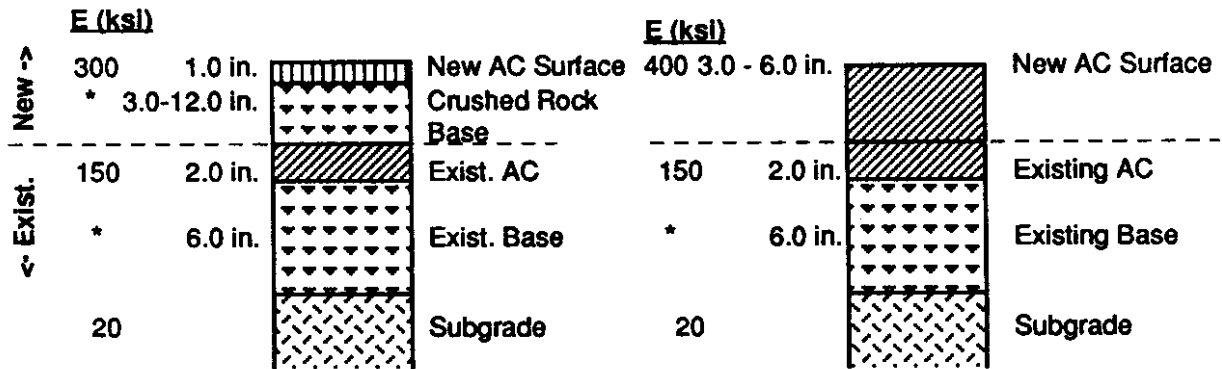
\* Stress sensitive moduli determined in EVERSTRS analysis

Figure 3.2. Pavement Structures Modelled by Sibal [26] Using ELSYM5

### Case 1 – Weak Subgrade



### Case 2 – Strong Subgrade



\* Stress sensitive moduli determined in EVERSTRS analysis.

$$\text{relationship: } E_B = K_1 (\theta)^{K_2} \text{ where } K_1 = 3200, 4000 \text{ or } 8000. \\ K_2 = 0.6$$

Figure 3.3. Pavement Structures Modelled by Sibal [26] Using Nonlinear Model for Crushed Rock Layers

converted to a granular overlay with an equivalency factor of 1.70, then the conversion would be:

$$\begin{aligned} 4 \text{ in. AC} &= 1.0 \text{ in. AC} + 3.0 \text{ in. of AC} \\ &= 1.0 \text{ in. AC} + 3.0 \times 1.70 \text{ of crushed rock} \\ &= 1.0 \text{ in. AC} + 5.1 \text{ in. of crushed rock (or 6.1 in. total thickness)} \end{aligned}$$

The results of Sibal's analyses are shown in Tables 3.2 and 3.3. The crushed rock moduli in Table 3.2 range from fixed values of 10 ksi to 80 ksi (69 to 551 MPa). Further, the modulus of the preexisting base course is set at twice the subgrade modules. In Table 3.3 the crushed rock layers (for the granular overlay and the preexisting base course) are based on three nonlinear moduli relationships.

- $E_{\text{Base}} = 8000 (\theta)^{0.6}$
- $E_{\text{Base}} = 4000 (\theta)^{0.6}$
- $E_{\text{Base}} = 3200 (\theta)^{0.6}$

These relationships were obtained from those reported in the AASHTO Guide [1] for dry, damp, and wet conditions estimated for the crushed limestone base course used at the AASHO Road Test.

The results in both Tables 3.2 and 3.3 reveal equivalency factors of about 2.0 for the "stiffer" crushed rock moduli. This is further illustrated in Figure 3.4 which is simply a plot of the equivalency factors shown in Table 3.2 (which was based on the ELSYM5 computations).

### **3.4 SOUTH AFRICAN STUDIES**

A series of South African studies investigated the effects of different parameters on the behavior of the crushed rock layer in inverted pavements. These studies provide verification that the modulus of the crushed rock layer can be quite high and offer insight into improved designs for this layer.



Table 3.2. Equivalent Thicknesses and Equivalency Factors Based on Most Critical Failure Mode Using Linear Elastic Moduli for Crushed Rock Layers (after Sibal [26])

Thickness of AC Overlay (in.)	Equivalent Thickness of Crushed Rock in Granular Overlay		Equivalency Factors (CR/AC)	
	Subgrade = 10 ksi	Subgrade = 20 ksi	Subgrade = 10 ksi	Subgrade = 20 ksi
<b>*ECR = 10 ksi</b>				
2	5.3	—	5.3	—
3	11.6	—	5.8	—
4	—	—	—	—
6	—	—	—	—
<b>*ECR = 20 ksi</b>				
2	3.7	3.8	3.7	3.8
3	6.4	6.6	3.2	3.3
4	8.9	—	3.0	—
6	—	—	—	—
<b>*ECR = 40 ksi</b>				
2	<3.0	<3.0	3.0	3.0
3	4.6	4.7	2.3	2.4
4	6.8	6.7	2.3	2.2
6	11.0	10.3	2.2	2.1
<b>*ECR = 60 ksi</b>				
2	<3.0	<3.0	3.0	3.0
3	3.8	3.9	1.9	2.0
4	5.6	5.7	1.9	1.9
6	9.6	9.2	1.9	1.8
<b>*ECR = 80 ksi</b>				
2	<3.0	<3.0	3.0	3.0
3	3.3	3.4	1.6	1.7
4	5.0	5.2	1.7	1.7
6	8.8	8.5	1.8	1.7

\*Modulus of crushed rock layer in granular overlay

Table 3.3. Equivalent Thicknesses and Equivalency Factors Based on Most Critical Failure Mode Using Nonlinear Moduli for Crushed Rock Layers (after Sibal [26])

Thickness of AC Overlay (in.)	Equivalent Thickness of Crushed Rock in Granular Overlay		Equivalency Factors (CR/AC)	
	Subgrade = 10 ksi	Subgrade = 20 ksi	Subgrade = 10 ksi	Subgrade = 20 ksi
Case A: *CR $K_1 = 8000$ $K_2 = 0.6$				
3	—	<3.0	—	1.5
4	—	4.2	—	1.4
5	—	6.1	—	1.5
6	—	7.1	—	1.4
Case B: *CR $K_1 = 4000$ $K_2 = 0.6$				
3	3.5	3.6	1.8	1.8
4	5.6	5.4	1.9	1.8
5	7.7	6.8	1.9	1.7
6	>8.0	>8.0	—	—
Case C: *CR $K_1 = 3200$ $K_2 = 0.6$				
3	3.9	4.1	2.0	2.0
4	6.2	5.7	2.1	1.9
5	>8.0	7.2	—	1.8
6	>8.0	>8.0	—	—

\*Crushed rock layers ( $E = K_1(\theta)^{K_2}$ )

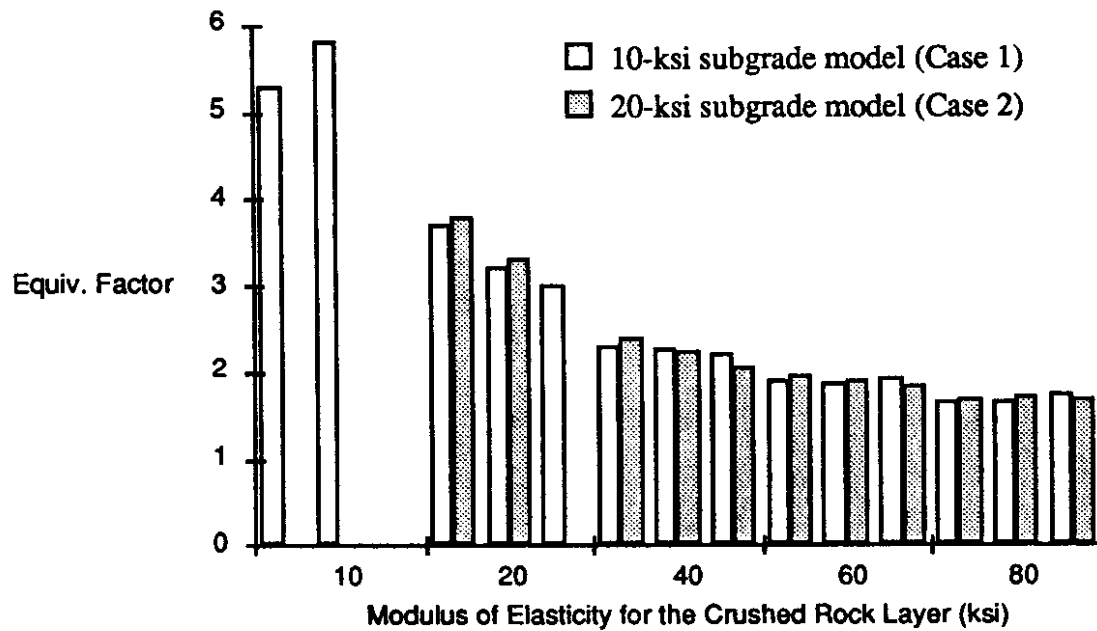


Figure 3.4. The Equivalency Factors versus the Modulus of Elasticity for the Crushed Rock Layer Based on Sibal's Calculations [26]

The South African system of classifying granular pavement materials is shown in Figure 3.5. The material generally used in the crushed rock layer was the G1 material, although G2 was used on occasion. The densities for the G1A material are listed in terms of “apparent density,” but no definition of this term was given.

In most cases multidepth deflectometers (MDD) were placed in the pavement and the pavement was loaded with a heavy-vehicle simulator (HVS). A 1.5 in. (38 mm) diameter hole 6.5 ft. (2.0 m) deep was drilled into the pavement and lined with a thin rubber tube. The MDD reference point for the deflection measurements is taken at 6.5 ft. (2.0 m). Sensors were placed to measure the deflections at various depths in the pavement (generally at layer interfaces). This system offered the advantage of directly measuring the response of the pavement layers to loading. The loading was done by the heavy-vehicle simulator which applied loads ranging from 4.5 to 22.5 kip (20 to 100 kN) dual-wheel loads (or single axle loads ranging from 9,000 to 45,000 lbs (40 to 200 kN)). Measurements that were taken included surface deflections, MDD deflections, road surface profile, temperature, precipitation, and depth to the water table. The testing is conducted on each road for a period of two to six months (Maree et al. [17])

The surface and depth deflections were then used to calculate the effective elastic moduli of the pavement layers with elastic layer theory and the ESLYM5 computer program (Maree et al. [16]). The bulk stress for the crushed rock layer was calculated by averaging the calculated principal stresses at the top, middle, and bottom of the layer.

After the material had been tested, the changes undergone by the pavement were correlated against the total number of repetitions of the wheel load. The total number of repetitions was then multiplied by the relative damage factor (Equation 3.4) to determine the total number of 18 kip (80 kN) equivalent single axle loads (ESALs). The relative damage factor is calculated as follows (after Maree et al. [17]):

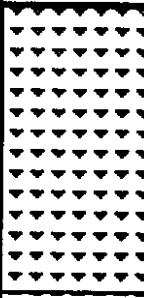
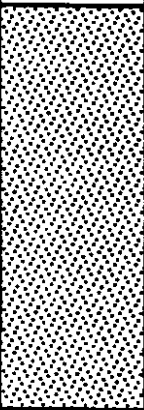
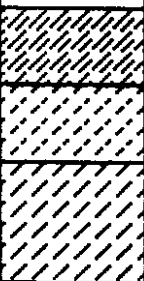
Symbol	Code	Material	Abbreviated Specifications
	G1	Graded crushed stone	Dense-graded unweathered crushed stone. Max. size 1.5 in. (37.5 mm) G1A: 86 - 88% of apparent density. G1B: 98% modified AASHTO (density lower than G1A)
	G2	Graded crushed stone	Dense - graded stone and soil binder. Max. size 1.5 in. (37.5 mm), min. 98% modified AASHTO
	G4	Natural gravel	CBR ≥ 80, PI ≤ 6
	G5	Natural gravel	CBR ≥ 45, PI ≤ 10 to 15, depending on grading; Max. size 2.5 in. (63 mm)
	G6	Natural gravel	CRB ≥ 25, Max. size ≤ 2/3 layer thickness
	G7	Gravel - soil	CRB ≥ 15, Max. size ≤ 2/3 layer thickness
	G8	Gravel - soil	CBR ≥ 10 at in situ density
	G9	Gravel - soil	CBR ≥ 7 at in situ density
	C3	Cemented natural gravel	Unconfined Compressive Strength 220 - 440 psi (1.5 - 3.0 MPa) at 100% mod. AASHTO; Max. size 2.5 in. (63 mm)
	C4	Cemented natural gravel	Unconfined Compressive Strength 110 - 220 psi (0.75 - 1.5 MPa) at 100% mod. AASHTO; Max. size 2.5 in. (63 mm)
	C5	Treated natural gravel	Modified mainly for Atterberg limits

Figure 3.5. South African Pavement Material Classifications  
(from Maree, et al. [16] and Maree, et al. [17])

$$\text{Relative Damage Factor} = \left(\frac{P_i}{9}\right)^n \quad (\text{Equation 3.4})$$

where  $P_i$  = applied dual wheel load,  
 9 kip = standard wheel load (or 18 kip single axle), and  
 n = generally taken to be 4.2.

### **3.4.1 Effective Moduli and Stress Dependence of Granular Layers**

An early study compared the effects of the different loadings on two "traditional," thin pavements and two inverted pavements (Maree et al. [16]). The test sections were all in the Transvaal Province (see map Figure 3.8) with pavement profiles as shown in Figures 3.6 and 3.7. The major difference between the light and inverted pavements was the use of higher quality crushed rock layers beneath the surfacing and cement stabilized subbases below the crushed rock layer.

The pavements were then loaded and tested as described above. Tables 3.4 through 3.7 show the results of these tests.

In every case, the base course that was supported by the cemented subbase had significantly higher bulk stresses and higher moduli of elasticity than did the light pavements. Most notable were the differences in quality between the base courses in the four roads. In both of the light pavements the base consisted of natural gravels (classified G5), whereas the inverted pavement base consisted of graded crushed stone (classified G1 and G2). This accounts for much of the difference in the moduli between the light and inverted pavement bases.

For a simple comparison of the WSDOT general model ( $E = 8500 \theta^{0.375}$ ) and the moduli for these four test roads, the bulk stresses shown in Tables 3.4 through 3.7 for the 9 kip (40 kN) dual wheel load were used to estimate an "analogous" WSDOT modulus (Table 3.8). Actually the WSDOT moduli would be different than shown due to corresponding differences in bulk stresses. At any rate the South African and WSDOT

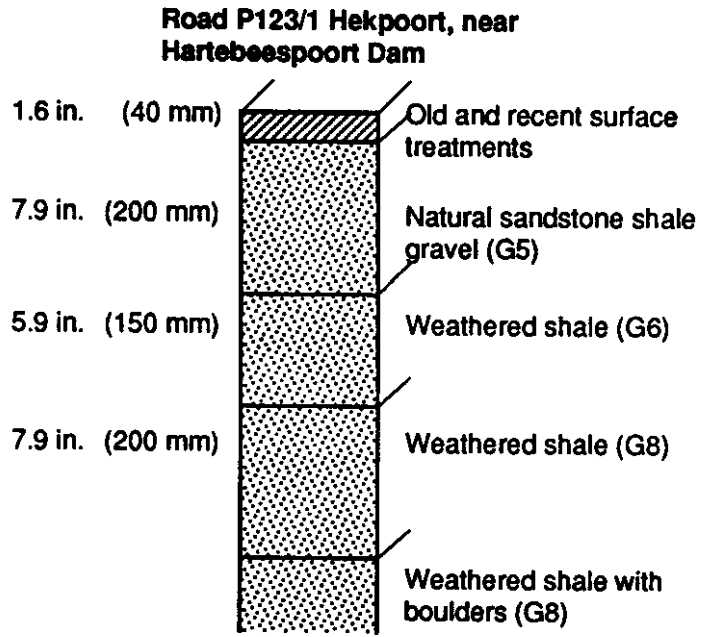
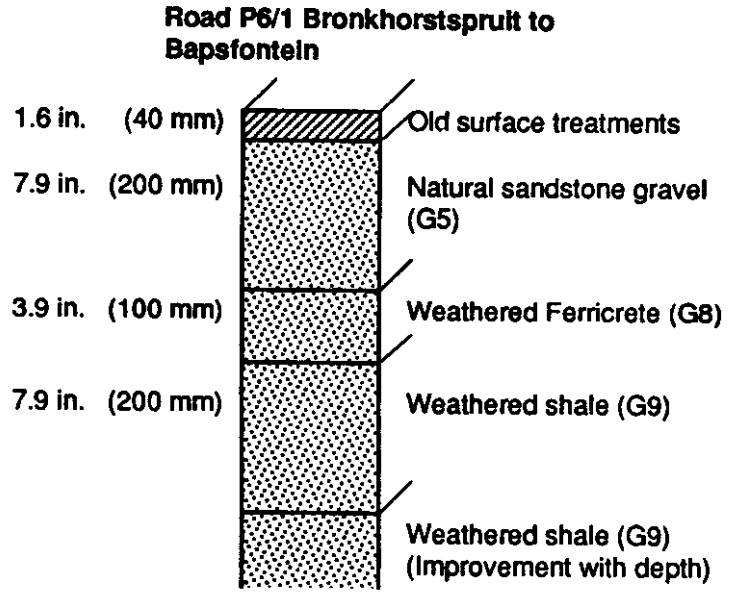
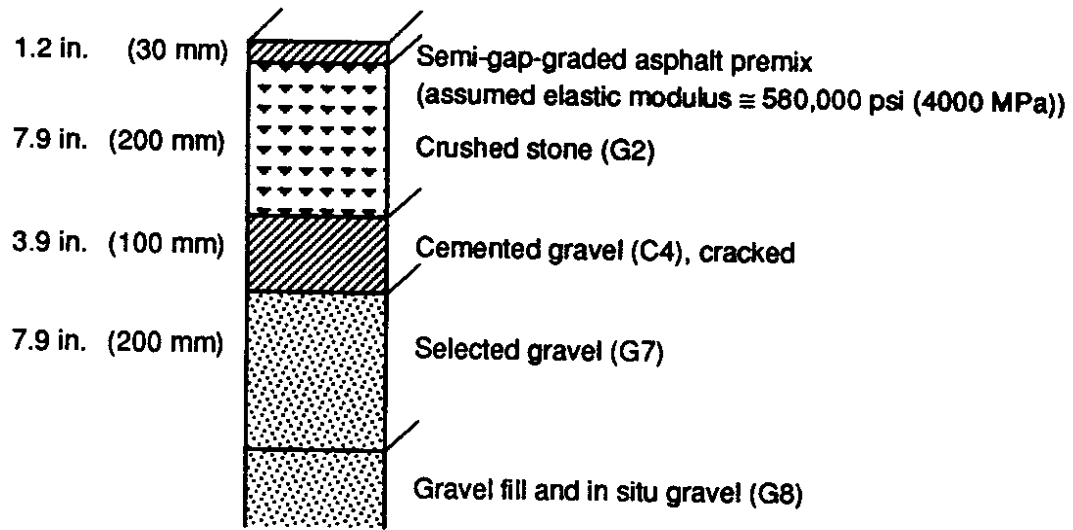


Figure 3.6. The Light Pavements, Road P 6/1 and Road P 123/1, Tested by the Heavy Vehicle Simulator (after Maree et al. [16])

**Road P157/1 Ollifantsfontein**



**Road P157/2 Jan Smuts Airport**

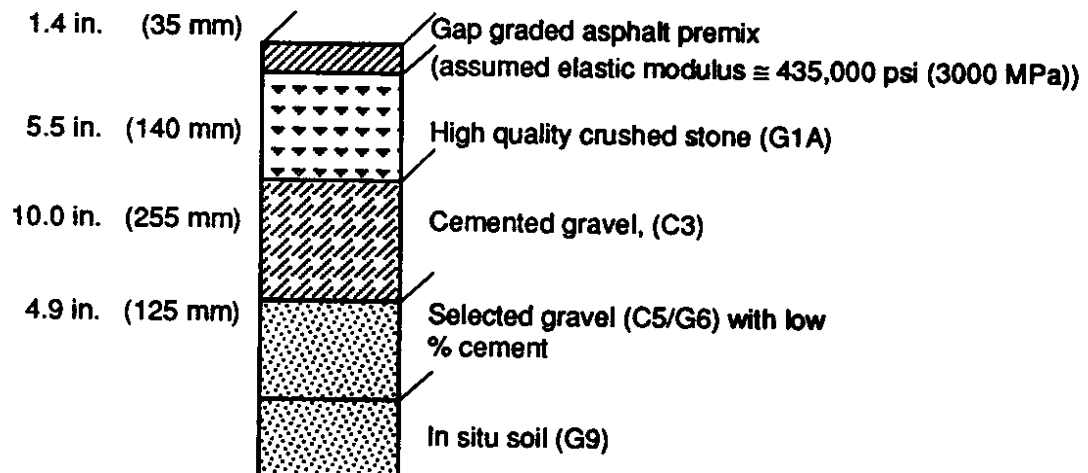


Figure 3.7. Inverted Pavements, Road P157/1 and P157/2, Tested with the Heavy Vehicle Simulator (after Maree et al. [16])



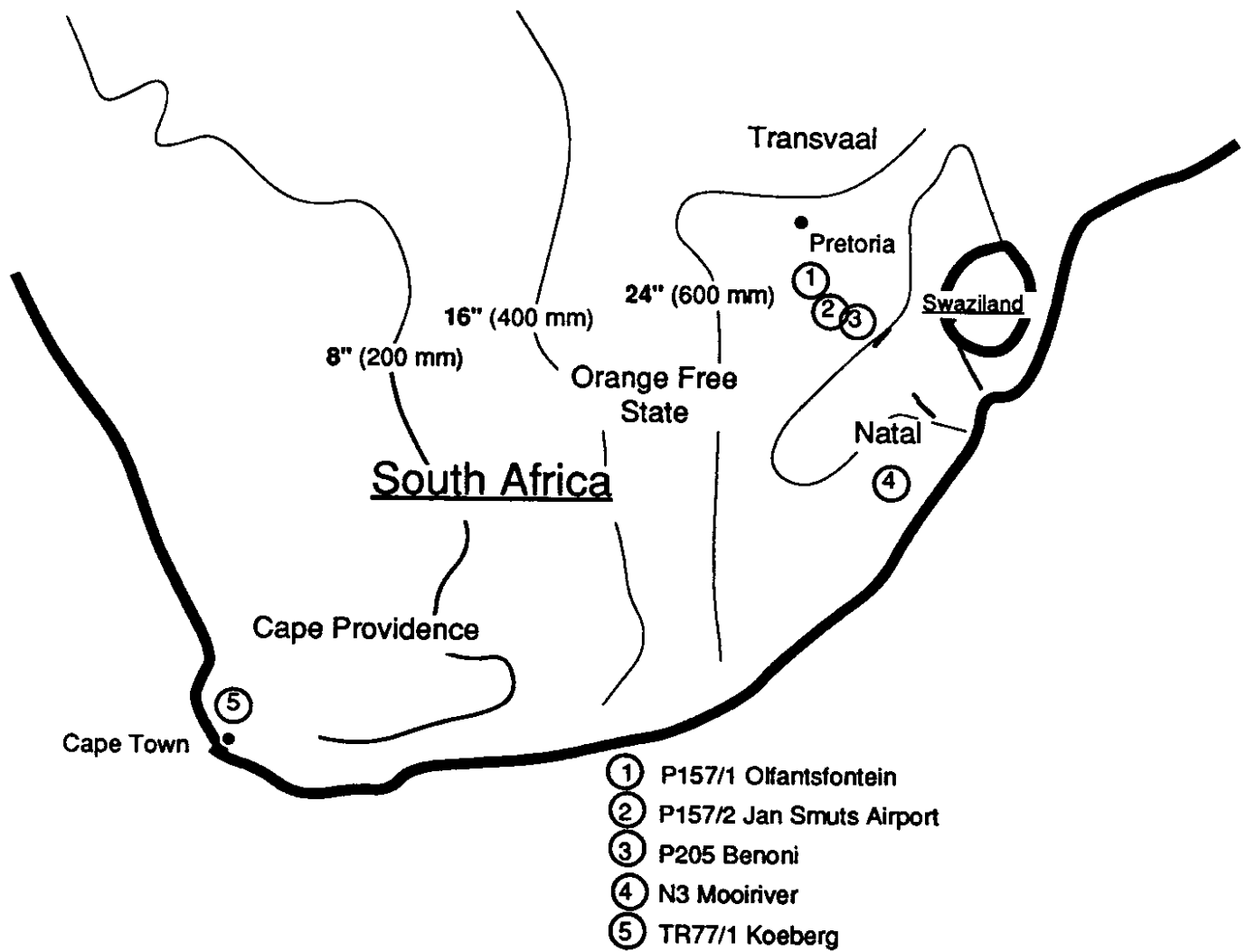


Figure 3.8. Map of South Africa Showing the Average Annual Precipitation (Jackson [11]) Location of Five Test Sites (Maree et al. [17])

**Table 3.4. The Moduli of Elasticity of the Base Course (G5) in a Light Pavement (Road P6/1) Tested with a Heavy-Vehicle Simulator**

Dual Wheel Load		Modulus of Elasticity		Bulk Stress (calculated)	
kip	kN	ksi	MPa	psi	kPa
4.5	20	8.7	60	12.6	87
9.0	40	8.7	60	21.5	148
13.5	60	10.2	70	26.5	183
18.0	80	12.3	85	39.4	272
22.5	100	16.0	110	46.5	321

**Table 3.5. The Moduli of Elasticity of the Base Course (G5) in a Light Pavement (Road P123/1) Tested with a Heavy-Vehicle Simulator**

Dual Wheel Load		Modulus of Elasticity		Bulk Stress (calculated)	
kip	kN	ksi	MPa	psi	kPa
4.5	20	5.8	40	19.0	131
9.0	40	7.2	50	34.5	238
13.5	60	8.0	55	52.8	364
18.0	80	10.2	70	62.9	434
22.5	100	11.6	80	75.3	519

**Table 3.6. The Moduli of Elasticity of the Base Course (G2) in an Inverted Pavement (Road P157/1) Tested with a Heavy-Vehicle Simulator**

Dual Wheel Load		Modulus of Elasticity		Bulk Stress (calculated)	
kip	kN	ksi	MPa	psi	kPa
9.0	40	29.0	200	38.3	264
15.7	70	43.5	300	58.4	403

**Table 3.7. The Moduli of Elasticity of the Base Course (G1A) in an Inverted Pavement (Road P157/2) Tested with a Heavy-Vehicle Simulator**

Dual Wheel Load		Modulus of Elasticity		Bulk Stress (calculated)	
kip	kN	ksi	MPa	psi	kPa
9.0	40	48.6	335	53.6	370
15.7	70	75.4	520	89.6	618
22.5	100	105.1	725	127.5	879

Table 3.8. Comparison of WSDOT and South African Granular Layer Moduli

Road	Dual Wheel Load		Bulk Stress		Moduli			
					Actual		WSDOT	
	kip	kN	psi	kPa	ksi	MPa	ksi	MPa
P6/1	9.0	40	21.5	148	8.7	60	26.9	185
P123/1	9.0	40	34.5	238	7.2	50	32.1	221
P157/1	9.0	40	38.3	264	29.0	200	33.4	230
P157/2	9.0	40	53.6	370	48.6	335	37.8	261

Table 3.9. Results of Increasing Load Repetitions on Road P157/1

Repetitions	Dual-Wheel Load		Modulus of Elasticity		Bulk Stress (calculated)	
	kip	kN	ksi	MPa	psi	kPa
10	9.0	40	29.0	200	38.3	264
	15.7	70	43.5	300	58.4	403
1.00E+06	9.0	40	23.5	162	38.6	266
	15.7	70	42.0	290	53.1	366
1.75E+06	9.0	40	25.8	178	35.8	247
	15.7	70	32.6	225	59.6	411
1.94E+06	9.0	40	28.3	195	30.5	210
	15.7	70	34.1	235	51.2	353

Table 3.10. Results of Increasing Load Repetitions on Road P157/2

Repetitions	Dual-Wheel Load		Modulus of Elasticity		Bulk Stress (calculated)	
	kip	kN	ksi	MPa	psi	kPa
10	9.0	40	48.6	335	53.7	370
	15.7	70	75.4	520	89.6	618
4.80E+05	9.0	40	36.2	250	53.6	370
	15.7	70	60.9	420	90.6	625
1.42E+06	9.0	40	37.7	260	55.0	379
	15.7	70	55.1	380	85.8	592
1.70E+06	9.0	40	27.6	190	53.8	371
	15.7	70	33.4	230	91.4	630

moduli were not at all similar for the light pavements (Roads P6/1 and P123/1) or Road P157/2. The moduli were somewhat similar for Road P157/1.

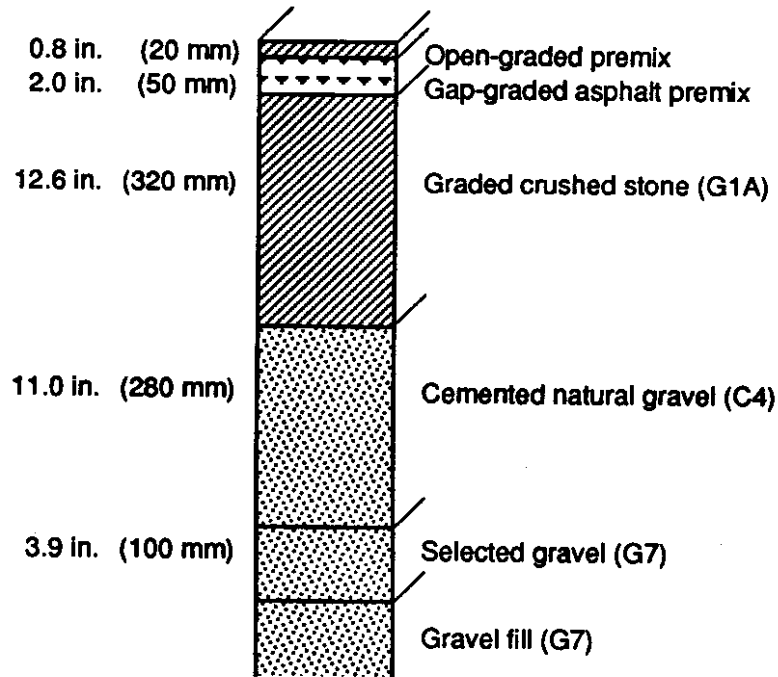
The heavy vehicle simulator tests were continued up to about two million repetitions of the 15.7 and 22.5 kip (70 and 100 kN) dual-wheel loads. (The pavement response and the estimated moduli were made at 9.0 and 15.7 kip (40 and 70 kN) loads.) As the loadings increased the moduli of the granular layer decreased (Tables 3.9 and 3.10). When the testing was finished, sections of the pavement were dug up. No degradation was observed in the crushed rock layer, but the cement stabilized subbase was fully cracked into small pieces on Road P157/1. The cement stabilized subbase on Road P157/2 was cracked, but not fully. Maree et al. [16] noted that a gradual decrease in soil suction (hence increasing moisture content and degree of saturation) occurred during the repeated loading by the HVS. In fact, for Road P157/1, the degree of saturation changed from less than 50 percent at the beginning of the repeated loadings to 85 to 100 percent at completion ( $1.94 \times 10^6$  repetitions). For Road P157/2, the initial degree of saturation also was less than 50 percent increasing to 50 to 85 percent after  $1.7 \times 10^6$  load repetitions. Clearly, the repeated loadings contributed to the increased moisture content thereby decreasing the modulus of elasticity.

### **3.4.2 Moisture Content**

A second South African study (Maree et al. [17]) investigated the effect of moisture on the crushed rock layer. The locations of the five pavements that were tested are shown in Figure 3.8 and the profiles of the pavements are shown in Figures 3.9 through 3.11. The tests involved loading the pavement with a heavy-vehicle simulator, measuring the rutting, wetting the pavement and loading it, then measuring the rutting again. The rutting was measured with a surface transverse profilometer as well as the MDDs. The tests were conducted from 1978 to 1981.

Four of these pavements were inverted pavements and the fifth had only a crushed stone subbase. The base course for the four inverted pavements ranged from G1A, a

**Road P205/1, Benoni**



**Road P157/1 Olifantsfontein**

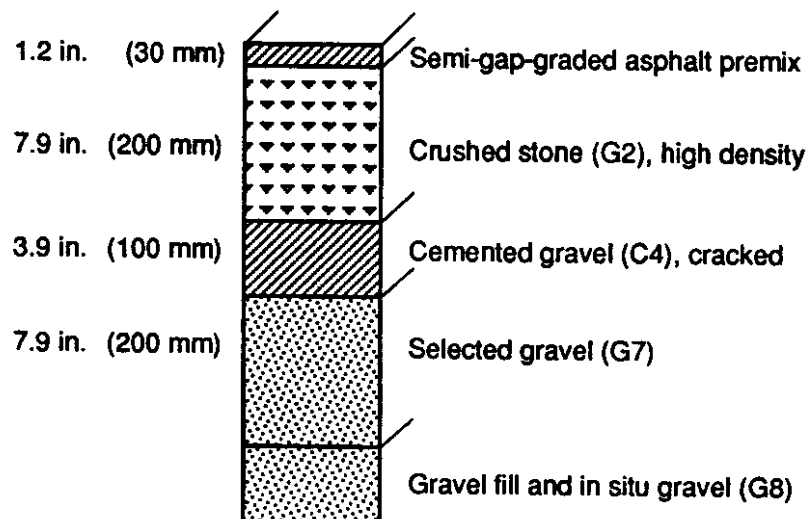


**Figure 3.9. Inverted Pavements, Road P205/1 and Road P157/1, Tested with the Heavy Vehicle Simulator (Maree et al [17])**

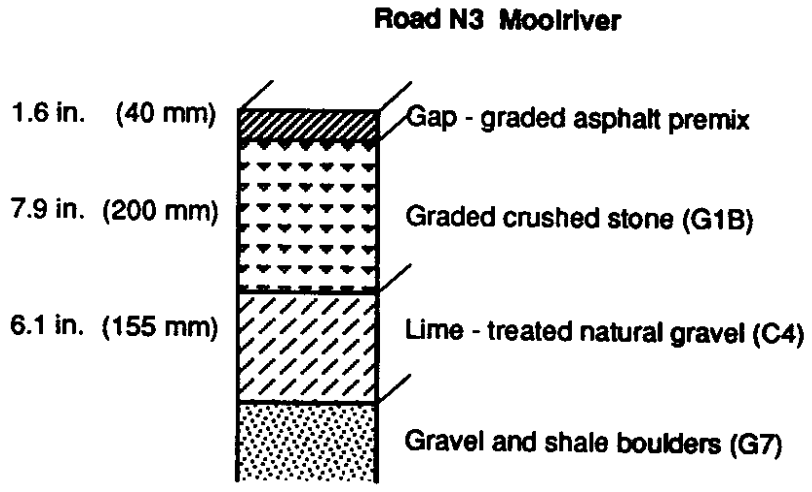
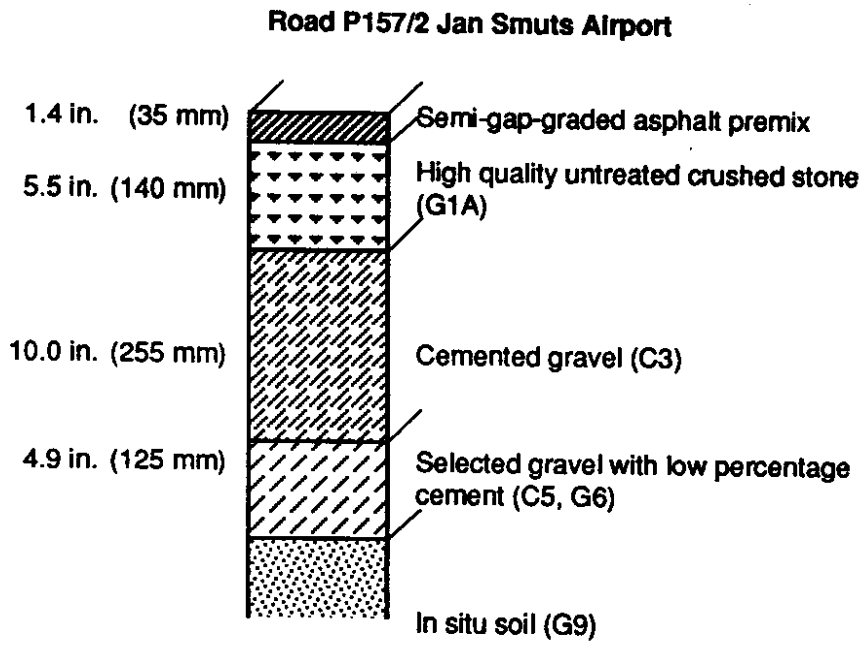


**Figure 3.10. Inverted Pavements, Road P157/2 and N3, Tested with the Heavy-Vehicle Simulator (Maree et al. [17])**

Road TR 77/1 Koeberg

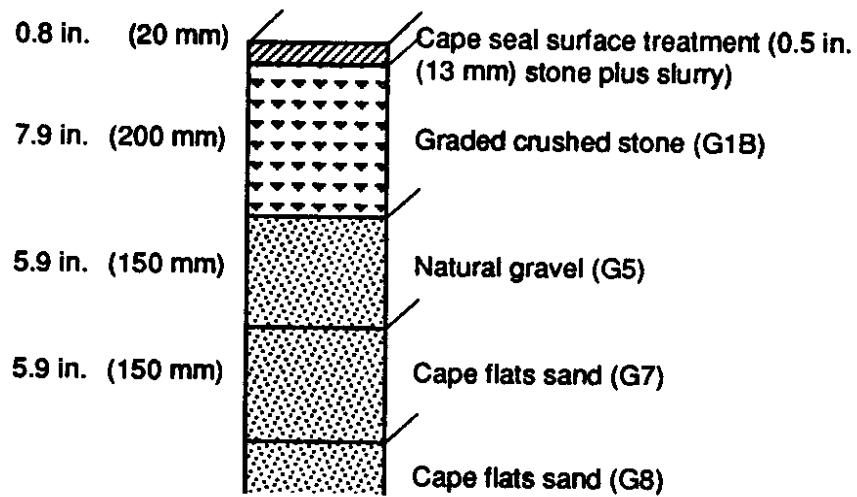
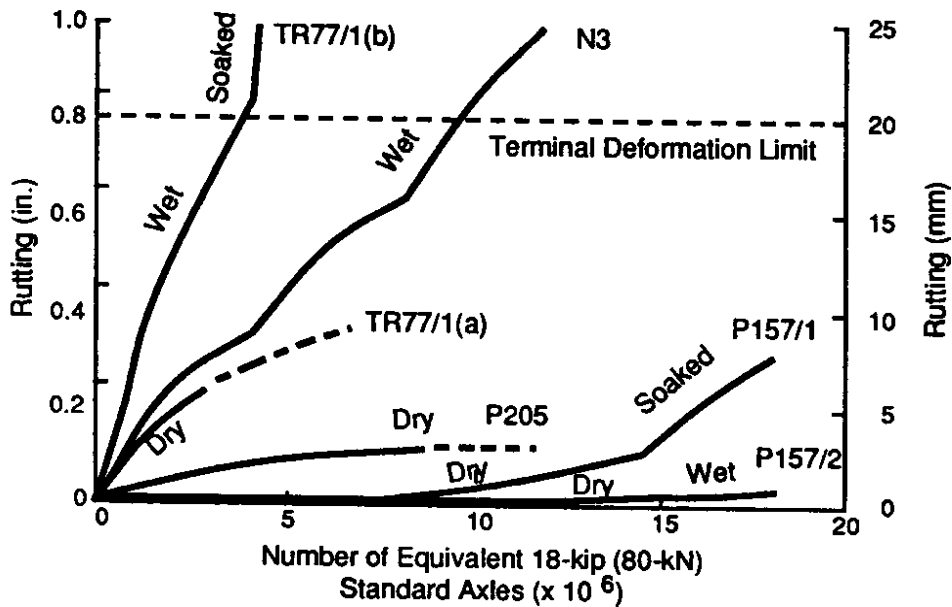


Figure 3.11. Light Pavement, Road TR 77/1, Tested with the Heavy Vehicle Simulator (Maree et al. [17])



Legend

- Dry = 50% Saturated
- Wet = 50 - 85% Saturated
- Soaked = >85% Saturated

Figure 3.12. The rutting of the five different pavement structures against the number of 18-kip (80-kN) ESALs

high-quality, dense-graded, high density material consisting of particles crushed solely from fresh rock, to G1B, a crushed stone compacted to a lower density, and G2, a dense-graded stone and soil binder compacted to greater than 98 percent modified AASHTO.

The two pavements with the highest quality bases, Roads P205/1 and P157/2, showed the lowest rutting after repeated loadings with the HVS, even when the base course was wet. After about two million HVS load repetitions (or  $15.4 \times 10^6$  18 kip (80 kN) ESALs) on P205 and  $50.3 \times 10^6$  18 kip (80 kN) ESALs on P157/2, neither pavement had ruts of more than 0.1 in. (3 mm). Further, water was injected into the base in P157/2 and the pavement was subjected to additional ESALs (about  $3 \times 10^6$ ). Although the rate of rutting increased slightly after water had been injected, the rutting still remained minimal.

These results illustrate that a well compacted, high-quality base course which is well supported can be very resistant to rutting. The only significant difference in the structure of the two pavements was that the base course in P205/1 was about 130 percent thicker than that in P157/2. Increasing the base by the additional 7.1 in. (180 mm) did not seem to have a significant impact on the performance of the pavement.

Figure 3.12 shows the rate of deformation for the five pavement sections versus the number of ESALs. In every case, when the base course became wet, the rate of rutting increased (however only slightly for Roads P205/1 and P157/2). The rate of increase was faster when the base course material was of a lower quality and when it was not confined.

In a later study, a newly built inverted pavement was tested with the HVS while the base was slowly wetted (van Zyle et al. [33]). The road was a major highway that had recently been rebuilt. The new pavement structure is shown in Figure 3.13. The base consisted of the high quality G1A material, similar to that in the roads P205/1 and P157/1 from the earlier study. Because the subgrade consisted of weathered mudstone and had CBRs of less than 5, the subbase was thicker than normal.



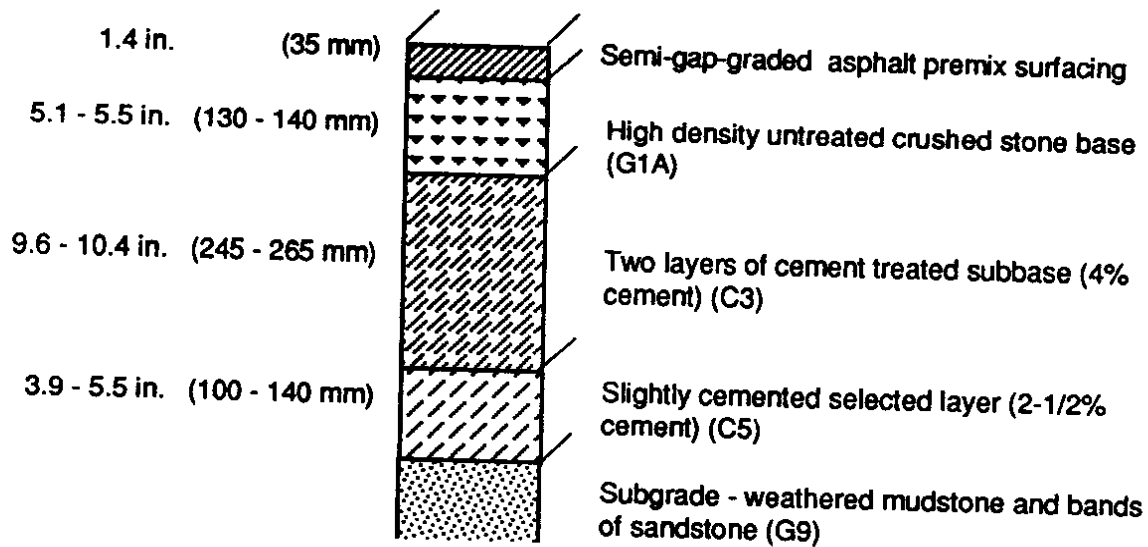


Figure 3.13. The Rebuilt Section of Road P157/2

The study was again conducted by loading the pavement with the HVS and measuring the deformation with MDDs and pavement profilometers. The pavement was kept at normal moisture conditions for the first  $39 \times 10^6$  18 kip (80 kN) ESALs, then slowly wetted and subjected to an additional  $14.4 \times 10^6$  18 kip (80 kN) ESALs. Water was introduced in the second half of the experiment through holes 1 ft (0.3 m) from one end of the section. A total of over  $31 \text{ ft}^3$  ( $1.1 \text{ m}^3$ ) of water was introduced over a period of 39 days.

At the end of the testing, the overall rut depth in the pavement was less than 0.08 in. (2 mm) and no surface cracks were observed. The introduction of water seemed to have little impact on the rate of deformation. However, when the deflection in the pavement under a load was measured, the deflections increased significantly as the pavement became more saturated. The deflections increased from approximately 15.7 mils (400  $\mu\text{m}$ ) to 27.5 mils (700  $\mu\text{m}$ ) at the end of the testing (deflections measured under 22.5 kip (100 kN) dual wheel load of HVS). Additionally, the resilient moduli and the stress-stiffening of the base decreased significantly. As can be seen in Figure 3.14 and in Table 3.11, the magnitude of the resilient modulus decreased after the first  $0.5 \times 10^6$  18 kip

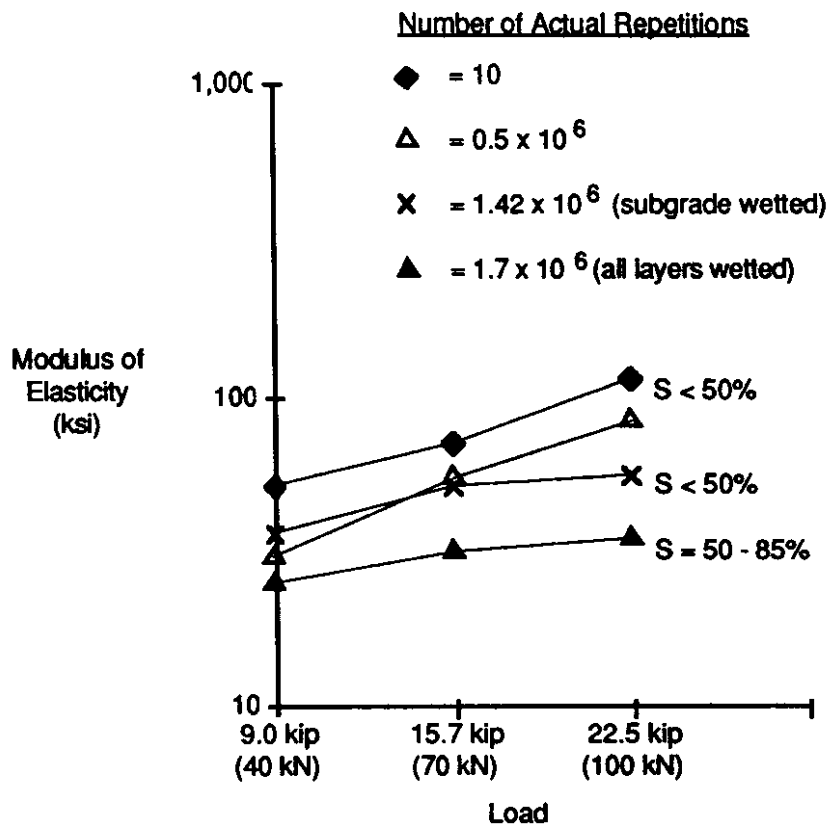


Figure 3.14. The Stress-stiffening Behavior of the Crushed Stone Base in Road P157/2

Table 3.11. Resilient Moduli for the Crushed Rock Base in P157/2

Dual Wheel Load		18 kip (80 kN) ESALs							
		10		$5 \times 10^6$		$44 \times 10^6$		$53 \times 10^6$	
kip	kN	E (ksi)	E (MPa)	E (ksi)	E (MPa)	E (ksi)	E (MPa)	E (ksi)	E (MPa)
9.0	40	53.7	370	31.9	220	36.3	250	26.1	180
15.7	70	72.5	500	58.0	400	53.7	370	33.4	230
22.5	100	116.0	800	87.0	600	58.0	400	36.3	250

(80 kN) ESALs, but the stress-stiffening (the slope of the line) did not change. After the material had been wetted, the stress-stiffening declined dramatically.

The loss of stiffness due to moisture was discussed in another South African study done by Horak et al. [6]. The study examined rehabilitation options for a rural road and considered the remaining life of the pavement and different options for stiffening it. One of the attempts at stiffening the pavement was to add a crushed rock layer on top of the existing pavement both with and without a lime stabilized sublayer. This was then covered with an AC surface. Although the specifications required the construction of a G1 base, tests done during construction showed that the initial requirement of 86 percent apparent density (as measured with the nuclear gauge) was not reached. The reasons stated for this failing were a lack of fines and a course overall grading of the crushed rock material. No specifics as to the actual grading were given. The base was instead classified as a G2 material.

After construction, the test sections with and without the lime stabilized sublayer were tested with the HVS. Both sections showed significant initial rutting with the amount tapering off. After approximately  $1.6 \times 10^6$  18 kip (80 kN) ESALs, the section without the lime stabilized sublayer had ruts of nearly 0.6 in. (15 mm), as opposed to 0.3 in. (7 mm) for the section with the lime stabilized sublayer. The authors suggested that this result emphasized the importance of having strong support for the granular layer. To test the moisture sensitivity of the granular base with the lime stabilized sublayer, water was injected into the base. This resulted in a rise in the amount of rutting from 0.3 in. (7 mm) to 0.4 in. (10 mm) in  $0.4 \times 10^6$  18 kip (80 kN) ESALs. The degree of saturation achieved through injecting the water was not given.

### **3.4.3 Gradation**

As Horak et al. [6] discovered, gradation specifications are very important for achieving the high densities required for optimal performance of confined crushed rock layers. Horak et al. [7] published a paper that dealt with the effects of tightening the

grading specifications beyond those normally required for the G1 base. Although they mentioned the importance of the strength, durability, shape and Atterberg limits of the aggregate, the report focused on changes to the specifications to produce a better compacted base.

For convenience, the gradation bands for the South African G1 material as well as somewhat similar gradations from AASHTO M147 (Gradings A and B) and WSDOT (Crushed Surfacing Top Course and Base Course) are listed in Table 3.12. The gradation band for the G1 material was obtained directly from a figure in Horak et al. [7]. It appears

Table 3.12. Gradation Bands for Various Crushed Rock Specifications

Sieve Designation		Percent Passing				
		South African G1*	AASHTO M147-65		WSDOT 9-03.9(3) Crushed Surfacing	
Standard	mm		Grading A	Grading B	Top Course	Base Course
2 in.	50	100	100	100		
1 1/4 in.	32	93 - 97				100
1 in.	25	82 - 92		75 - 95		
3/4 in.	19	72 - 85				
5/8 in.	15.9	64 - 78			100	50 - 80
3/8 in.	9.5	50 - 67	30 - 65	40 - 75		
1/4 in.	6.35	40 - 57			55 - 75	30 - 50
No. 4	4.75	35 - 52	25 - 55	30 - 60		
No. 10	2.00	23 - 39	15 - 40	20 - 45		
No. 30	0.600	14 - 26				
No. 40	0.425	11 - 24	8 - 20	15 - 30	8 - 24	3 - 18
No. 200	0.075	5 - 12	2 - 8	5 - 20	10 max	7.5 max.

\* South African G1 grading taken from plotted gradation band [7]

that most similar gradations to the G1 is AASHTO Grading B and WSDOT Base Course (it should be noted that the majority of granular overlays constructed by WSDOT to date used the Crushed Surfacing Top Course grading).

The base course Horak et al. [7] worked with was compacted to 99 to 103 percent of modified AASHTO and had a gradation that fell within the specifications for a G1 base, but with the added requirements listed below. They found that the greater effort required to set up the crusher and obtain the correct gradation was more than offset by the increased ease in compacting the material to a higher density. These added requirements were:

1. 40 to 45 percent passing No. 4 (4.75 mm)
2. 7 to 9 percent passing No. 200 (0.075 mm)
3. A coarse sand ratio of 30 to 50 percent. Coarse sand ratio defined as ratio of fraction passing No. 10 (2.00 mm) divided by fraction passing No. 40 (0.425 mm)

#### **3.4.4 Reflection Cracking**

The resistance of different overlays to reflective cracking was studied by Vilojoen et al. [30]. Cracks were measured through the use of crack-activity meters. These instruments consist of two linear variable transformers (LVDTs), one to measure horizontal displacement and the other to measure vertical displacement. These instruments are then affixed to the road surface across a spot likely to crack.

The pavement that was overlain was a plain jointed PCC pavement 7.9 in. (200 mm) thick with a 15 ft. (4.5 m) joint spacing that had a large number of hairline cracks. These cracks were caused by an alkali-aggregate reaction and resulted in a pattern of cracks 10 in. x 10 in. x 4 in deep (250 mm x 250 mm x 100 mm deep). These blocks had very high relative movements under traffic loading, as high as 23.6 mils (600  $\mu\text{m}$ ) under a 9.0 kip (40 kN) load. Horizontal thermal movement was low because of the cracked state of the pavement, averaging 7.9 mils (200  $\mu\text{m}$ ).

The overlays that were tested are summarized in Table 3.13. They include granular overlays, open-graded bitumen-rubber overlay, gap-graded AC overlay, and AC overlay with a geofabric interlayer.

The pavements were then loaded until the surface began to crack. A comparison of the loadings until the first cracks appeared is shown in Figure 3.15. The time to cracking was identified as being due to either temperature or traffic stresses. The relative construction costs are shown in Figure 3.16.

Table 3.13. Description of the Reflection Crack Test Sections

Section	Description
H	A continuously graded crushed stone overlay consisting of 5.9 and 7.9 in. (150 and 200 mm) of crushed rock covered with a 1.6 in. (40 mm) semi-gap-graded asphaltic wearing course which included 0.75 in. (19 mm) of rolled-in chips.
A	A 1.2 in. (30 mm) bitumen-rubber overlay with a semi-open aggregate grading. The grading was selected to provide a stable coarse aggregate packing to prevent plastic deformation and at the same time contain a relatively high percentage of voids in mineral aggregate, enabling the mix to accommodate high binder contents to promote resistance to reflection cracking.
B	A conventional gap-graded AC(with no interlayers) varying in thickness from 1.2 to 3.5 in. (30 mm to 90 mm).
D	A 2.4 in. (60 mm) gap-graded asphaltic concrete with rolled-in chips on top of a non-woven geofabric interlayer (Bidum U24) on top of a 1.2 in. (30 mm) leveling course. The leveling course consisted of a fine continuously graded AC with 100 percent of the aggregate passing the No. 4 (4.75 mm) sieve and with 8.6 percent 150/200 pen bitumen. The interlayer was soaked with a 60 percent stable grade emulsion by spraying 0.025 gal/ft <sup>2</sup> (1 l/m <sup>2</sup> ) before laying and 0.012 gal/ft <sup>2</sup> (0.5 l/m <sup>2</sup> ) after laying the geofabric layer.
E	A 2.4 in. (60 mm) gap-graded asphaltic concrete with rolled-in chips on top of a bitumen-rubber, single seal interlayer (0.04 gal/ft <sup>2</sup> , 1.8 l/m <sup>2</sup> ) on top of the leveling course described in Section D.
C	A 2.4 in. (60 mm) gap-graded asphaltic concrete with rolled-in chips on top of a single seal with a woven geofabric interlayer on top of the leveling course described in Section D. The woven geofabric was a 0.80 in. (20 mm) square mesh made of a bitumen-impregnated polyester fibre called Hatelit. After the layer was placed, 0.015 gal/ft <sup>2</sup> (0.6 l/m <sup>2</sup> ) of stable grade emulsion was sprayed on it.

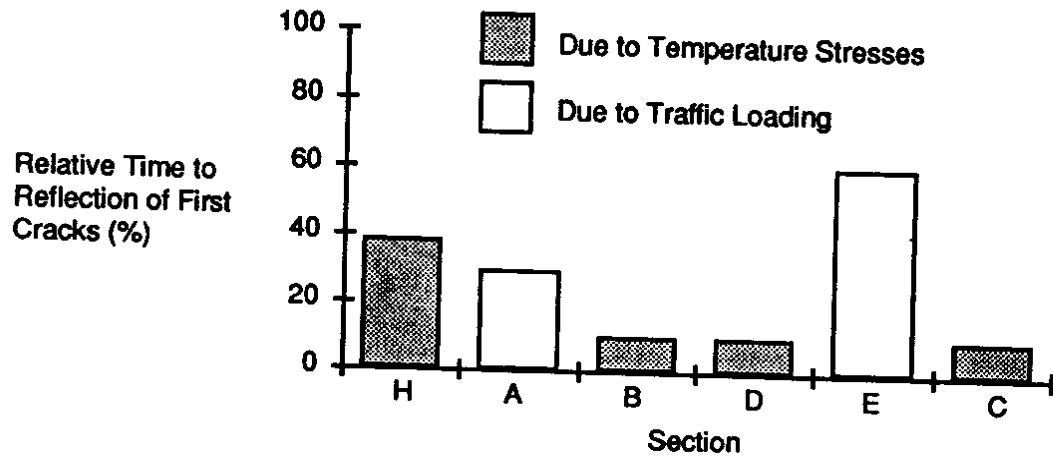


Figure 3.15. Relative Time to First Reflection Crack

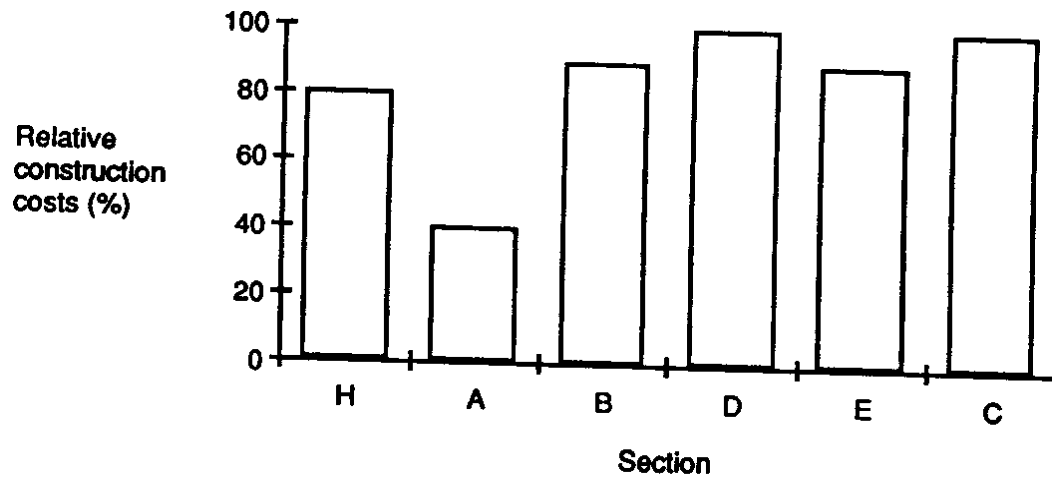


Figure 3.16. Relative Construction Costs for the Different Sources of Overlays

An overall comparison shows the granular overlay to be cost effective. Sections A and E could be more effective (depending on how one "weights" cost and performance).

In another reflection cracking experiment in Ontario, Canada, granular overlays consisting of 3.0 in. (75 mm) and 6.0 in. (150 mm) crushed rock layers surfaced with 5 in. (125 mm) of bituminous mix and a 5.0 in. (125 mm) bituminous surface with no crushed rock layer were placed over a cracked AC pavement. After four years of exposure to traffic, the 3.0 in. granular overlay showed 66 transverse cracks per mile (41/km), the 6.0 in. showed 47 per mile (29/km) and the control section showed 183 per mile (114/km). Additionally both granular overlays showed two longitudinal cracks per mile (1.2/km), while the control section showed 42 per mile (26/km) (Sherman [27]).

### **3.5 CONSTRUCTION OF THE CRUSHED ROCK LAYER**

As was discussed in the prior sections, the crushed rock layer is stiffer and more durable if it is well constructed. The compaction and integrity of the crushed rock layer is very important. The material for the crushed rock layer must be durable. As was mentioned by Horak et al. [6], the easiest method of obtaining the highest compaction is to use an optimum gradation. Interviews during 1990 with WSDOT project engineers on granular overlay construction projects (Reister [24], Stokes [29], Murray [21]) indicated that the moisture content is also important. Since the crushed rock is being spread in a thin layer, the moisture from the rock tends to evaporate rapidly. The surface must therefore be sprayed with water to maintain the optimal moisture content.

A significant problem that WSDOT has encountered in the construction of the granular overlay is traffic. When there is no possible diversion, the traffic has to pass over the crushed rock layer during construction. This frequently results in washboarding. The granular surface must therefore be rebladed immediately before placing the surface layer. WSDOT currently requires that its crushed surfacing have at least one fractured face (WSDOT [31]). Washboarding may be reduced if this requirement is raised.



## **3.6 THE SURFACE LAYER**

The surface layer, when thin, serves mainly to protect the crushed rock layer. As was discussed in prior sections, the infiltration of moisture into the crushed rock layer causes significant reduction in the stress-sensitivity of the crushed rock. Additionally, the surface protects the integrity of the crushed rock layer. Since the crushed rock layer's stiffness is related to its compaction, the crushed rock layer must be kept intact. The surface layer's main roles are therefore to protect the crushed rock layer from moisture and loss of integrity.

### **3.6.1 Surface Layer Options**

The two choices for the surface layer are BSTs and AC. Although AC is stronger than BSTs, BSTs have several advantages for use in granular overlays. First, since the major means of failure of a thin surface over a crushed rock layer is bending (Freeme [4]), a more flexible layer works better. Also since the crushed rock layer already adds strength to the pavement, it is not essential that the surface layer add substantial strength as well. It has been shown that thicker, stiffer surface layers reduce the bulk stresses in the granular layer with a corresponding reduction in stiffness. Finally since BSTs are less expensive and require less equipment, they are more appropriate for the type of roads that receive granular overlays. In instances where a granular overlay is used on a road with traffic levels that are higher than is acceptable for BSTs, an AC surface is required.

### **3.6.2 Improvement in BST Construction**

A recent study by WSDOT examined the effects that construction practices have on the problems associated with BSTs (Jackson et al. [10]). The main problems that were investigated included flushing of excess asphalt, windshield damage due to loose rock, and aggregate loss due to poor embedment. Through a review of the use of BSTs in other western states and an examination of BST construction projects, a series of design and construction guidelines were developed.

The guidelines stressed different methods for assuring that the chips were 50 to 70 percent embedded in the asphalt binder. These techniques included using the minimum amount of chips and emulsion possible, requiring that the chips be applied within one minute after the asphalt emulsion has been applied and using choke stones and fog seals. These guidelines led to a significant reduction in the problems of aggregate loss and windshield damage.

The study also recommended several guidelines for the proper choice of roads to be overlain with BSTs. The report suggested that the BST be applied only to roads that are not considered high risk from a traffic standpoint. The high risk roads were those with average daily traffic (ADT) counts in excess of 5,000. If a BST surface is used on granular overlays, these same limitations hold. (WSDOT mostly requires BSTs on routes with ADTs of 2,000 or less and discourages the use of BSTs on routes with ADTs of 5,000 or more.)

### **3.7 EXISTING PAVEMENT**

Although granular overlays are good at reducing the rate of reflective cracking, they are also sensitive to moisture infiltration through breaks in the existing pavement surface. As mentioned in Section 3.4.2, infiltration of moisture lowers the stress-sensitivity of the crushed rock layer.

To circumvent the problem of an inconsistent base for the overlay, the highway department in Zimbabwe rips and spreads the existing base and shoulder then stabilizes with two percent cement or lime (if required) and recompacts it. In this manner the granular overlay is assured of having a solid base (Mitchell [19]). Normally all that would be required is to patch any holes and seal any cracks in the existing pavement surface.

### **3.8 OTHER ADVANTAGES AND LIMITATIONS**

#### **3.8.1 Insulation**

An advantage of the granular overlay is that it protects the existing pavement from the daily extremes in temperature. This is important during hot summer months and in tropical countries where pavement surface temperatures can approach and exceed 160°F (70°C) (Mitchell [19]). Since the stiffness of the pavement is directly proportional to the temperature, the hotter the pavement is, the less stiff it is. The reduced stiffness increases the potential for rutting and leads to early pavement failure. However, the crushed rock layer is unaffected, thus providing a relatively stiff layer.

#### **3.8.2 Increased Frost Resistance**

Frost heaves and thaw weakening can cause significant problems in areas with seasonal freezing weather. Frost heaving is caused by ice crystallization within the larger soil voids and usually a subsequent extension to form continuous ice lenses, layers, veins, or other ice masses. Thaw weakening is the result of melting snow and/or ice lenses infiltrating the pavement and leaving the entire structure saturated until it can drain (Irick [8]). Although there are several methods for preventing or reducing these problems, including sealing the pavement and removing soils that are frost-heave susceptible, one common method is to build thicker pavements.

Since the frost heave and thaw weakening problems are often a result of the subgrade freezing, if the subgrade is insulated from the cold then these problems are reduced. Several states including Alaska, Iowa, Oregon and Washington use frost protection in their pavement thickness design calculations (Rutherford et al. [25]). Most of these states design the pavement thickness to be at least 50 percent of the total expected frost depth. In this manner the subgrade is at least partially insulated against frost.

In Washington State, designing the overall pavement depth to be equal to 50 percent of the total frost depth has worked well for controlling all but the most severe frost problems (Mahoney et al. [13]). Unfortunately, many of the state's low volume rural

roads were built in the 1950s before this design procedure was adopted. These roads frequently consist of only a thin BST over 6 to 9 in. (150 to 225 mm) of base course when the frost design thicknesses are 15 to 24 in. (380 to 610 mm). Rehabilitating these roads typically consists of adding a granular overlay with a minimum of 4.2 in. (107 mm) of crushed rock.

In order to prevent the crushed rock layer from contributing to frost heave, it may be necessary to limit the amount of material passing the No. 200 sieve (0.075 mm). Researchers have observed that the fines content of soils is an important indicator of frost-susceptible soils (Irick [8]). Specifications from the different pavement design agencies surveyed specified the maximum percentage passing the No. 200 sieve to be 5 to 15 percent. The lower range of this specification is lower than the range suggested by Horak et al. [7] for obtaining the maximum compaction (Section 3.4.4).

### **3.8.3 Change in Road Geometry**

By adding 3 to 6 in. (75 to 150 mm) to the overall pavement structure, the granular overlay can alter the road geometry. It can be used to increase drainage, improve the road profile and to level off inconsistencies in the pavement. This additional height makes it unusable in areas where the road geometry is restricted by curb height or other considerations.

### **3.8.4 Resistance to Shear**

Little information could be found concerning the ability of confined crushed rock layers to resist shear. However, this is a potential problem. Although granular materials are very strong in compression, they have little resistance to tension. When subjected to a high confining pressure, the crushed rock particles can distort, be crushed, shift, roll or slide. The amount of movement caused by any of these actions is directly proportional to the confining pressure. If the shear stress becomes sufficiently large, the combined movement from these actions will result in a shear failure (Sowers [28]). No calculations were found as to the effective shear stress at failure.

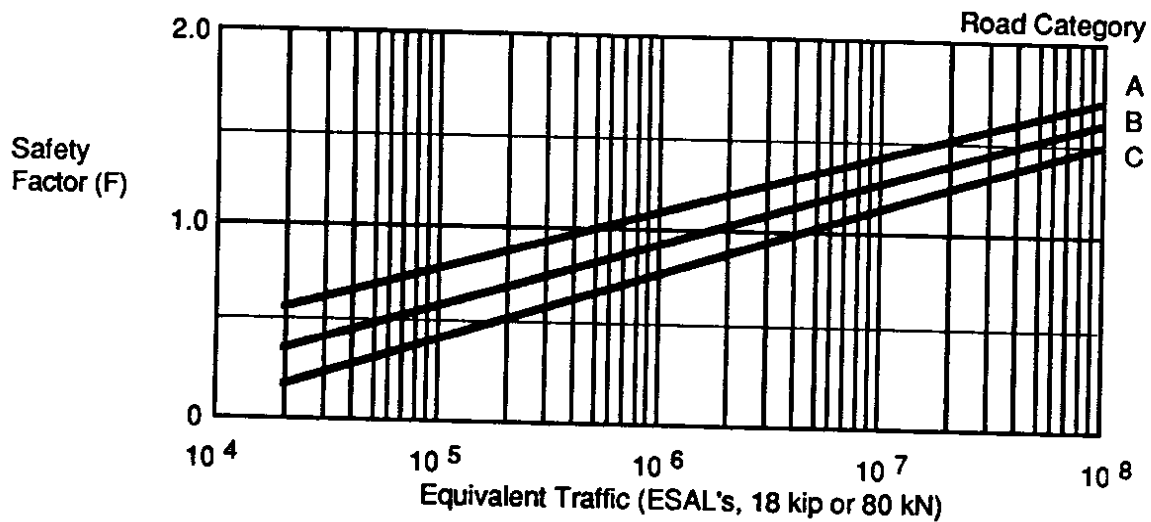


Figure 3.17. Safety Factors for Shear Stress (after Freeme et al. [4])

Table 3.14. Typical Granular Material Shear Properties (after Freeme et al. [4])

Material	Degree of Saturation	Cohesion (C)		Internal Friction (°)
		psi	kPa	
High Density Crushed Stone	45	9.4	65	55
	90	6.5	45	55
Moderate Density Crushed Stone	45	8.0	55	52
	90	5.8	40	52
Crushed Stone and Soil Binder	45	7.2	50	50
	90	5.1	35	50
Gravel, Base Quality	45	6.5	45	48
	90	5.1	35	48
Gravel, Subbase Quality	Moderate	5.8	40	43
Gravel, Low Subbase Quality	Moderate	4.4	30	40

Freeme et al. [4] provided typical shear properties for a range of granular materials used in South Africa (Table 3.14). These properties (cohesion and the angle of internal friction) are shown for two levels of saturation — 45 percent for dry to moderate regions and 90 percent for wet regions. The shear strength can be calculated by use of Coulomb's equation (after Bowles [34] and Terzaghi and Peck [35]):

$$\text{Shear Strength (s)} = c + \sigma_n \tan \phi \quad (\text{Equation 3.5})$$

where

- $c$  = cohesion (psi or kPa)
- $\phi$  = angle of internal friction
- $\sigma_n$  = normal stress  
 $= \frac{\sigma_1 + \sigma_3}{2} + \frac{\sigma_1 - \sigma_3}{2} \cos 2\theta$
- $2\theta$  =  $90^\circ + \phi$
- $\sigma_1, \sigma_3$  = principal stresses (psi or kPa)

For example, use of  $\sigma_1 \approx 50$  psi (345 kPa) results in a shear strength of about 16 psi (110 kPa) for the high density crushed stone at the 45 percent saturation level.

Freeme et al. [4] further discussed how to safeguard against shear failure (or excessive gradial shear deformation). This is done by limiting the shear stresses by the following formula:

$$\text{Safety Factor} = F = \frac{\text{Maximum Safe Shear Stress}}{\text{Working Shear Stress}} \quad (\text{Equation 3.6})$$

Further, Freeme recommended that the safety factors be calculated at the mid-length of the layer at two points:

1. directly under the wheel, and
2. at the center of the dual wheel.

The limiting safety factors vary according to expected traffic loads (refer to Figure 3.17).

The road categories shown in Figure 3.17 are:

**Road  
Category**

- A Interurban freeways, major interurban roads (3 to 50 million ESALs)
- B Interurban collectors, major rural roads (0.2 to 12 million ESALs)
- C Lightly trafficked rural roads (less than 3 million ESALs)

In Chapter 6, estimated shear stresses will be shown.

To limit the problem of shear, granular overlays should not be used in areas where shear forces will be high. Areas where the granular overlay may be commonly subjected to non-vertical stresses are on steep curves and grades and at stopping locations. In the first instance, centrifugal force pulls a vehicle across the pavement. In the other two instances, a vehicle's braking force (downhill) or drive torque (uphill) induces a horizontal shear force into the pavement. To avoid potential problems, granular overlays should not be used in situations where shear forces like these are likely to be high.

**3.9 DESIGN OF GRANULAR OVERLAYS**

There are two basic techniques in designing granular overlays. One is based on mechanistic calculations. The studies done by Sibal [26] and Deoja [3] are such examples. Another technique is based on practical construction considerations.

**3.9.1 Mechanistic Design**

Mechanistic design is based on designing the appropriate thickness of crushed rock to provide the necessary strength to ensure the desired life for the overlay. Designing an overlay with the mechanistic approach is similar to designing an AC overlay. Since there has been much research done on determining the appropriate thicknesses of AC for different road conditions, one approach to designing granular overlays is to design an AC overlay and determine the equivalent thickness for a granular overlay. These equivalency factors were investigated by Sibal [26] (Section 3.3).

### **3.9.2 One Thickness Approach**

The second design approach is to use the maximum thickness of granular material that can be easily compacted in one lift. This suggestion was made in the report by Maree et al. [17] (Section 3.4.2) in which the authors found that a crushed rock layer of 12.6 in. (320 mm) did not perform significantly better than one of 5.5 in. (140 mm) thick (both crushed rock layers were on cement stabilized subbases). Maree concluded that the crushed rock layer need not exceed the maximum thickness that can be placed and compacted in one lift (6 in. (150 mm)).

A study done by Otte and Monismith [23] resulted in similar conclusions. They used a layer elastic program, PSAD2A, to model the behavior of several different inverted pavement structures. The computations were made for a 9.0 kip (40 kN) dual wheels, 13.0 in. (330 mm) apart. The pavement that was simulated was an inverted pavement with a 1.4 in. (35 mm) BST surface. The thicknesses of the crushed rock layer and the cement stabilized base and subbase were varied over a wide range of thicknesses.

The authors found that the primary stresses in an inverted pavement were on the surface course and cement stabilized layers. They found that because of stress-stiffening, as the thickness of the crushed rock layer increased from 5 to 20 in. (125 to 500 mm), the equivalent elastic modulus of the granular base declined about 30 percent. Otte and Monismith [23] recommended the following:

1. The bituminous surfacing for "inverted" pavement designs should not exceed 1.2 to 1.4 in. (30 to 35 mm).
2. For typical highway traffic loads, the granular layer should have a thickness of about 5.0 to 6.0 in. (125 to 150 mm).
3. The cement stabilized layers supporting the granular layer should be:
  - a. Two layers each 6 in. (150 mm) thick if subgrade has a CBR = 15 or better.
  - b. One layer 6 in. (150 mm) thick for light traffic (rural).



The one thickness approach is also used in Zimbabwe (Mitchell [19]). The highway department in Zimbabwe has found that the practical range for the construction of the crushed rock layer in an overlay is 5 to 6 in. (120 to 150 mm). Thinner layers tend to shear under a roller. If a thicker layer is needed, then the road probably needs to be reconstructed.

In Washington state, granular overlays are generally built with thicknesses of 3 to 6 in. (most with a 4.2 in. (107 mm) thickness).

### **3.10 OVERLAY COSTS**

Two sources of data were used in comparing overlay costs, Means construction data and WSDOT estimates. The Means [18] data is intended to provide a national average while the WSDOT data is specific to Washington State.

The Means price for both the crushed rock and the surfacing include the cost of hauling the material less than 30 miles (48 km), placing and compacting the material and overhead and profit. The material for the crushed rock material is the material listed as pavement base and no information is given as to the quality of the material or the amount of compaction.

In Table 3.15, the cost of constructing BST and AC surfacings are listed. The price of the AC layer is based on approximately 1000 tons of AC per mile of 32 ft wide road. Although these prices are the prices for a new surface, they are assumed to be representative of the cost of overlays and surfacings for granular overlays.

The price for constructing the crushed rock layer are listed in Table 3.16. Although these are prices for a pavement base, they are assumed to be representative of the cost of the crushed rock layer in the granular overlay. The values for the 4.0 and 5.0 in. (100 and 125 mm) thickness are extrapolated from the prices provided for the 3.0 and 6.0 in. (75 and 150 mm) thicknesses.

Table 3.15. Material and Construction Costs for AC and BST Wearing Course Surfaces Based on Means Construction Data (1989). Costs Reflect Haul Distances of 30 Miles or Less

Surface	Thickness		Means (1989)	
	in.	mm	\$/yd <sup>2</sup>	\$/m <sup>2</sup>
BST	Double Layer		1.63	1.95
AC	1	25	2.16	2.58
AC	1.5	38	3.20	3.83
AC	2	50	4.19	5.01
AC	2.5	64	5.15	6.16
AC	3.0	75	6.15	7.36

Table 3.16. Material and Construction Costs for Pavement Base Courses with a Maximum Aggregate Size of 3/4 in. (19 mm) Based on Means Construction Data [18]

Layer Thickness		Cost	
in.	mm	\$/yd <sup>2</sup>	\$/m <sup>2</sup>
3.0	75	2.84	3.40
4.0	100	3.59	4.29
5.0	125	4.35	5.20
6.0	150	5.10	6.10

Table 3.17. Comparison of Costs for AC Overlays and Granular Overlays with BST Surfacing Based upon an Equivalency Factor of 2.0

AC Thickness		Cost of AC		Equivalent C.R. Thickness		Cost of GO with BST Surface	
in.	mm	sy	m <sup>2</sup>	in.	mm	sy	m <sup>2</sup>
1.5	38	\$3.20	3.83	3.0	75	\$4.47	5.35
2.0	50	\$4.19	5.01	4.0	100	\$5.22	6.24
3.0	75	\$6.15	7.36	6.0	150	\$6.73	8.05

Finally the price of an AC overlay is compared with the price of an equivalent granular overlay with a BST surface (Table 3.17). The comparison is made by using an Equivalency Factor of 2.0. In comparing the costs listed in Table 3.17, it appears that granular overlays are more expensive than the equivalent thickness of AC. The difference in price is greater for the thinner AC layers but never decreases to less than 10 percent. Since it is more expensive to transport AC than crushed rock, the price for the granular overlay may be more competitive if hauling distances are longer than 30 miles (48 km).

Next the information from the WSDOT price estimates was examined. It was decided that WSDOT's estimate should be used rather than the actual contractor's bid to avoid problems with front-end loading and other bid modifications. The information shown came from seven granular overlay construction projects built since 1985.

In Table 3.18, the costs for the AC and BST surfacings are listed. The prices for the AC and BST layers are the prices for the surfacing on the granular overlay but are also considered to be accurate for the price of a normal overlay. These prices include the cost of preparing the surface, placing a tack coat, laying the surface and applying any other treatments or materials that were used (e.g., additives such as anti-strip and treatments such as fog seals).

In each of the estimates, the cost of the AC surfacing material is \$21 to \$22 per ton (\$23 to \$24 per metric ton) as illustrated in Table 3.19. The AC surfacings for SR281 and SR261, based on the WSDOT estimate, are 6 and 33 percent lower than the costs for the equivalent AC thickness based on the Means data; however, when adjusted for inflation these differences are minor. The prices for the BSTs are quite similar when adjusted for inflation. The "typical" price (SR24) for WSDOT double shot BST is \$1.22 as compared to the price of \$1.63 for Means. (Additional details about the WSDOT BST's are shown in Table 3.20.)

The cost of the crushed rock layer was determined from the same estimates used for the surface layer thicknesses and are shown in Table 3.21. This price is the line item price

Table 3.18. WSDOT Construction Costs for AC and BST Surfaces on Granular Overlays

Route No.	Year	Length		Thickness		Surfacing Material	Total Cost <sup>1</sup>	Cost <sup>2</sup>	
		miles	km	in.	mm			\$/yd <sup>2</sup>	\$/m <sup>2</sup>
281	1985	11.34	18.24	2.4	61.0	AC	\$986,880	4.64	\$5.55
261	1987	8.20	13.19	2.4	61.0	AC	508,000	3.30	3.95
231	1985	8.64	13.90	0.7	17.8	BST	213,960	1.32	1.58
24	1986	13.62	21.91	0.7	17.8	BST	312,900	1.22	1.46
25	1987	14.60	23.49	0.7	17.8	BST	359,880	1.31	1.57
155	1989	12.96	20.85	1.1	27.9	BST	373,280	1.53	1.83
20	1989	7.95	12.79	1.1	27.9	BST	301,375	2.00	2.39

<sup>1</sup> Includes AC mix, prime coat, anti-strip, etc.

<sup>2</sup> Cost per unit area based on assumption of road and shoulder width of 32 ft. (9.8 m)

Table 3.19. Quantity and Costs of AC Estimated for the AC Surface Granular Overlays (Based on WSDOT Estimates)

Route No.	Length		AC Quantity*		AC Unit Cost	
	miles	km	ton	metric ton	\$/ton	\$/metric ton
281	11.34	18.25	42,460	38,600	20.80	22.90
261	8.20	13.19	20,500	18,600	22.00	24.20

\*WSDOT Class B asphalt concrete

Table 3.20. Bituminous Surface Treatment Details Which Influence Costs

Route No.	Year Constructed	Type of BST	Aggregate	
			Layer	Gradation
231	1985	Single	First	1/2" - 1/4"
			Choke Stone	1/4" - 0
24	1986	Double	First	1/2" - 1/4"
			Second	3/8" - No. 10
25	1987	Single	First	1/2" - 1/4"
			Choke Stone	1/4" - 0
155	1989	Triple	First	3/4" - 1/2"
			Second	1/2" - 1/4"
			Third	3/8" - No. 10
			Choke Stone	1/4" - 0
20	1989	Triple	First	3/4" - 1/2"
			Second	1/2" - 1/4"
			Third	3/8" - No. 10
			Choke Stone	1/4" - 0

Table 3.2.1 Quantities and Costs of Crushed Rock Layer in Granular Overlays  
(Based on WSDOT Estimates)

Route No. 1	Length		Crushed Rock Quantity		Crushed Rock Unit Price		Typical Thickness		Total Costs <sup>2</sup>	Cost/Unit Area	
	miles	km	ton	metric ton	\$/ton	\$/metric ton	in.	mm		\$/sy	\$/m <sup>2</sup>
281 (CSTC)	11.34	18.25	128,450	116,770	4.80	5.28	3.0	75	616,560	2.90	3.45
261 (CSBC)	8.20	13.19	74,200	67,450	4.75	5.22	3.0	75	352,450	2.29	2.73
231 (CSTC)	8.64	13.90	62,720	57,020	5.00	5.50	4.2	105	313,625	1.93	2.30
24 (CSTC)	13.62	21.91	78,200	71,090	4.25	4.68	3.6	90	332,350	1.30	1.55
25 (CSTC)	14.60	23.49	125,000	113,640	4.80	5.28	6.0	150	600,000	2.19	2.61
155 (CSTC)	12.96	20.85	83,120	75,560	4.50	4.95	3.6	90	374,040	1.54	1.83
20 (CSTC)	7.95	12.79	59,260	53,870	5.25	5.78	4.2	105	311,115	2.08	2.48

1 CSTC: Crushed Surfacing Top Course (5/8" max. aggr.)

CSBC: Crushed Surfacing Base Course (1 1/4" max. aggr.)

2 Includes costs of material, hauling, compaction

for the crushed surfacing top course and includes the cost of hauling and compacting the material. The unit price of crushed surfacing top course varied from \$4.25 to \$5.25 per ton (\$4.68 to \$5.78 per metric ton).

The price of the crushed rock layer from the WSDOT estimates ranges from having good agreement with Means to substantially lower. The differences are mostly due to variable thickness (within project) and lower crushed rock costs.

When the price of the surfacing is combined with the cost of the crushed rock layer, the total construction cost of the granular overlay is obtained. These costs are listed in Table 3.22 and are shown in Figure 3.18.

Although the costs vary considerably, several trends are clear. In every case where an AC surface was used, the AC surface represented about 60 percent of the total costs. The cost of a BST surface represented 40 to 50 percent.

A straightforward comparison of the cost of a "traditional" AC overlay to an "equivalent" BST surfaced granular overlay is as follows:

1. Assume 2.4 in. conventional AC overlay.
2. Assume EF = 2.0 for converting AC to crushed rock.
3. Granular Overlay = (2.4 in) x (2) = 4.8 in.
4. Assume crushed rock in granular overlay will receive 0.7 in. BST surface.
5. Assume density of AC  $\approx$  145 lb/ft<sup>3</sup>

Assume density of Crushed Rock  $\approx$  135 lb/ft<sup>3</sup>

Assume AC at \$22/ton

Assume crushed rock at \$5/ton

Assume BST at \$1.30/square yard

Then

AC overlay  $\approx$  \$2.87/yd<sup>2</sup>

Granular overlay (with BST)  $\approx$  \$2.52/yd<sup>2</sup>

6. Thus, AC overlay is about 12 percent more expensive.

Table 3.22. Summary of Total Construction Cost of Granular Overlays Based on WSDOT Projects

Route No.	Year Constructed	Length		Type	Surface Course		Crushed Rock Thickness		Total Costs	
		miles	km		Thickness	Thickness	in.	mm	\$/sy	\$/m <sup>2</sup>
281	1985	11.34	18.25	AC	in.	mm	in.	mm	\$/sy	\$/m <sup>2</sup>
					2.4	60	3.0	75	7.54	8.97
261	1987	8.20	13.19	AC	2.4	60	3.0	75	5.59	6.65
231	1985	8.64	13.90	BST	0.7	18	4.2	105	3.25	3.87
24	1986	13.62	21.91	BST	0.7	18	3.6	90	2.52	3.00
25	1987	14.60	23.49	BST	0.7	18	6.0	150	3.50	4.16
155	1989	12.96	20.85	BST	1.1	28	3.6	90	3.07	3.65
20	1989	7.95	12.79	BST	1.1	28	4.2	105	4.08	4.49

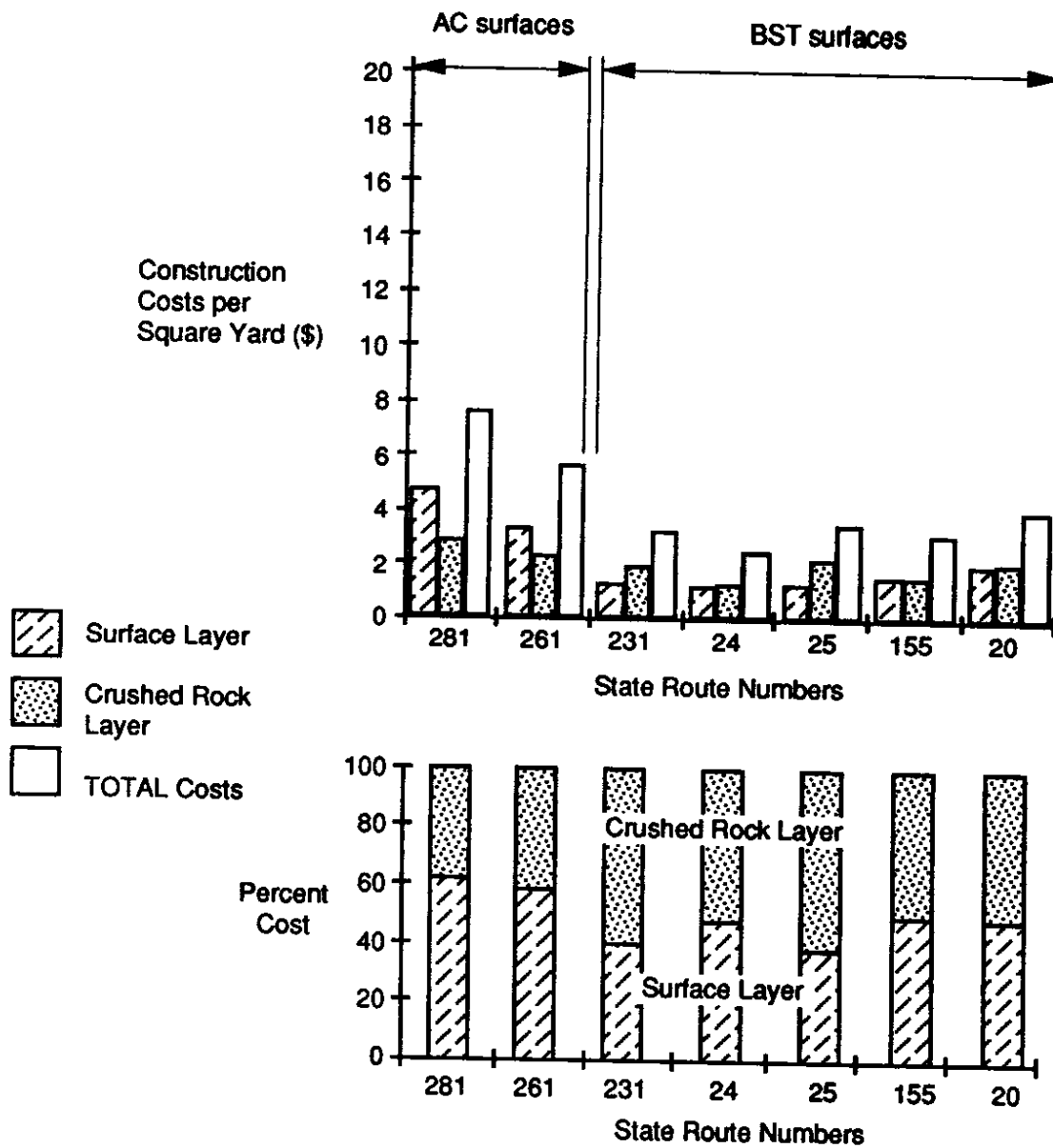


Figure 3.18. Comparison of the Cost of the Different Layers in a Granular Overlay Based on WSDOT Cost Estimates



If a straightforward comparison of the seven projects summarized in Table 3.22 is made, then AC granular overlays (at \$6.56/yd<sup>2</sup>) are twice as expensive as the BST granular overlays (at \$3.28/yd<sup>2</sup>). Further, the bottomline costs are more skewed toward the granular overlays (either surfacing) when the quantities of leveling course materials are compared. It is much cheaper to levelup with crushed rock than AC. It is not uncommon to see levelup quantities constituting 25 to 50 percent of the total crushed rock quantity.



## CHAPTER 4

### SURVIVAL LIVES AND PERFORMANCE PERIODS

#### 4.1 INTRODUCTION

The survival life of a pavement is the amount of time between a pavement's construction and its resurfacing. The performance period is the amount of time from initial construction to the time it reaches a minimally acceptable level. Both survival lives and performance periods provide valuable estimates of pavement "life." In this portion of the report, the survival lives and performance periods of AC overlays, BST resurfacings and granular overlays are estimated and compared.

This part of the study considered only the ages of the different types of surfaces. Other factors, such as traffic loadings, weather conditions, and soil support, affect the amount of time that a pavement lasts but these were not considered. Since the study was conducted within a small geographic area, the weather and subgrade effects were assumed to be constant for all roads. The effects of higher traffic loadings were expected to be somewhat cancelled by the thickness of the resurfacing.

An important point to be noted was the difference in characteristics of the roads overlain by the different techniques. In general, roads with AC surfaces had higher traffic counts than roads with BST surfaces. Additionally, granular overlays were often used as a method for repairing badly distressed roads. Most roads that received a granular overlay had either thermal cracking or roughness problems and therefore required special treatment.

Two methods for calculating the life of the pavement were used: survival time and performance period. Each technique had its own advantages and disadvantages, but taken together they provided a reasonable overall picture of how long the resurfacings can last.

The survival time is defined as the amount of time between the construction of the overlay and its subsequent resurfacing. Since this method measures the amount of time that resurfacing is used rather than the amount of time until it deteriorates to a minimally

acceptable level, it does not necessarily reflect the true performance of the resurfacing. Ideally, a road receives resurfacing as soon as it reaches a minimally acceptable condition. However, this is frequently not the case. Other factors such as the available budget, maintenance schedules, and other considerations also affect the timing of resurfacing. An advantage to this method is that it was relatively easy to obtain data. Since only the resurfacing construction dates were required, it was possible to use construction data dating back to the WSDOT's earliest records that are contained in the WSPMS. However, the use of the early records did provide some problems. Many of the resurfacings from the 1940s showed survival lives that were two to three times greater than the average. These findings may have been a reflection of the prevailing economic conditions of this period, the result of incomplete records, or reality. These early data points were included in all summaries; however, they did not significantly alter the overall averages.

The second method of calculating the life of the resurfacing involved analyzing the rate at which a pavement deteriorated and using this to predict at what point it will need to be resurfaced (or reconstructed). In effect, the deterioration curves similar to Figure 3.1 were examined for each road section, and the amount of time necessary to reach the minimally acceptable condition was calculated. The performance period calculation, therefore, avoided the problem of other factors influencing useable life times. The disadvantage was that it was difficult to obtain information on the actual deterioration of the different types of pavements. Because of this constraint, only a small number of data were available.

In comparing the results of the survival time and the performance periods, it is important to remember that the sets of data did not come from the same time period. Since the performance life equations were only calculated for the present road surface, they represented only resurfacings built since the late 1970s. The data for calculating the survival lives, on the other hand, were equally spread from the 1980s to the 1960s, with some dating as far back as the 1940s. Because of the problems previously mentioned with

the "old" survival life data, the old information tended to increase the average survival life slightly.

#### **4.2 SOURCE OF DATA**

The source of data for this analysis was the WSDOT Pavement Management System (WSPMS) [32]. WSPMS contains records of work done on the roads and the pavement condition analyses. Data from WSPMS were spot checked against as-built plans and pavement conditions and were found to be accurate.

The data on the construction projects included the construction date, the type of layer (AC, BST, crushed rock, etc.) and the layer thicknesses. An example of this information is listed in Table 4.1. Therefore, the list of layers represented a historical record of the work done on that pavement section. By subtracting the consecutive years of work from the previous years, it was possible to determine how long each layer lasted until being resurfaced. These survival times were then grouped together with the other survival times for the same type of resurfacing and basic statistics calculated.

**Table 4.1. WSPMS Construction Data for SR 21, Milepost 46.95 to 50.50**  
(The survival lives are calculated for all layers except the original, which is not a resurfacing.)

Year	Contract	Type of Construction	Thickness	Surfacing Type
1984	#012715	Resurfacing	0.04 ft.	BST
1976	#010275	Resurfacing	0.06 ft.	BST
1971	Unknown	Resurfacing	0.06 ft.	BST
1962	Unknown	Resurfacing	0.06 ft.	BST
1955	Unknown	Resurfacing	0.06 ft.	BST
1947	Unknown	New Construction	0.06 ft.	BST
1947		Bases	0.59 ft.	Untreated Base

Survival times:

1984	-	1976	=	8 years
1976	-	1971	=	5 years
1971	-	1962	=	9 years
1962	-	1955	=	8 years

The pavement condition ratings (PCR) were collected from surveys that WSDOT had conducted at least every other year since 1969 (Mahoney and Jackson [14]). The rating was on a scale with a maximum of 100 and an open-ended bottom. Examples of the PCR ratings for pavement sections are shown in Table 4.2. These ratings roughly corresponded to the AASHTO Present Serviceability Index (PSI) with a PCR of 100 corresponding to a PSI of 5.0 and a PCR of 40 corresponding to a PSI of 3.0. The road being analyzed was divided into 1 mile (1.6 km) sections and each section was analyzed separately. The ratings for the sections were then averaged together to give an overall rating for the road.

WSDOT has developed a program entitled Management Information Data Access Linkage (MIDAL) to manipulate the information in WSPMS. This system takes the PCRs for a road section and attempts to develop a pavement performance prediction equation. If there are enough PCRs, the program calculates a regression curve for the data (PCR vs. Age). If the root mean square error (RMSE) (Section 6.3.5) of this curve was high indicating a poor fit of the data, or if the equation did not follow the expected trend, then the program modified the equation to better represent the expected trend. If the pavement surface was too new to have enough points to define a curve, then the program adapted the standard (default) pavement equations to fit the data. Only equations that were based entirely on the actual PCR data and on road segments that were more than 5 years old were used in this analysis (i.e., no default equations were used). Of the over 600 road sections examined, only 67 had useable equations.

In Figure 4.1, the regression equation for a road with a granular overlay built in 1983 is plotted. The predicted performance equation for this road section is:

$$\text{PCR} = 98.4 - 0.682 (\text{Age})^{2.00} \quad (\text{Equation 4.1})$$

where PCR = Pavement Condition Rating

Age = Time (years) since granular overlay placed.

Table 4.2. Typical PCR Survey Data as Reported in WSPMS  
(Data from the 1989 Survey of SR231)

MP 7.06 to 8.06	
Rutting 1/4 to 1/2	Deduct value = 0.0
Alligator Cracking, Spalled, 1-24% Wheel Tracks	Deduct value = 35.0
Raveling Localized, Slight	Deduct value = 0.0
Longitudinal Cracking, less than 1/4", 1-99 per station	Deduct value = 5.0
Transverse, Spalled, 1-4 per station	Deduct value = 15.0
Patching, Blade, Over 25%	Deduct value = 40.0
Segment Rating =	5.0

MP 4.05 to 5.06	
No Rutting	Deduct value = 0.0
Alligator Cracking, Hairline, 1-24% Wheel Tracks	Deduct value = 20.0
Raveling/Flushing-None	Deduct value = 0.0
Longitudinal Cracking, Over 1/4", 1-99 per station	Deduct value = 15.0
Transverse, Spalled, 1-4 per station	Deduct value = 15.0
Patching, Blade, 1-5%	Deduct value = 25.0
Segment Rating =	25.0

MP 5.06 to 6.06	
No Rutting	Deduct value = 0.0
Alligator Cracking-None	Deduct value = 0.0
Raveling/Flushing-None	Deduct value = 0.0
Longitudinal Cracking, Over 1/4", 1-99 ft/station	Deduct value = 15.0
Transverse, Spalled, 1-4 per station	Deduct value = 15.0
Patching, Blade, 6-25%	Deduct value = 30.0
Segment Rating =	40.0

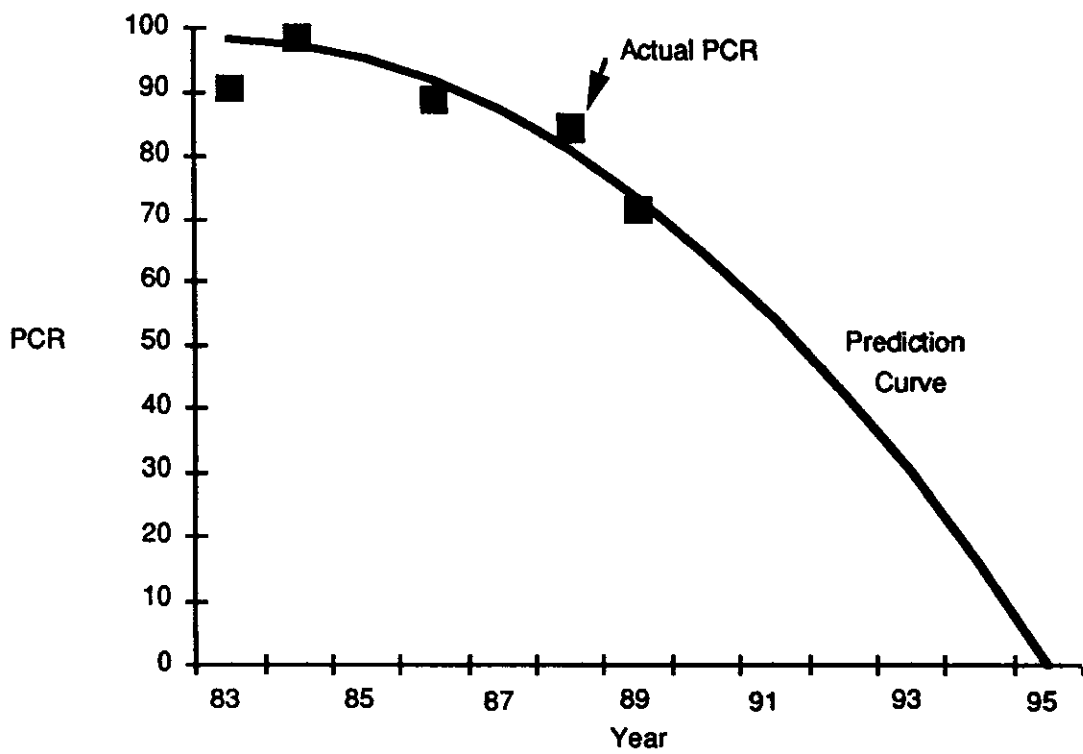


Figure 4.1. Plot of Regression Equation for SR21A Milepost 44.73 to 46.95

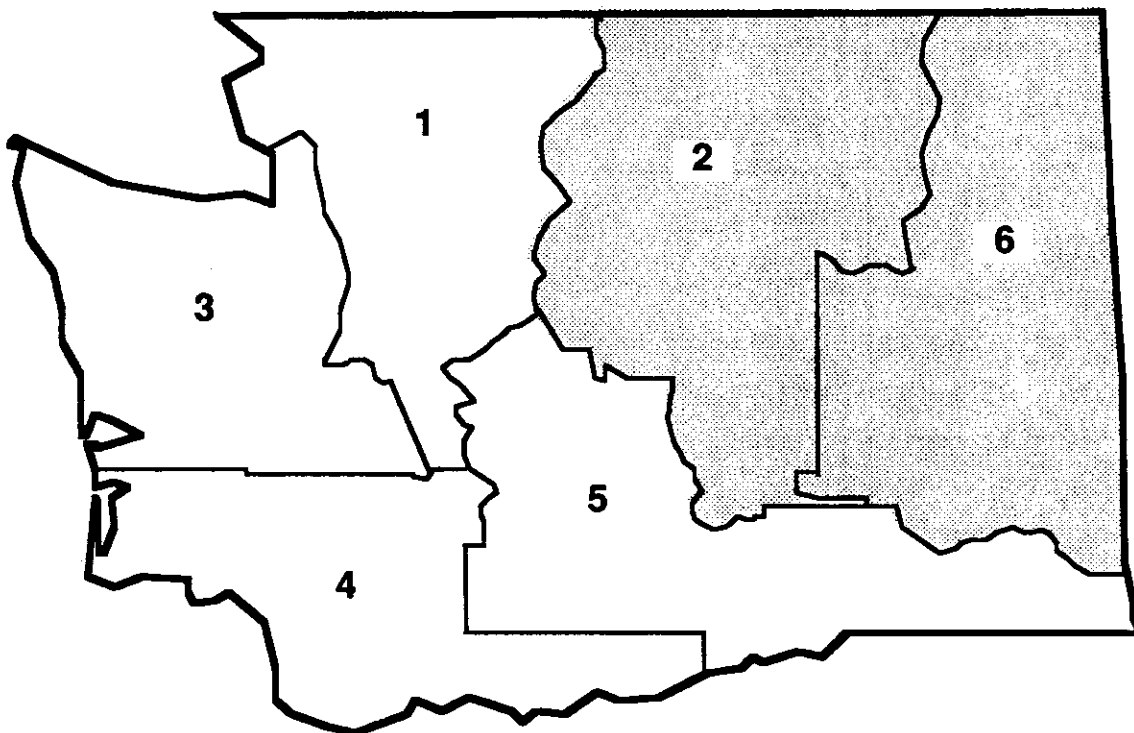


Figure 4.2. Map of the Granular Overlay Study Area and WSDOT District Boundaries



For illustration purposes, the predicted performance periods for the above performance equation and PCR levels are shown in Table 4.3.

The estimation of survival lives and performance periods was restricted to WSDOT Districts 2 and 6 (Figure 4.2). These two districts are generally rural areas where the topography ranges from mountainous to rolling hills. The average annual precipitation is 16.7 in. (424 mm) in Spokane (Hoffman [5]) but the area has severe frost in the winter. These are also the two districts that contained the majority of the roads with granular overlays.

The WSPMS was searched to locate all roads containing BST, AC and granular resurfacings. First, the actual survival time for the different layers of pavement surfaces was calculated by subtracting consecutive resurfacing construction years from the previous years. Next, PCR data on the most recent resurfacing were examined to determine whether the regression equation in the model represented a "true" regression equation. Finally, the survival lives and the performance periods were compared for each type of resurfacing and among the types of resurfacings.

The reader should keep in mind that WSDOT normally uses granular overlays on pavement sections in very poor condition. Thus, general statistics on performance of BST and AC surfacings are not completely fair comparisons to the performance of granular overlays. At any rate, such comparisons will be made since such information was available.

Table 4.3. Performance Periods for SR21A Milepost 44.73 to 46.95

Final PCR	Initial Year	Final Year	Performance Period
40	1983	1992	9 years
20	1983	1994	11 years
0	1983	1995	12 years

### **4.3 BITUMINOUS SURFACE TREATMENTS**

The actual survival time for BST resurfacings is shown in Figure 4.3. The figure is similar to a skewed, normal distribution, with the exception of the peaks at 5, 7, 10 and 13 years. The long tail to the right was the result of special cases. All of the survival lives over 26 years are from resurfacings in the 1930s.

The reader should keep in mind that WSDOT normally uses granular overlays on pavement sections in very poor condition. Thus, general statistics on performance of BST and AC surfacings are likely not fair comparisons to the performance of granular overlays. At any rate, such comparisons will be made since such information was available.

Next, the PCR equations were examined to determine the performance periods. Although over 200 road sections were analyzed, only 21 had useable regression equations. The histogram showing their distribution is shown in Figures 4.4 through 4.6 and the results are summarized in Table 4.4.

The graph for a PCR of 0 has the least uniform distribution of predicted PCRs. Since most data represented points within the first 7 years of a resurfacing's life, predictions of the pavement condition beyond 7 years will contain higher errors than those of under 7 years. These errors should have been symmetric, so that the average results from these predictions should be reasonable.

The differences between the actual survival time and predicted performance periods have already been discussed. If the historical differences are ignored and the other effects are assumed to balance out, then a comparison of the values for the actual survival times and the performance periods reveals that WSDOT resurfaces BST roads when their PCR is between 20 and 0.

### **4.4 ASPHALT CONCRETE OVERLAY**

The actual survival times for AC overlays are shown in Figure 4.7. The figure shows a basically normal distribution. The statistical summary of this data is shown in Table 4.5.

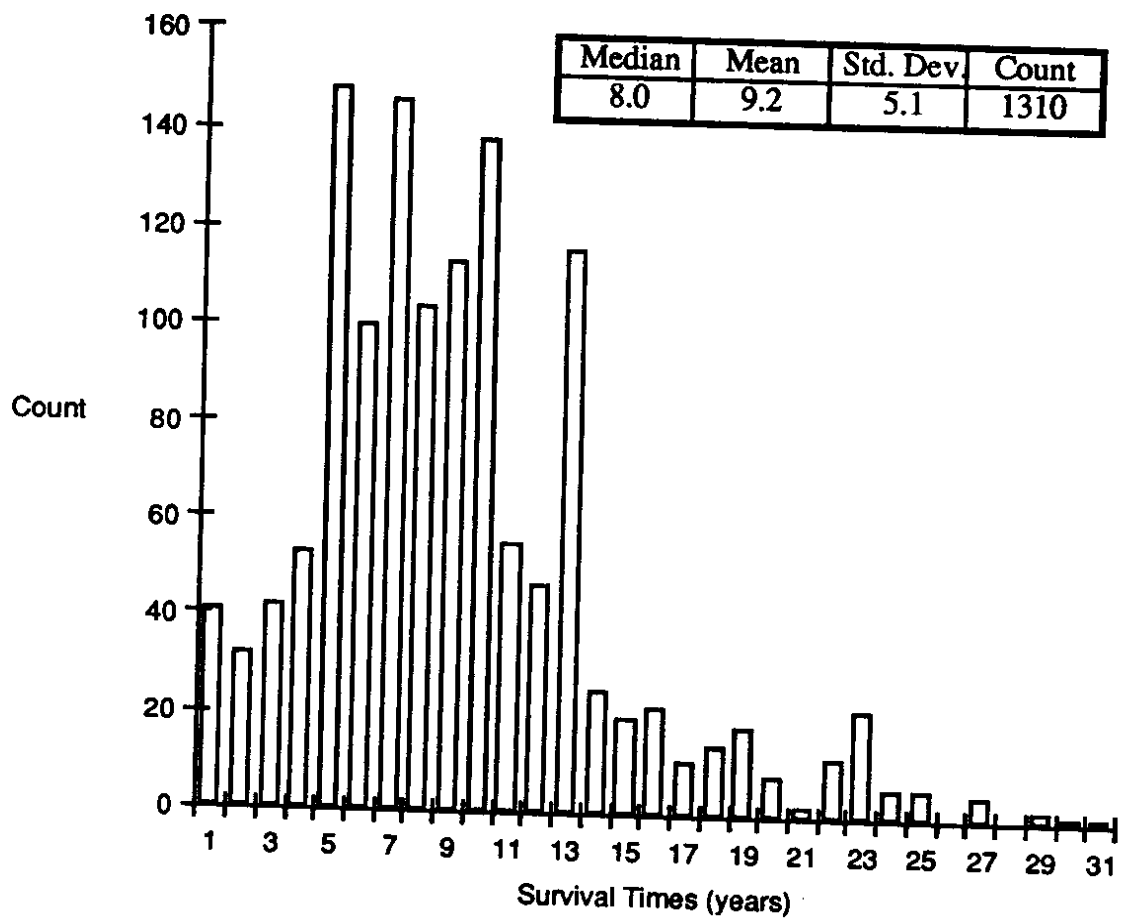


Figure 4.3. Survival Times for BSTs in Districts 2 and 6

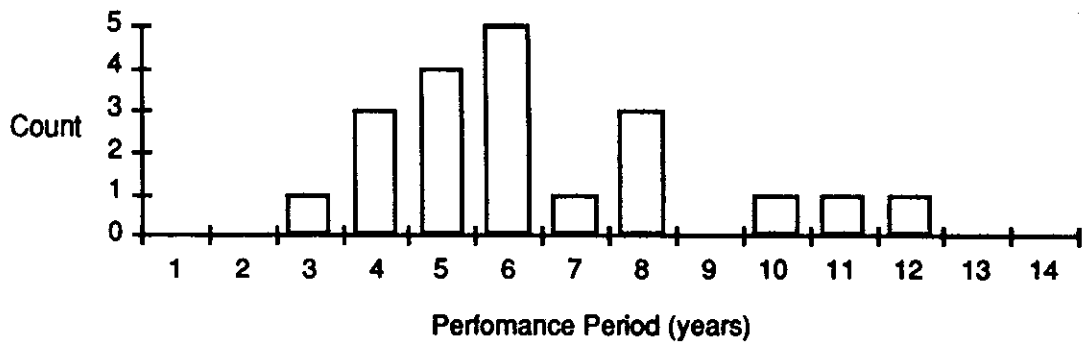


Figure 4.4. The Predicted Amount of Time for BSTs to Reach a PCR of 40, Based on Project Specific Regression Equations

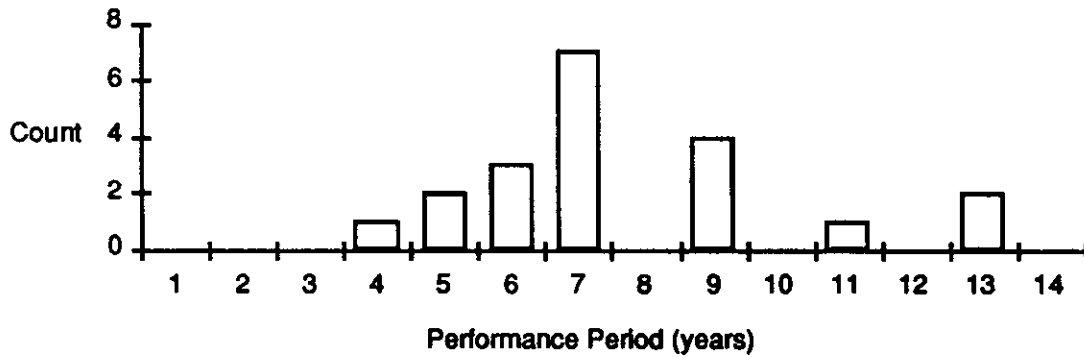


Figure 4.5. The Predicted Amount of Time for BSTs to Reach a PCR of 20, Based on Project Specific Regression Equations

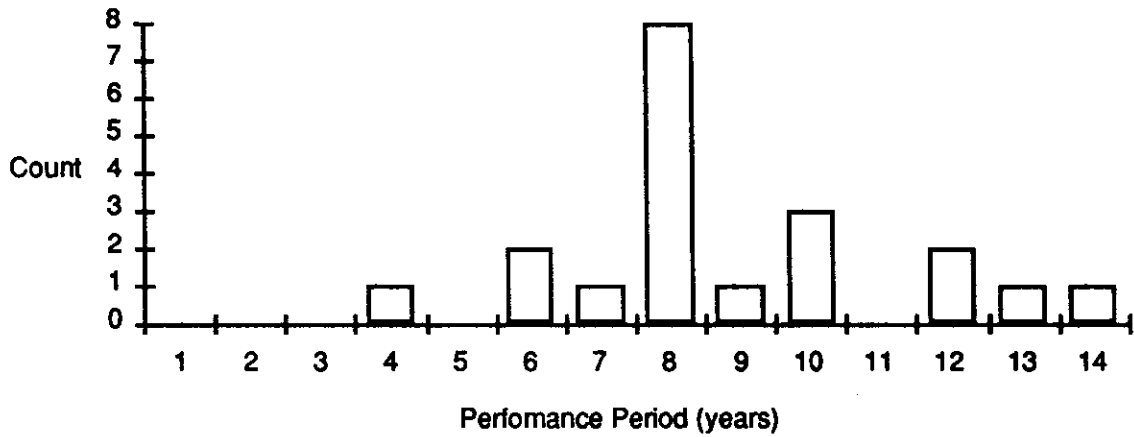


Figure 4.6. The Predicted Amount of Time for BSTs to Reach a PCR of 0, Based on Project Specific Regression Equations

Table 4.4. Basic Statistics for the Performance Periods of BSTs  
(Based on 21 Data Points)

PCR Level	Median	Mean	Std. Dev
PCR 40	6.1	7.0	2.5
PCR 20	7.4	8.2	2.4
PCR 0	8.7	9.3	2.4

Table 4.5. Basic Statistics for the Survival Times of AC Overlays in Districts 2 and 6

AC Thicknesses	Median	Mean	Std. Dev	Count
Overall	10	9.4	4.2	328
< 1.2 in. (30 mm)	8	8.7	2.8	91
> 1.2 in. (30 mm)	10	9.7	4.5	237

Table 4.6. Basic Statistics for the Performance Periods for AC Overlays in Districts 2  
and 6 (Statistics Based on 29 Data Points)

PCR Level	Median	Mean	Std. Dev
PCR 40	10.6	10.2	1.7
PCR 20	11.4	11.3	1.7
PCR 0	12.2	12.1	1.8

The survival times based upon AC overlays with thicknesses of less than 1.2 in. (30 mm) were separated out. According to the 1988 WSDOT specifications, only AC overlays thicker than 1.2 in. (30 mm) are subject to compaction control. It is evident from Figure 4.7 that the values representing the thin overlays represented the majority of the data in the lower range of survival times.

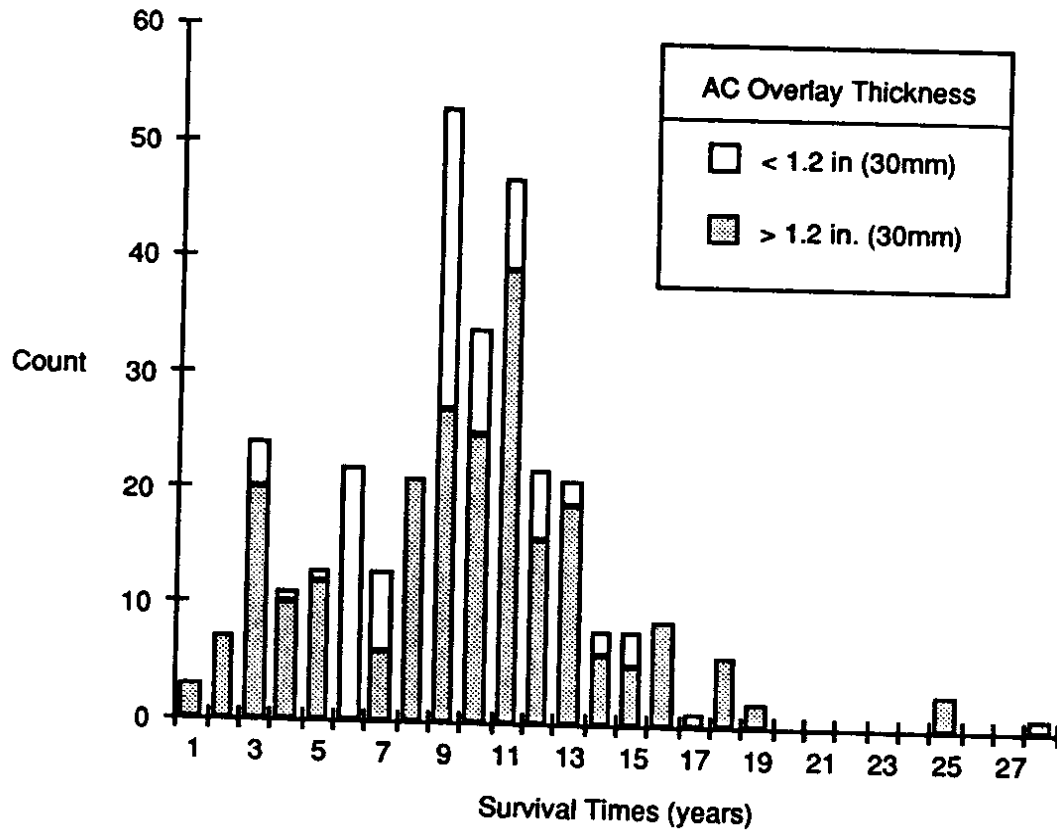
There are also a significant number of survival times of 5 years and less. If only the survival times of AC overlays thicker than 1.2 in. (30 mm) and lasting more than 5 years are considered, the average survival life increased to 11.5 years.

The predicted performance periods are shown in the histograms in Figures 4.8 to 4.10. The data from this analysis is summarized in Table 4.6.

#### **4.5 GRANULAR OVERLAY**

Unlike the other two resurfacings (or overlays) that were examined, there are not a large number of granular overlays on the WSDOT route system. Additionally, since granular overlays have only been used with greater frequency since the mid-1980s, few data are available concerning survival times. Therefore, the authors did not have enough data with which to analyze the actual survival times for granular overlays. This left examining the performance periods. To increase the number of available data, all roads with granular overlays in eastern Washington were examined rather than just Districts 2 and 6. The histograms showing the distribution of performance periods are shown in Figures 4.11 through 4.13 and summarized in Table 4.7.

These three histograms show a marked decrease in normality. This decrease is probably due to the difficulty in projecting far beyond the actual data available for developing the predicted equations. For example, the point at 18 years in Figure 4.13 is the result of a pavement deterioration curve that is a straight line. Since this line begins in 1979, it is accurate for the PCR of 40, but it probably does not necessarily accurately portray the deterioration after 18 years.



Thickness	Median	Mean	Std. Dev.	Count
<1.2"	8	8.7	2.8	91
>1.2"	10	9.7	4.5	237

Figure 4.7. Survival Times for AC Overlays in Districts 2 and 6

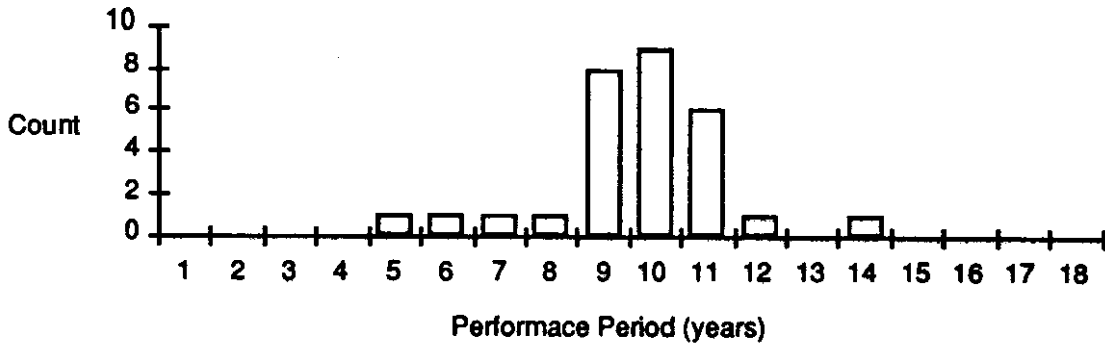


Figure 4.8. Predicted Amount of Time for AC Overlays to Reach a PCR of 40, Based on Project Specific Regression Equations (Districts 2 and 6)

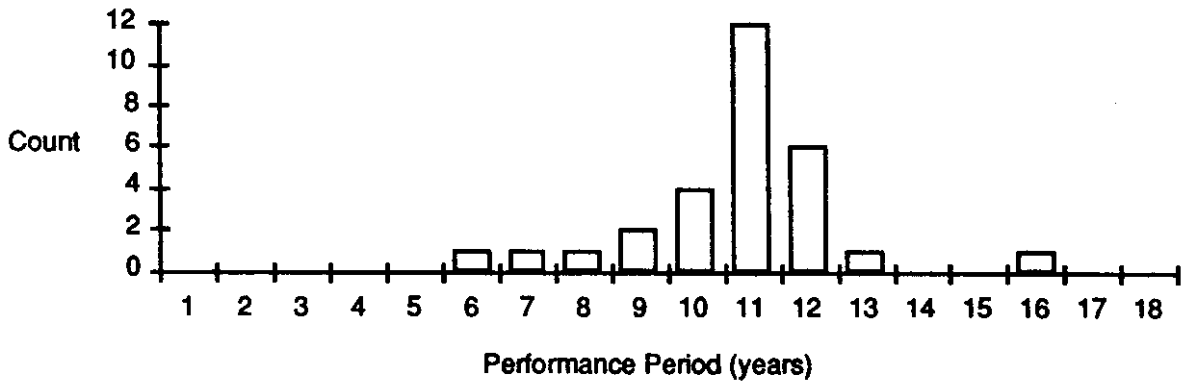


Figure 4.9. Predicted Amount of Time for AC Overlays to Reach a PCR of 20, Based on Project Specific Regression Equations (Districts 2 and 6)

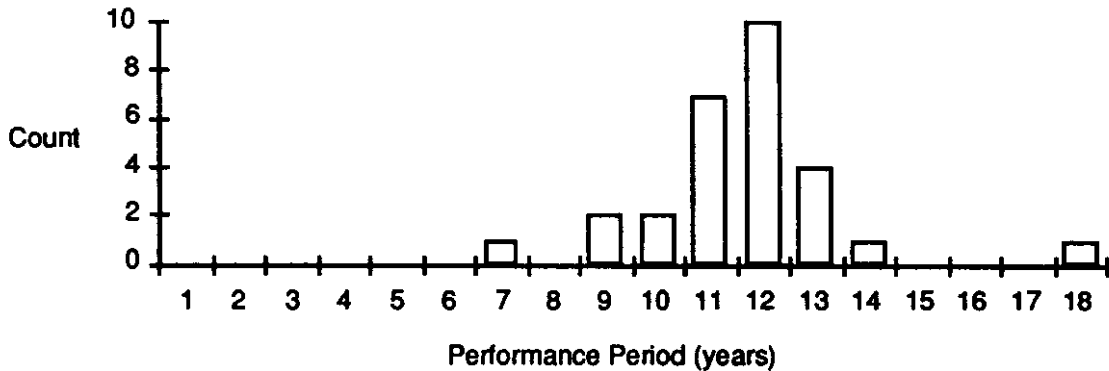


Figure 4.10. Predicted Amount of Time for AC Overlays to Reach a PCR of 0, Based on Project Specific Regression Equations (Districts 2 and 6)



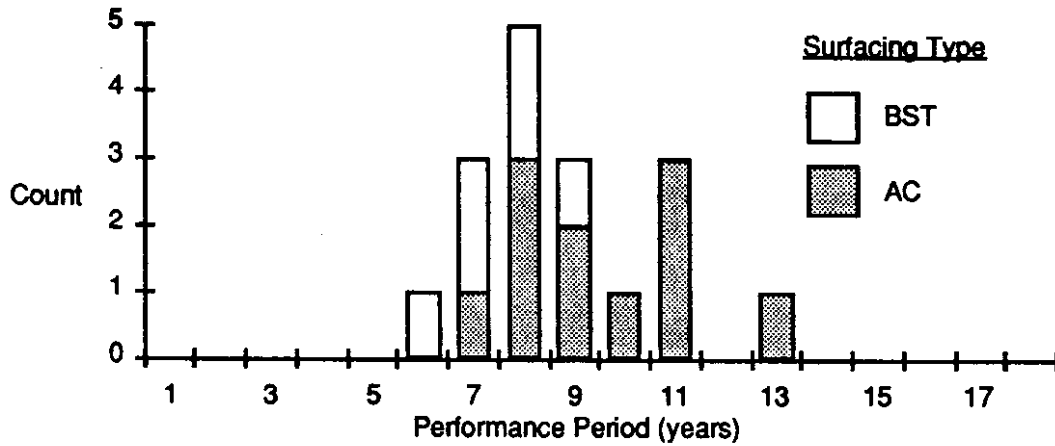


Figure 4.11. The Predicted Amount of Time for Granular Overlays to Reach a PCR of 40, Based on Project Specific Regression Equations

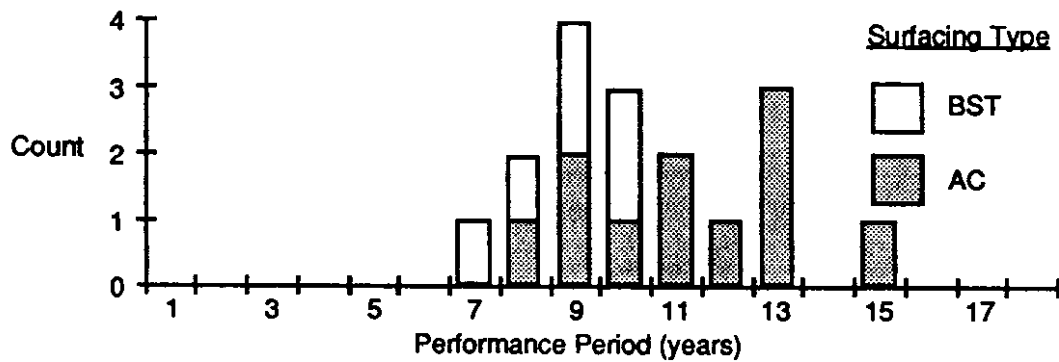


Figure 4.12. The Predicted Amount of Time for Granular Overlays to Reach a PCR of 20, Based on Project Specific Regression Equations

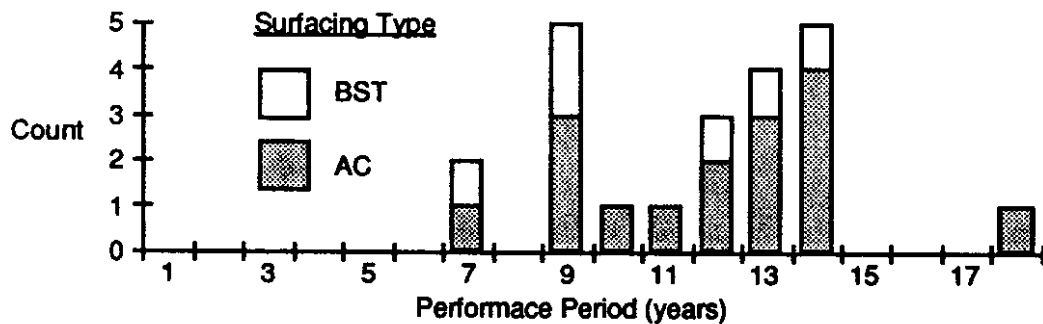


Figure 4.13. The Predicted Amount of Time for Granular Overlays to Reach a PCR of 0, Based on Project Specific Regression Equations

Table 4.7. Basic Statistics for the Performance Periods of Granular Overlays  
(Based on 17 Data Points)

PCR Level	All Surfaces			Only BST Surfaces	Only AC Surfaces
	Median	Mean	Std. Dev	Mean	Mean
PCR 40	8.7	9.2	1.8	7.5	9.5
PCR 20	10.7	10.8	2.1	8.3	11.3
PCR 0	12.0	12.2	2.6	11.0	11.8

Table 4.8. Survival Times and Predicted Performance Periods for the Resurfacings.

Type of Resurfacing	Actual Survival Life	Predicted Performance Period		
		PCR 40	PCR 20	PCR 0
BST Only	8	6.1	7.4	8.7
GO w/BST surface	-	7.5	8.3	11.0
AC Only (> 1.2 in. (30 mm))	10	10.6	11.4	12.2
GO w/AC surface	-	9.5	11.3	11.8

\*GO = Granular Overlay

The granular overlays were separated by their surfacing type (Table 4.7).

#### **4.6 CHAPTER SUMMARY**

Although both methods used for calculating the useable life of the resurfacings has uncertainty, the two methods together provide reasonable estimates of useable life. The average times are shown in Table 4.8.

By comparing BST resurfacings to granular overlays with BST surfaces, the difference in predicted performance is relatively small (7 percent) at a PCR of 40 but increases (18 percent) at a PCR of 0 (the granular overlays in both cases last longer than a simple BST). However, for AC, the granular overlays surfaced with AC do not last as long as a conventional AC overlay (7 percent less at a PCR of 40 and 2 percent less at a PCR of 0). Again, it is interesting to note that the granular layer is of extra benefit if the pavement structure is allowed to deteriorate significantly (say to a PCR of 0).

Although these comparisons do not show the granular overlay as performing significantly better than the resurfacings without the crushed rock layer, this is likely due to the current use of the granular overlay. As was stated at the beginning of this chapter, granular overlays are generally used to repair a pavement structure with significant distresses. If the granular overlay had been used on a pavement in better condition, these comparisons would have likely been more favorable to the granular overlay.



## CHAPTER 5

### INITIAL ANALYSIS OF NONDESTRUCTIVE TESTING DATA

#### **5.1 INTRODUCTION**

To assess the actual performance of roads with granular overlays, over 50 centerline miles (80 km) of roads were tested using a Dynatest Falling Weight Deflectometer (FWD) Model 8000. These roads were located throughout WSDOT Districts 2 and 6 and had a variety of different structures, ages, and conditions. The tests were designed to provide evidence as to the comparative performance and stiffness of granular overlays. This chapter will be used to present the initial results of the deflection testing. Chapter 6 will be used to present the results of backcalculation of layer moduli.

#### **5.2 TESTING APPARATUS DESCRIPTION AND TESTING PROCEDURE**

The stressed area under the impulse load of a FWD is shown in Figure 5.1. Since the stresses caused by the load are spread over a wider area at deeper depths, the deflection measured at the surface at wider radii is the primary result of stresses on deeper sections. The slope at which the stressed area expands in each layer depends upon the stiffness of that layer. Typical deflection basins are shown in Figure 5.2.

The testing was conducted by WSDOT under the direction of Mr. John Livingston. The tests were conducted at one-tenth of a mile intervals in both lanes of the road. The FWD was aligned on the center of the outer wheel path of the lane. The load was dropped twice from its maximum height causing approximately a 15.0 kip (67 kN) force to "seat" the load plate. The deflection readings from these drops were ignored. The weight was then dropped four times from consecutively lower heights to cause loads of approximately 13.0 kips (58 kN), 10.0 kips (44 kN), 9.0 kips (40 kN) and 5.0 kips (22 kN). The results from these tests were stored in the computer. Additionally at least once each test section,

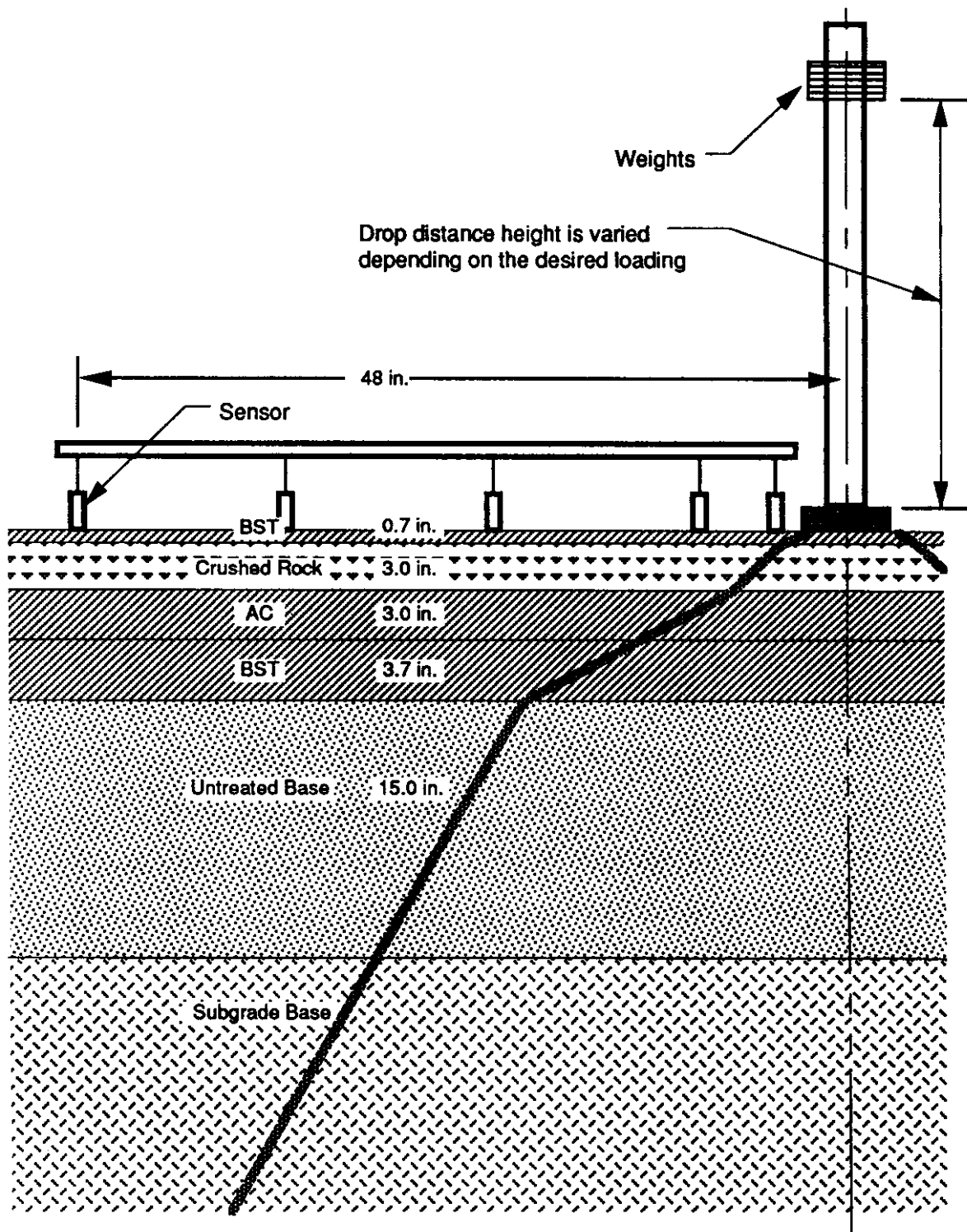


Figure 5.1. Profile of the FWD Sensors and Weights (SR28B at Milepost 57.0)

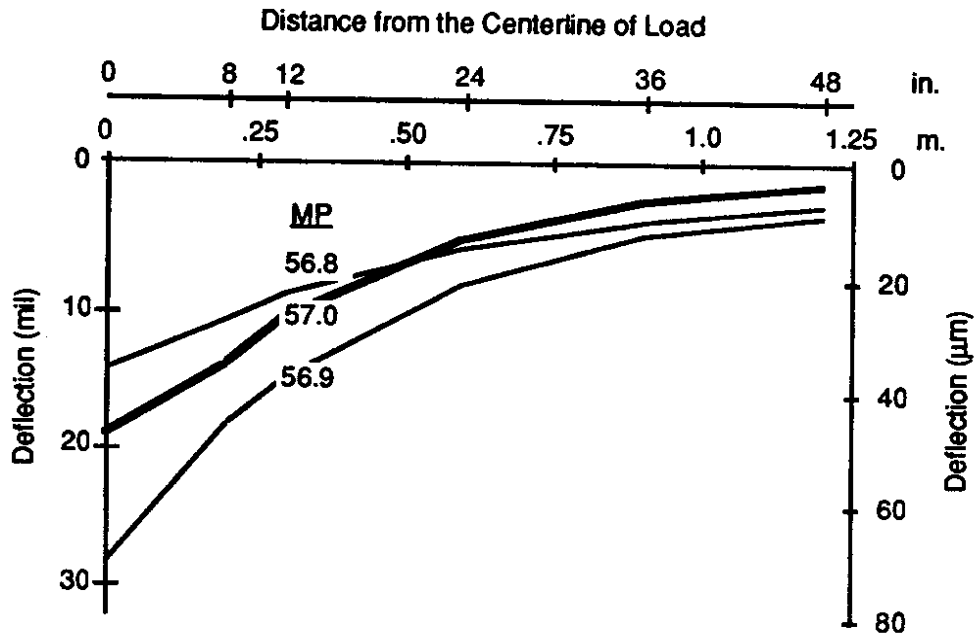


Figure 5.2. Deflection Basins for SR28B, Mileposts 56.8, 56.9, and 57.0

the temperature of the pavement was taken and the surface was drilled to determine surface depth. The testing methods used are discussed further in Section 5.3.

While the FWD tests were being conducted, notes were taken on the pavement condition and surroundings. These notes included information on pavement distress, weather conditions, any sign of bedrock, and other indicators of subsurface conditions.

The tests in District 2 were conducted at the beginning of June 1990. Little rainfall was reported by District personnel to have fallen in the weeks prior to the testing; however, a light drizzle fell during the testing of SR17. Small test pits dug in the shoulders of SR24 at Milepost 60.0 showed the base to be damp.

District 6 was tested in late August 1990. No rainfall was reported by District personnel to have fallen in the three weeks preceding the testing and none fell during the tests. A hole dug in the shoulder of SR231A at Milepost 7.25 showed that the granular base material was dry for the first 3.0 in. (76 mm) and damp at greater depths.

### **5.3 SELECTION OF TEST SECTIONS**

All of the roads that were selected were in rural eastern Washington. Traffic on these roads was mostly local, with occasional long haul trucks. The topography of eastern Washington ranges from mountainous to rolling hills and most of the land is either dry land wheat farms or scrub fields. The bedrock consists of generally horizontal layers of fractured basalt.

A representative sample of roads having enough different characteristics to be representative of all of the other roads in these two districts was sought. Characteristics that were considered included age, pavement structure, traffic flow and road location. The roads that were selected are shown in Figure 5.3 and are further summarized in Table 5.1. Where more than one section was tested on a specific road, each section was designated by a letter.

The ESAL count for each road was estimated by multiplying the average number of trucks per year for each road as listed in WSPMS by 1.03, the average number of ESALs/truck for Washington State (Mahoney et al. [13]). These ESAL estimates are considered to be only approximate at best.

In Table 5.2 the thicknesses of the surface layer as listed in the WSPMS and as measured during the testing are listed. The field measurements were made by drilling the surface with a 3/4 in. (19 mm) drill and measuring the depth of the surface layer. In cases where the surfacing was AC, it was relatively easy to discern the interface between the surface layer and the crushed rock layer. When the surface was BST, this was frequently not possible.

Table 5.2 also lists the surface temperatures that were taken during testing. A temperature reading was taken at the start of each test section and additional measurements were taken as needed. The temperature was measured for AC surfaces by drilling half way through the surfacing, cooling the hole with water then inserting a temperature probe in the hole. The water was sprayed in the hole to dissipate the heat caused by the drill. For BST



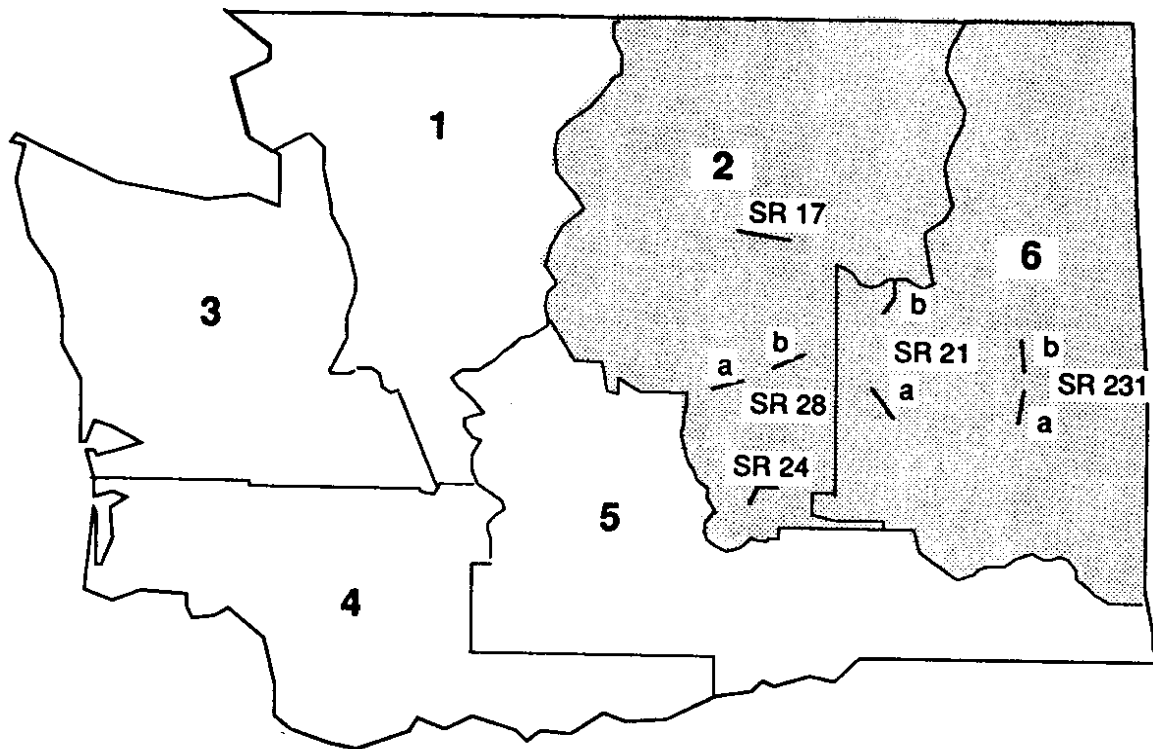


Figure 5.3. Sections of Roads Tested during the Granular Overlay Study

Table 5.1. Road Sections Tested with the FWD

Location	Surfacing Type	Granular Thickness		Age at testing (years)	Test Length		Average Daily Traffic <sup>1</sup>	Annual 18kip (80 kN) ESAL <sup>2</sup>
		in.	mm		miles	km		
District 2								
SR17	BST	2.4-12 <sup>3</sup>	60-300	6	8.0	12.8	960	107,000
SR 24	BST	3.6	90	4	11.0	17.6	920	26,000
SR 28A	AC	3.0	75	6	5.0	8.0	4,700	180,000
SR 28B	BST	3.6	90	6	5.8	9.3	640	29,000
District 6								
SR21A	AC	4.2	107	11	5.0	8.0	330	28,000
SR21B	BST	3.0	75	10	5.0	8.0	280	13,000
SR231A	BST/AC	4.2	107	11	5.0	8.0	180	5,700
SR231B	BST/AC	4.8	122	8	5.0	8.0	230	6,400

<sup>1</sup>WSPMS, 1990

<sup>2</sup>Calculation is based on WSDOT's estimate of truck count (MIDAL, 1990)

<sup>3</sup>Thickness varies

**Table 5.2. Test Sections Surface Thicknesses and Temperatures  
Taken During FWD Testing**

Location	Surfacing Type	Surface Thickness				Temperature			
		WSPMS		Measured		North or East Lane		South or West Lane	
		in.	mm	in.	mm	°F	°C	°F	°C
<b>District 2</b>									
SR17	BST	1.2	30	*	*	52/56 <sup>1</sup>	17/19 <sup>1</sup>	68/74 <sup>2</sup>	20/23 <sup>2</sup>
SR 24	BST	1.4	36	1.7	43	102	39	72/98 <sup>3</sup>	22/37 <sup>2</sup>
SR 28A	AC	2.4	61	2.4	61	78	26	60	16
SR 28B	BST	0.7	18	*	*	77	25	68	20
<b>District 6</b>									
SR21A	AC	1.8	46	1.0 &1.5	25 & 38	92	33	92	33
SR21B	BST	0.7	18	0.75 & 3.0	19 & 76	58	14	70	21
SR231A	BST/AC	0.7/ 1.8	18/ 46	*	*	65	18	89	32
SR231B	BST/AC	0.7/ 1.8	18/ 46	1.5	38	65	18	59	15

\*Surface thickness could not be determined from drill hole.

<sup>1</sup> Second temperature was taken at Milepost 124.0

<sup>2</sup> Second temperature was taken at Milepost 124.05

<sup>3</sup> Second temperature was taken at Milepost 55.0

surfaces, a flat thermometer was placed directly on the pavement. When more than two readings were taken during the testing, both are listed in the table.

### **5.3.1 Overlay Analysis Methods**

The pavement sections were evaluated with both the AASHTO Structural Number (AASHTO [1]) and the Asphalt Institute effective thickness overlay design techniques (Asphalt Institute [36]). In both cases, a design life of 10 years, the annual ESAL counts from Table 5.1 with 0 percent growth and the subgrade moduli in Table 5.21 were used. The additional factors used in the overlay design are shown in Tables 5.3 and 5.4.

**Table 5.3. AASHTO Factors Used in Overlay Design Calculations**

<b>Reliability</b>	<b>90%</b>
<b>Standard Deviation</b>	<b>0.50</b>
<b>Design Serviceability Loss</b>	<b>2.5</b>
<b>Remaining life of existing pavement factor (RLX)</b>	<b>20%</b>
<b>Remaining life of overlay factor (RLY)</b>	<b>30%</b>
<b>Remaining life factor (FRL)</b>	<b>0.62</b>
<b>Structural Layer coefficients</b>	
<b>Asphalt Concrete</b>	<b>0.40</b>
<b>Old Asphalt Concrete (&gt;6 years old)</b>	<b>0.35</b>
<b>BST</b>	<b>0.35</b>
<b>Confined Crushed Rock</b>	<b>0.25</b>
<b>Base Course</b>	<b>0.07</b>

**Table 5.4. Asphalt Institute Equivalency Factors Used in Overlay Design Calculations**

<b>Asphalt Concrete</b>	<b>0.70</b>
<b>Old Asphalt Concrete (&gt;6 years old)</b>	<b>0.60</b>
<b>BST</b>	<b>0.50</b>
<b>Confined Crushed Rock</b>	<b>0.50</b>
<b>Base Course</b>	<b>0.15</b>

Average factors were used for all of the pavement sections to create a direct method for comparing the pavement structures. The effect of these assumptions are discussed in Section 5.9. The structural layer coefficient (AASHTO) and the effective thickness factor (Asphalt Institute) for the granular layer were always assumed to be one-half of the factor for an average AC layer in keeping with the design equivalency factor of 2.0, as discussed in Section 3.3.

### 5.3.2 Test Section Pavement Cross-Sections

The section of SR17 (refer to Figure 5.4) that was tested, Mileposts 120-128, was east of Bridgeport, Washington. The road was well elevated and had adequate drainage. The ditches were in good condition and showed slight signs of erosion. There were basalt cliffs nearby and large boulders every few miles. Three road cuts showed a sandy loess (Mileposts 120.3, 124.8 and 126.7), while one other showed basalt (Milepost 125.2). A few small cracks and ruts were in the surface and occasional thin (skin) patches were at the shoulder (fog) line. The crushed rock layer thickness varied from 2.4 to 12 in. (60 to 300 mm). This variation was intended to compensate for changes in strength of the existing pavement (Stokes [29]). In the PCR surveys (Table 5.5), a BST applied in 1976 had deteriorated to a PCR of 12 in 3 years (a loss of 28 PCR points per year). The granular overlay applied in 1984 was still at a PCR of 85 after 5 years (a loss of about 1 PCR point per year). (This section illustrates a commonly observed trend in that granular overlays are usually placed on pavements which have deteriorated to a very low condition.) The overlay designs, based on Figure 5.4, are shown in Table 5.6.

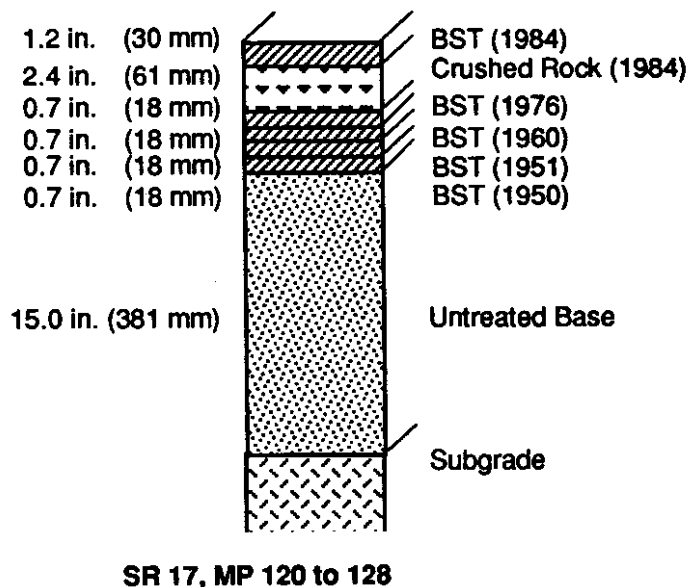


Figure 5.4. Cross-section of SR17 Mileposts 120 to 128

Table 5.5. Average PCR Survey Results for SR17 Milepost 120 to 128

Survey Year	'75	'77	'79	'81	'83	'84	'86	'88	'89
PCR	15	96	12	21	25	91	94	95	85

Table 5.6. Overlay Calculations Based on AASHTO and Asphalt Institute Design Procedures for SR17 Milepost 120 to 128

	Thickness		AASHTO SN	AI Equiv. Thick	
	in.	mm		in.	mm
Total	21.4	544	1.89	5.57	141
Required			2.6	7.2	183
Overlay			0.71	1.63	41
AC thickness (in)			1.77	1.63	41

1 in. = 25.4 mm

Table 5.7. Average PCR Survey Results for SR24 Milepost 49 to 60

Survey Year	'75	'77	'79	'81	'83	'84	'86	'88	'89
PCR	60	72	55	49	18	7	93	98	98

Table 5.8. Overlay Calculations Based on AASHTO and Asphalt Institute Design Procedures for SR24 Milepost 49 to 60

	Thickness		AASHTO SN	AI Equiv. Thick	
	in.	mm		in.	mm
Total	17.7	450	1.88	5.49	139
Required			2.20	5.8	147
Overlay			0.32	0.31	8
AC thickness (in)			0.80	0.31	8

1 in. = 25.4 mm

The section of SR24 that was tested (refer to Figure 5.5), Mileposts 49 to 60, passed through the Saddle Mountain Wildlife Refuge. The road was in an open area with hills a mile away. There were no sign of any rock outcroppings. The ditches were dry and the only vegetation was scrub brush. There were narrow transverse cracks approximately every mile and occasional longitudinal cracks. These are averaged into the PCRs (Table 5.7). The overlay designs are listed in Table 5.8.

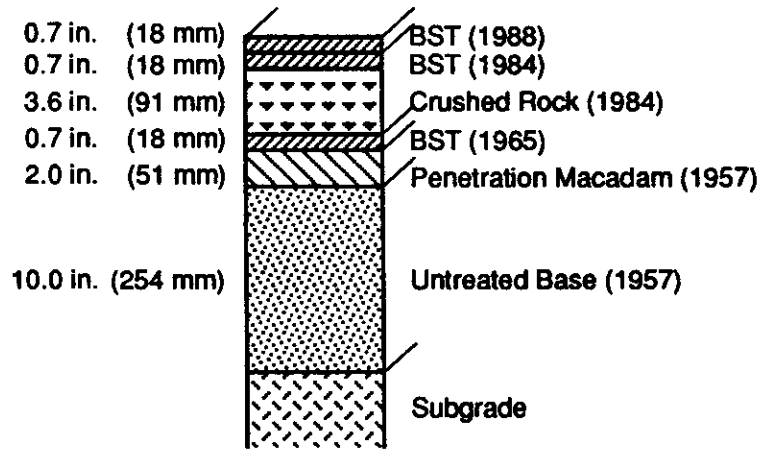


Figure 5.5. Cross-section of SR 24, Milepost 49 to 60

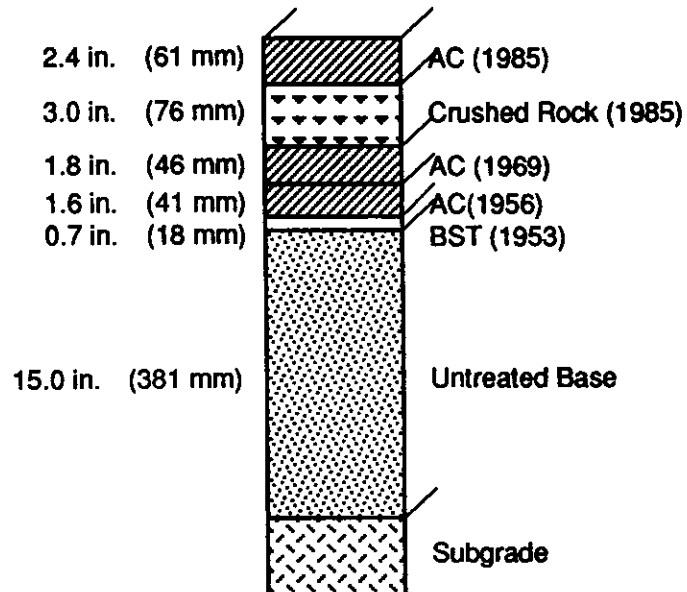


Figure 5.6. SR 28 Section A Milepost 31.7 to 36.5 (with Granular Overlay)

The first section of SR28 that was tested (refer to Figure 5.6), Mileposts 31.7 to 36.5, was between Quincy and Ephrata, Washington, and had the highest volume of traffic of any of the roads tested. It was in a flat agricultural area and there were no signs of rock outcroppings. The ditches were dry except for irrigation water. There were a few transverse cracks, most notably the five between Mileposts 36.10 and 36.20. Additionally, a nearly continuous longitudinal crack extended from Milepost 35.2 to 36.5. The town of Winchester was between Milepost 36.2 and 36.7. A hole drilled at Milepost 31.6 showed 2.4 in. (61 mm) of AC. The final mile of this section did not have a granular overlay (Figure 5.7) but did have an AC overlay of the same thickness (2.4 in. (61 mm)) placed in 1977. The PCR data and the overlay designs for the sections of this road with and without the granular overlays are shown in Tables 5.9 and 5.10.

Table 5.9. Average PCR Survey Results for SR28A Milepost 31.7 to 37.5

Survey Year	'75	'77	'79	'81	'83	'84	'86	'88	'89
MP 31.7-36.5	85	64	55	31	4	8	100	99	100
MP 36.5-37.5	-1	100	99	99	96	82	95	90	86

Table 5.10. Overlay Analysis for SR28A Milepost 31.7 to 37.5

	Thickness				AASHTO SN		AI Equivalent Thickness			
	w/o GO		w/GO		w/o GO	w/GO	w/o GO		w/GO	
	in.	mm	in.	mm			in.	mm	in.	mm
Total	24.5	622	19.7	500	2.21	1.74	6.6	168	5.1	130
Required					2.5	2.5	7.2	183	7.2	183
Overlay					0.29	0.76	0.6	15	2.1	55
AC thickness					0.72	1.89	0.6	15	2.1	55

Table 5.11. Average PCR Survey Results for SR28B Milepost 55 to 60

Survey Year	'75	'77	'79	'81	'83	'84	'86	'88	'89
PCR	42	20	6	6	-26	99	93	94	96

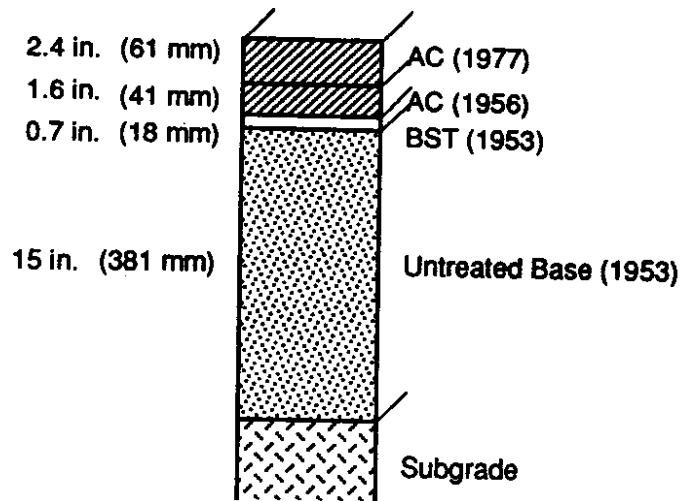


Figure 5.7. SR28 Section A, Mileposts 36.5 to 37.5 (without Granular Overlay)

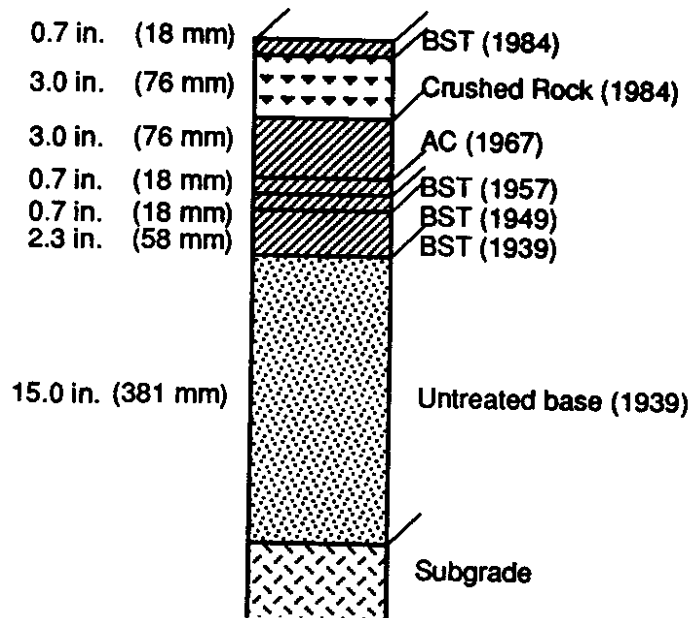


Figure 5.8. SR28 Section B Mileposts 55 to 60



The second section of SR28 that was tested (refer to Figure 5.8), Mileposts 55 to 60, went up to a plateau east of Soap Lake, Washington. The road passed through several cuts (basalt at MP 55.0-55.1; glacial till at MP 56.9, 57.4, 58.6) and over several fill sections (MP 56.0, 57.1 and 57.3). The road was in excellent condition except that it had two to three transverse cracks per mile. The PCR data and the overlay designs are shown in Tables 5.11 and 5.12.

The first section of SR21 that was tested (refer to Figure 5.9), Mileposts 40 to 45, was just north of Odessa, Washington. The terrain was slightly rolling with exposed basalt cliffs on the hills. The land alternated between agricultural and scrub. The road went up to a plateau from Milepost 42.0 to 43.8. A hole drilled at Milepost 45 showed 1.0 in. (25 mm) of AC. The road had significant transverse cracking and rutting. The PCR data and the overlay analyses are listed in Tables 5.13 and 5.14. (Note that a BST placed in 1976 (refer to Figure 5.9) had lost 44 PCR points (assuming a PCR = 100 after paving) in one year (refer to Table 5.13). The granular overlay placed in 1979 took 10 years to lose the same amount of PCR points.)

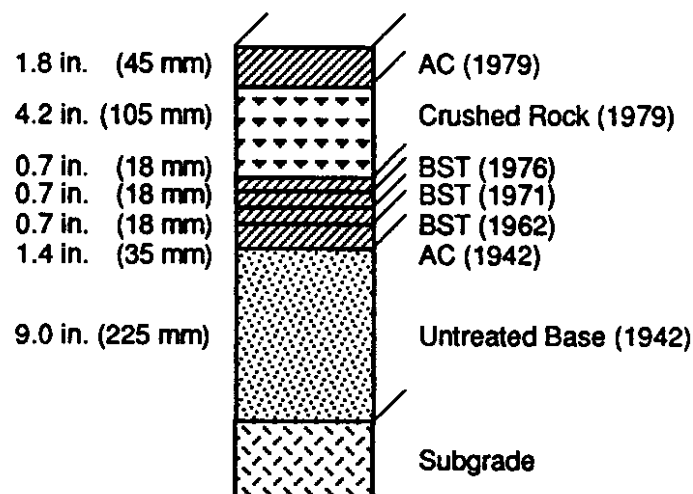


Figure 5.9. Cross-section of SR21 Section A, Milepost 40 to 45

Table 5.12. Overlay Analysis for SR28B Milepost 55 to 60

	Thickness (in.)		AASHTO SN	AI Equiv. Thick	
	in.	mm		in.	mm
Total	25.4	645	1.74	7.75	197
Required			2.5	7.2	183
Overlay			0.76	-0.55	-14
AC thickness (in)			1.89	-0.55	-14

Table 5.13. Average PCR Survey Results for SR21A Milepost 40 to 45.

Survey Year	'75	'77	'79	'81	'83	'84	'86	'88	'89
PCR	6	56	55	99	99	99	90	78	54

Table 5.14. Overlay Analysis for SR21A Milepost 40 to 45

	Thickness (in.)		AASHTO SN	AI Equiv. Thick	
	in.	mm		in.	mm
Total	12.3	312	2.15	5.40	137
Required			2.20	6	152
Overlay			0.05	0.60	15
AC thickness (in)			0.13	0.60	15

Table 5.15. Average PCR Survey Results for SR21B Milepost 70 to 75

Survey Year	'75	'77	'79	'81	'83	'84	'86	'88	'89
PCR	12	-20	-6	99	84	78	72	56	19

Table 5.16. Overlay Analyses for SR21B Milepost 70 to 75

	Thickness		AASHTO SN	AI Equiv. Thick.	
	in.	mm		in.	mm
Total	12.3	312	1.44	5.4	137
Required			2.20	5.3	135
Overlay			0.76	-0.1	-2.5
AC thickness (in.)			1.90	-0.1	-2.5

The second section of SR21 that was tested (refer to Figure 5.10), Mileposts 70 to 75, was just north of Wilbur, Washington on a plateau above the Colombia River. The land was slightly rolling and alternated between agricultural and scrub land. The BST surface was covered by a leveling course, which varied in thickness from 0 to 3.0 in. (0 to 75 mm). Additionally it is possible (based on conversations with District personnel) that leveling courses may exist on other pavement layers. The surface was drilled at Milepost 70.0, where the thickness measured 0.75 in. (20 mm) and at 74.90, where the surface thickness measured 3.0 in. (76 mm). Basalt bedrock was evident in a cut on the west side of the road at Mileposts 73.60 to 73.85. The average PCR are listed in Table 5.15 and the overlay design is in Table 5.16. (Note that the BST placed in 1971 (Figure 5.10) had lost 88 PCR points in four years (Table 5.15). The granular overlay lost about the same number of PCR points in eight years. Further, the granular overlay, when placed, was on a pavement with a very low PCR (-6).)

The first section of SR231 that was tested (refer to Figures 5.11 and 5.12), Mileposts 0.0 to 7.3, began just outside of Sprague, Washington. The topography consisted of rolling hills and numerous basalt outcroppings. In most cases, the basalt was several hundred yards from the road, but the road did cut through it at Mileposts 3.65, 4.55 and 5.00. Mileposts 3.45 to 3.55 were in a marshy bottom land. The road was well elevated and well drained. In the initial survey of the road in June 1990, a significant number of longitudinal, transverse and alligator cracks were observed. A new BST surface was applied during the summer so that no cracks could be documented during the FWD testing. The PCRs indicate that the granular layer was used on the pavement beginning at Milepost 2.7 to compensate for extensive distresses prior to the 1979 overlay (Table 5.17). The overlay designs are listed in Table 5.18. (Note that both sections had the same thickness overlay (1.8 in. (45 mm)). The section with the granular overlay was in poorer condition at the time of construction but both sections performed about the same.)

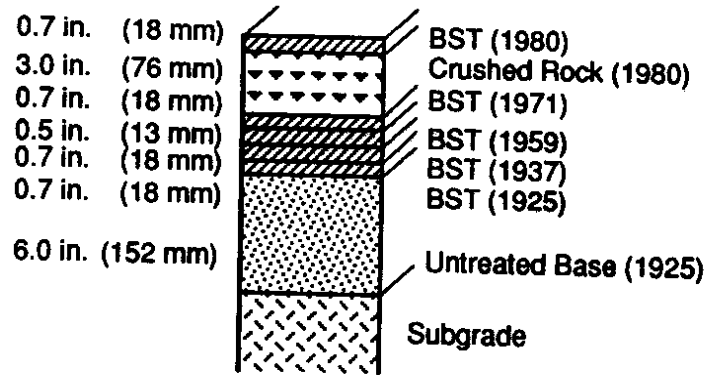


Figure 5.10. Cross-section of SR21 Section B, Milepost 70 to 75.

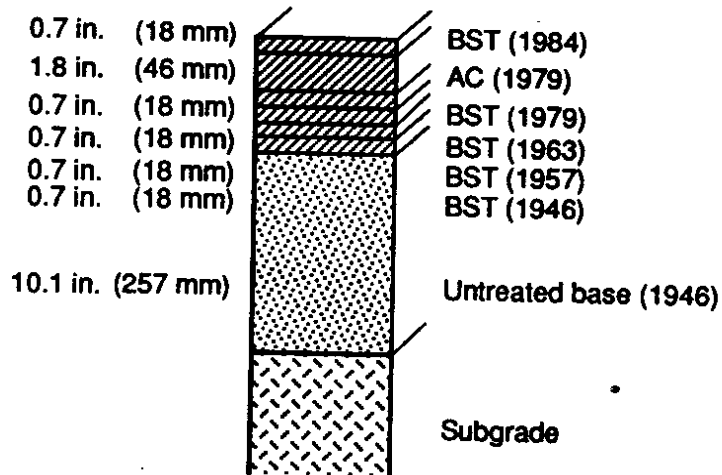


Figure 5.11. Cross-section of SR 231 Section A, Milepost 0.0 to 2.7 (without Granular Overlay)

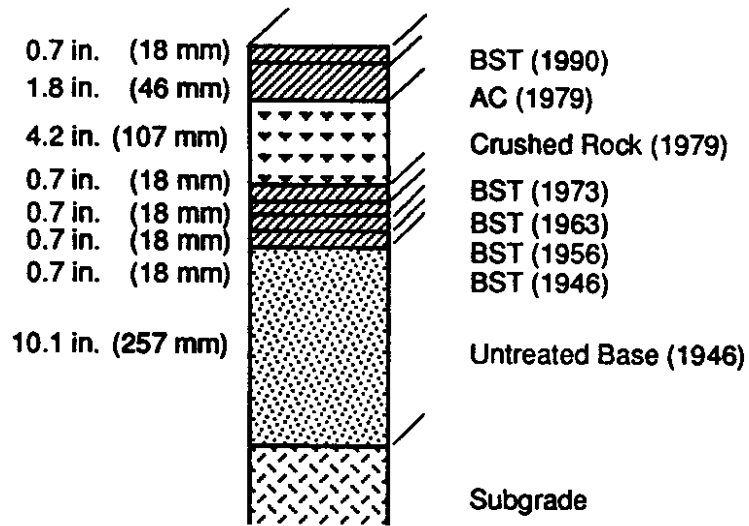


Figure 5.12. Cross-section of SR231 Section A, Milepost 2.7 to 7.3 (with Granular Overlay)

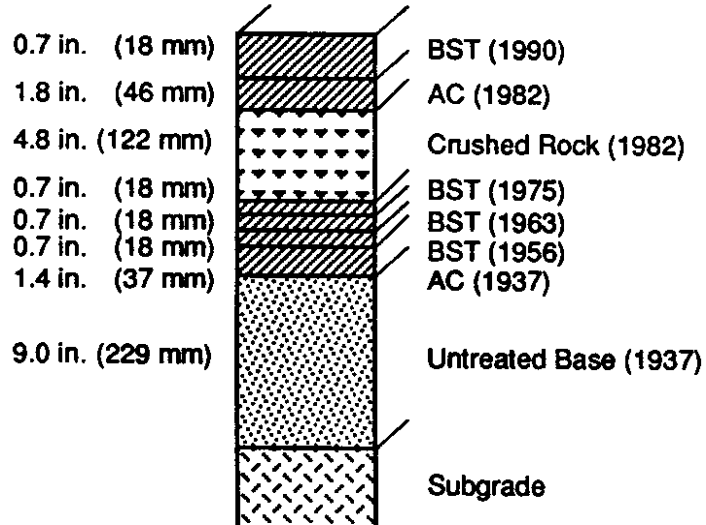


Figure 5.13. Cross-section of SR231 Section B, Milepost 22.0 to 27.0

Table 5.17. Average PCR Survey Results for SR 231A, Milepost 0.0 to 7.3

Survey Year	'75	'77	'79	'81	'83	'84	'86	'88	'89
MP 0.0-2.7	74	96	89	99	89	89	55	74	50
MP 2.7-7.3	36	41	67	100	97	93	59	70	44

Table 5.18. Overlay Analysis for SR231A, Milepost 0.0 to 7.3

	Thickness				AASHTO SN		AI Equiv. Thick			
	w/o GO		w/GO		w/o GO	w/GO	w/o GO		w/GO	
	in.	mm	in.	mm			in.	mm	in.	mm
Total	15.4	391	19.6	498	1.59	2.24	4.35	110	6.45	164
Required					1.60	1.60	4.0	102	4.0	102
Overlay					0.01	-0.64	-0.35	-26	-2.45	-62
AC thickness					0.03	-1.60	-0.35	-26	-2.45	-62

Table 5.19. Average PCR Survey Results for SR231B, Milepost 22 to 27

Survey Year	'75	'77	'79	'81	'83	'84	'86	'88	'89
PCR	12	42	15	-12	99	99	100	84	92

Table 5.20 Overlay Analysis for SR231B, Milepost 22 to 27

	Thickness		AASHTO SN	AI Equiv. Thick	
	in.	mm		in.	mm
Total	19.8	502.9	2.44	7.1	179.6
Required			1.70	4.3	109.2
Overlay			-0.75	-2.8	-70.4
AC thickness (in)			-1.86	-2.8	-70.4

The second section of SR231 that was tested was between Mileposts 22 to 27 (Figure 5.13). There were no basalt outcroppings, and most of the land was irrigated farmland. The road was well elevated and drained. Milepost 24.6 was in a marshy area. The surface was a new BST and no cracking was apparent. A test hole was drilled at Milepost 27.0 and the AC was measured to be 1.5 in. (38 mm) thick. The PCR's for this section of the road are listed in Table 5.19 and the overlay designs are listed in Table 5.20. (Note that the BST placed in 1975 (Figure 5.13) lost 58 PCR points in two years (or about 30 PCR points per year). At the time of construction of the granular overlay, the pavement condition was extremely low (PCR = -12) but it has lost only 1 to 2 PCR points per year.).

#### **5.4 DEFLECTION BASINS**

The shape and magnitude of the deflections from the FWD is an indication of the stiffness of the pavement layers. For example, if the surface is weak but the subgrade is stiff, then the deflection readings near the load plate are high but the deflections further out are low.

A primary source of deflection variation is simply the nonhomogeneity of what we hope are homogeneous pavement sections. As an illustration of this nonhomogeneity, the basins shown in Figure 5.3 all came from adjacent tests taken a tenth of a mile apart on a "uniform" section of pavement. Some of the deflections varied by 100 percent. For the roads tested in the study, the standard deviation of the deflection under the loading plate ( $D_0$ ) was about 25 percent of the mean and the lowest value was generally only half of the highest. These differences could be the result of localized pavement failures, subgrade changes, inconsistent construction or any other factor that affects the stiffness of the pavement layers. This variability naturally influences the results of any analysis of FWD data.

## 5.5 ANALYSIS OF THE SUBGRADE

A most important parameter to understand in a pavement system is the subgrade. Since the deflections at a distance of several feet from the center of the load are little affected by the surface layers (Figure 5.2), these deflections provide a means of estimating the moduli of the subgrade. Equation 5.1 is one such equation (Newcomb [22]):

$$E_s = -111 + 0.00577(P/D_4) \quad \text{(Equation 5.1)}$$

where:  $E_s$  = Modulus of Elasticity of the Subgrade (psi)

$P$  = Applied Load (lbs), and

$D_4$  = Deflection 4.0 ft (1.22 m) from applied load.

The results of this calculation on the roads tested are shown in Table 5.21. The moduli for District 2 are generally higher than those of District 6. The effect of this will be seen in the subsequent analyses.

Table 5.21. Calculated Subgrade Moduli for the Test Sections

Route Number	Direction of Travel	Subgrade Modulus of Elasticity	
		Average (psi)	Standard Dev. (psi)
District 2			
SR17	North	16,200	4,300
	South	16,500	5,200
SR24	North	15,800	2,000
	South	15,700	2,300
SR 28A w/o GO	East	25,000	4,000
w/GO	East	24,400	4,900
w/o GO	West	22,200	3,600
w/GO	West	22,000	3,500
SR28B	East	22,300	6,300
	West	22,500	5,800
District 6			
SR21A	North	14,300	4,200
	South	15,100	7,500
SR21B	North	11,000	4,000
	South	13,000	7,200
SR231A w/o GO	North	18,100	5,200
w/GO	North	20,300	24,500
w/o GO	South	13,100	4,300
w/GO	South	15,800	12,500
SR231B	North	14,400	10,100
	South	12,100	3,400

1 psi = 6.89 kPa



## 5.6 ANALYSIS OF $D_0$

One method for analyzing deflection basins is to examine the measurements taken directly under the load,  $D_0$ . This measurement is important because it is the only deflection that results from stresses on all of the pavement layers. Therefore, it is a reflection of the stiffness of both the pavement system and the subgrade. By comparing the magnitude of  $D_0$  between different pavement sections, it is possible to determine the relative stiffness of the different pavements. Table 5.22 summarizes the  $D_0$  readings for the pavements tested in this study.

Table 5.22 Summary of  $D_0$  Values Normalized to a 9000 lb (40.0 kN) Load and 77° F (25° C) (Temperatures were normalized using WSDOT temperature correction procedure.)

Route Number	Direction of Travel	$D_0$ (mils)		
		Average ( $\bar{x}$ )	Standard Deviation	$\bar{x} + 2SD$
<u>District 2</u>				
SR17	North	26.6	5.1	36.8
	South	23.2	4.3	31.9
SR24	North	16.7	2.1	20.9
	South	19.2	3.0	25.2
SR 28A	w/o GO East	14.0	2.2	18.5
	w/o GO West	15.3	2.7	20.8
	w/ GO East	12.1	1.9	15.8
	w/ GO West	13.1	2.1	17.3
SR28B	East	15.7	3.5	22.7
	West	18.0	4.5	27.0
<u>District 6</u>				
SR21A	North	26.4	4.1	34.6
	South	26.4	5.1	36.5
SR21B	North	48.6	12.3	73.2
	South	38.9	11.4	61.8
SR231A	w/o GO North	25.1	4.4	33.9
	w/o GO South	30.5	6.9	44.4
	w/ GO North	33.6	7.6	48.9
	w/ GO South	31.2	9.2	49.7
SR231B	North	29.8	5.8	35.6
	South	32.7	5.4	43.8

1 mil = 25.4  $\mu\text{m}$

To compare these results, typical pavements were modeled with the linear elastic layer program, ELSYM5 (Section 3.2.2). The AC thicknesses were chosen to represent thin, medium and thick pavements. The elastic moduli for the subgrade were varied to represent common moduli from the test sections. The layer properties are listed in Table 5.23 and their Asphalt Institute equivalent thicknesses are listed in Table 5.24. Based upon a linear elastic layer analysis, ELSYM5, the  $D_0$  for these sections is listed in Table 5.25.

The values for  $D_0$  were higher in District 6 than in District 2 (again, refer to Table 5.22). As shown in Table 5.21, the subgrades under the roads in District 6 were less stiff than those in District 2. This reduced stiffness accounts for a large part of the difference.

Table 5.23. Layer Properties in the Typical Pavement Sections

Material	Thickness		Elastic Modulus		Poisson's Ratio
	(mm)	(in)	(mPA)	(ksi)	
Asphalt Concrete	76, 127, 178	3.0, 5.0 and 7.0	3,445	500	0.35
Crushed Stone Base	152	6.0	172	25	0.40
Subgrade	semi-infinite	semi-infinite	103 and 152	15 and 22	0.45

Table 5.24. Asphalt Institute Equivalent Thicknesses for the Typical Pavements. (Equivalency Factors are 1.0 for the AC and 0.15 for the Base)

Thickness AC		AI Equivalent for AC		Thickness of Base		AI Equivalent for Base		Total AI Equivalent	
(mm)	(in)	(mm)	(in)	(mm)	(in)	(mm)	(in)	(mm)	(in)
76	3.0	76	3.0	152	6	23	0.9	99	3.9
127	5.0	127	5.0	152	6	23	0.9	150	5.9
178	7.0	178	7.0	152	6	23	0.9	201	7.9

Table 5.25.  $D_0$  Values for the Typical Pavement Sections

Thickness AC		Subgrade Elastic Modulus		$D_0$	
(mm)	(in)	mPA	(psi)	mm	(mils)
76	3.0	103	15000	.67	26.3
127	5.0	103	15000	.47	18.7
178	7.0	103	15000	.37	14.5
76	3.0	151	22000	.67	21.3
127	5.0	151	22000	.47	15.0
178	7.0	151	22000	.37	11.7

For each road, one lane had higher deflections than the other. The subgrades were approximately equal and the pavement structures were assumed to be equal. One possible explanation for the difference is that one of the lanes had received higher traffic loadings than the other and therefore had deteriorated more.

For SR28A, the section of road with the granular overlay had a lower  $D_0$  than the section without the granular overlay. Although the AC is slightly thicker (the section with the granular overlay has a total of 5.8 in. of AC versus 4.0 in. for the section without the granular overlay), the granular layer is probably also serving to increase the stiffness of the pavement.

The section of SR231A without the granular overlay has a lower  $D_0$  than does the section with the granular overlay. The difference is likely due to the poor condition of the road that was overlain with the granular overlay and the lower subgrade elastic moduli. In the last PCR survey taken before the road was resurfaced, the PCR for the section without the granular overlay was twice as high as the section with the granular overlay (PCR of 96 versus 41 in 1977). Therefore, the granular overlay was probably applied to remedy a problem in the pavement from Milepost 2.7 to 7.3. The overlay for Milepost 0.0 to 2.7 might have been applied for other reasons.

## 5.7 ANALYSIS OF THE AREA PARAMETER

Although  $D_0$  is a good indicator of the relative, overall stiffness of the pavement, it is strongly influenced by the stiffness of the subgrade. To reduce the effect of the subgrade, the Area Parameter uses the measurements taken by several of the sensors, thus providing a measurement of the shape of the deflection basin. The equation upon which the Area Parameter analysis is based is as follows:

$$\text{Area Parameter} = (6/D_0)(1 + 2D_1 + 2D_2 + D_3) \quad (\text{Equation 5.3})$$

$D_n$  = the deflection at a distance of 'n' feet from the load.

By "normalizing" the deflections at some distance from the load plate with  $D_0$ , the Area Parameter gives an indication of the relative stiffness of the pavement structure, more or less eliminating the influence of the subgrade. In the extreme case, where there is no pavement structure (e.g., the testing is conducted directly on the subgrade), the ratios of:

$$\frac{D_1}{D_0}, \frac{D_2}{D_0}, \frac{D_3}{D_0}$$

will result in ratios of 0.26, 0.125 and 0.083 (for a one layer pavement system). Inserting these into Equation 5.3, the Area Parameter is

$$\text{Area Parameter} = 6(1 + 2(0.26) + 2(0.125) + 0.083) = 11.1$$

Therefore, 11.1 is the minimum possible value for the Area Parameter.

Conversely, if the pavement is very rigid, the values of  $D_1$  through  $D_3$  is very close to  $D_0$ . In the case of a pavement that is absolutely rigid, all of the deflections are equal to 1.0.

$$\frac{D_1}{D_0} = \frac{D_2}{D_0} = \frac{D_3}{D_0} = 1.0$$

Therefore, the Area Parameter is

$$\text{Area Parameter} = 6(1 + 2(1.0) + 2(1.0) + 1.0) = 36.0$$

Thus, the maximum value for the Area Parameter is 36.0.

The average Area Parameters for the test sections are given in Table 5.26. The Area Parameters for the "typical" pavement sections are given in Table 5.27.

Table 5.26 Comparison of the Area Parameters for the Tested Roads  
 (All deflections were normalized to a 9.0 kip (40.0 kN) load and 77° F (25° C).)

Route Number	Direction of Travel	Area Parameters	
		Average	Standard Deviation
<b>District 2</b>			
SR17	North	15.9	1.1
	South	17.2	1.6
SR24	North	21.2	1.0
	South	19.5	1.1
SR 28A w/o GO w/o GO w/GO w/GO	East	18.0	1.3
	West	18.3	0.5
	East	19.5	1.5
	West	19.7	1.6
SR28B	East	18.2	1.7
	West	16.8	1.3
Overall Mean		18.4	
<b>District 6</b>			
SR21A	North	18.2	1.2
	South	18.2	1.6
SR21B	North	15.3	1.4
	South	16.1	1.8
SR231A w/o GO w/o GO w/ GO w/ GO	North	18.8	1.9
	South	18.2	1.9
	North	17.3	1.8
	South	18.3	2.7
SR 231B	North	17.2	1.7
	South	17.0	1.2
Overall Mean		17.5	

Table 5.27. Area Parameters for the Typical Pavement Sections

Thickness AC (in.)	Subgrade Elastic Modulus (psi)	Area Parameter
3	15000	16.5
5	15000	20.2
7	15000	22.7
3	22000	15.1
5	22000	18.6
7	22000	21.0

The Area parameters for the test sections in District 2 ranged from 15.9 to 21.2 and had a mean value of 17.5. This is between the values for the Area Parameter of the 3.0 and 5.0 in. AC pavement over the 22 ksi subgrade. The Area Parameters for District 6 varied from 17.0 to 18.8 and averaged in between the values of the Area Parameter for the 3.0 and 5.0 in. pavement over the 15 ksi subgrade.

In each road, one lane had a higher Area Parameter than the other. As was discussed for  $D_0$ , this was likely the result of higher traffic in one lane.

In SR28A, the section of road with the granular overlay had a higher Area Parameter than did the section without the granular overlay. This was not true for SR231A. The reasons for this were the same as the reasons stated for the difference in  $D_0$  (Section 5.6).

### **5.8 COMPARISONS OF $D_0$ AND THE AREA PARAMETER**

By comparing the Asphalt Institute effective thickness,  $D_0$  and the Area Parameter of the different pavement structures, it is possible to gain insight into the behavior of the different pavement systems. Figure 5.14 is a plot of these different values for the typical pavement sections. The Asphalt Institute equivalent thickness and the Area Parameter varied directly with each other and inversely with  $D_0$ . Both  $D_0$  and the Area Parameter were lower for pavements with the higher subgrade elastic moduli. These parameters are plotted for Districts 2 and 6 in Figure 5.15. The same trends are evident.

By comparing  $D_0$ , the Area Parameter and the subgrade elastic moduli of the test sections with the typical pavement sections, it was possible to determine the thickness of pavement that were equivalent to the existing pavement structure. By then comparing the Asphalt Institute equivalent thickness of the test section with the equivalent thickness of the typical pavement, it was possible to determine how accurate the Asphalt Institute thickness were.

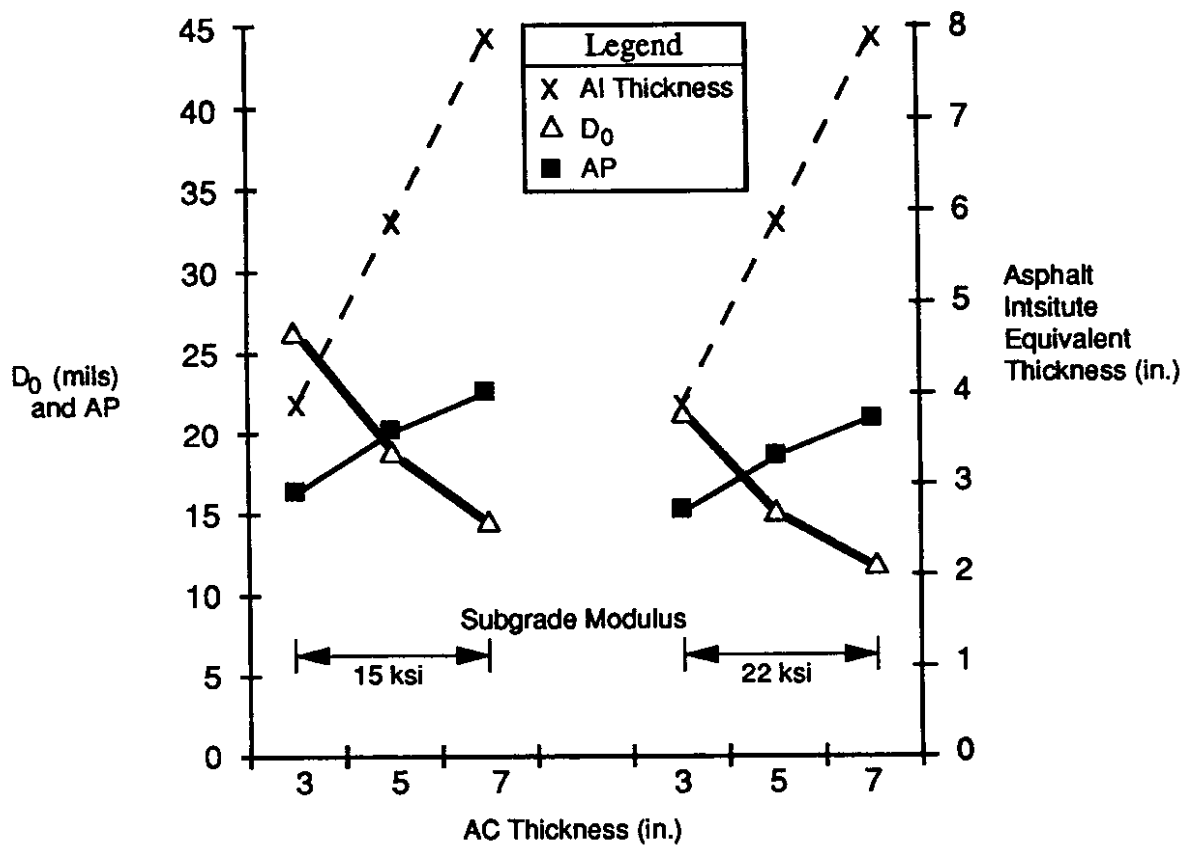


Figure 5.14. Comparison of the Asphalt Intsiteute Effective Thicknesses (Right Hand Scale), Area Parameters (Left Hand Scale) and  $D_0$ 's (Left Hand Scale) for the Typical Pavements

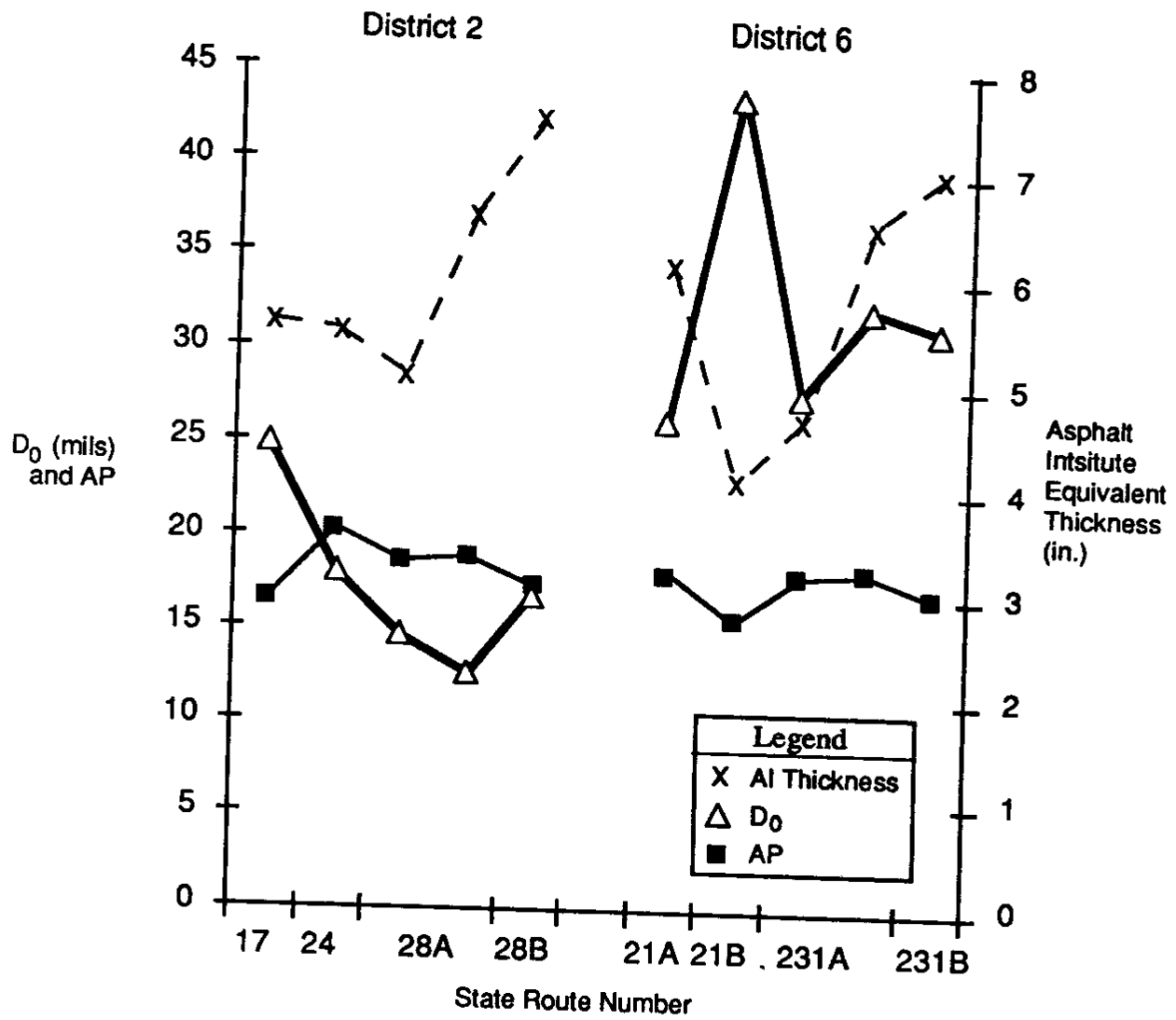


Figure 5.15. Comparison of the Asphalt Institute Effective Thicknesses (Right Hand Scale), Area Parameters (Left Hand Scale) and  $D_0$ 's (Left Hand Scale) for the Tested Roads



A pavement having the same  $D_0$  and Area Parameter values as those of the typical AC pavements were assumed to be equally stiff. Therefore by comparing the  $D_0$  and Area Parameters of the test sections with those of the typical pavements, it was possible to determine the thickness of typical AC pavement that had the same stiffness as the test section. By then comparing the equivalent thickness of the typical pavement to the Asphalt Institute thickness calculated in Section 5.3.2, it was possible to check the assumptions used in calculating the Asphalt Institute thicknesses.

In performing the comparison,  $D_0$ , Area Parameter, and subgrade elastic moduli for both lanes were averaged. The section is then compared to the typical pavement with the subgrade moduli that most closely corresponds to the calculated moduli for that section. The equivalent thickness of the pavement is then compared with the equivalent thicknesses of the model pavements (from Table 5.24).

SR17 had both a  $D_0$  and an Area Parameter approximately equal to those of the 3.0 in. AC pavement structure (on 15,000 psi subgrade). The Asphalt Institute effective thickness was 5.6 in. based on the thinnest section of the crushed rock layer. The large difference between these values indicated that some or all of the equivalency factors that were used, were not accurate.

SR24 had both  $D_0$  and Area Parameter values approximately equal to the 5.0 in. AC pavement structure (15,000 psi subgrade). The Asphalt Institute equivalent thickness for the pavement structure was 5.5 in. as compared to 5.9 in. for the typical pavement (refer back to Table 5.24). This close comparison indicated that the Asphalt Institute value was reasonable.

SR28A with a granular overlay had a  $D_0$  slightly higher than that of the 7.0 in. AC pavement structure (22,000 psi subgrade) and an Area Parameter slightly greater than that of the 5.0 in. AC pavement structure (22,000 psi subgrade). The Asphalt Institute equivalent thickness of 6.6 in. for the granular overlay portion of SR28 was between that of the 5.0 and 7.0 in. AC typical pavements.

SR28A without the granular overlay was comparable to just under the 5.0 in. AC pavement structure. The Asphalt Institute equivalent thickness of 5.1 in. for the test section was lower than the 5.9 in. for the typical 5.0 in. AC structure.

SR28B had an average  $D_0$  and Area Parameter between the values for the 3.0 in. and 5.0 in. AC pavements (22,000 psi subgrade) with an Asphalt Institute equivalent thickness of 7.3 in. Almost half of its Asphalt Institute equivalent thickness came from AC and BST layers applied between 1939 and 1967. The equivalency factor of 0.35 assigned to these layers may have been too high. The required thickness was only 4.80 in. which matched the thickness of the typical pavement very closely. Additionally, there was a large difference in the overlay design based on the AASHTO and Asphalt Institute methods, indicating that there was some problem in the overlay calculations.

SR21A had an average  $D_0$  equal to that of the 3.0 in. AC pavement (15,000 psi subgrade) and an Area Parameter between the 3.0 in. and 5.0 in. AC pavement. Its Asphalt Institute equivalent thickness was 5.4 in.

SR21B had a  $D_0$  significantly higher and an Area Parameter slightly lower than the corresponding values for the 3.0 in AC pavement (15,000 psi subgrade). Part of this difference was that the calculated subgrade for this section was only 11 ksi, as compared to the 15 ksi in the model. The Asphalt Institute equivalent thickness is 4.1 in., but again the layers were all at least 10 years old.

SR231A without the granular overlay had a  $D_0$  higher than that of the 3.0 in. AC pavement (15,000 psi subgrade) and an Area Parameter between that of the 3.0 and 5.0 in. pavement. The section with the granular overlay had a slightly higher  $D_0$  and approximately the same Area Parameter. The Asphalt Institute equivalent thickness was 4.4 in. for the section without the granular overlay and 6.4 for the section with the overlay, but because of the age of the pavement and the distresses observed in the granular overlay surface, the assumed Asphalt Institute equivalency factors were probably high.

SR231B had a  $D_0$  slightly higher than that of the 3.0 in pavement (15,000 psi subgrade) and an Area Parameter between that of the 3.0 and 5.0 in. AC pavement but an Asphalt Institute equivalent thickness of 7.1 in. The PCR at the time the road was overlain was -12 indicating that the old pavement was severely distressed. These distresses indicate that the equivalency factors for the old pavement should have been lower.

The comparisons between the typical pavements and the Asphalt Institute equivalency factors are summarized in Table 5.28.

Table 5.28. Summary of the Comparisons Between the Asphalt Institute Effective Thicknesses and the Equivalent Pavement Thicknesses

		Confined Crushed Rock Equivalency Factor			
		0.50		0.25	
Route No.	Equivalent Pavement Thickness (in.) <sup>1</sup>	AI Effective Thickness (in.) <sup>2</sup>	$\Delta$ (in.)	AI Effective Thickness (in.) <sup>3</sup>	$\Delta$ (in.)
District 2					
SR17	3.9	5.6	+1.7	5.0	+1.1
SR24	5.9	5.5	-0.4	4.6	-1.3
SR 28A w/ GO	6.9	6.6	-0.3	5.8	-1.1
SR 28A w/o GO	5.9	5.1	-0.8	5.1	-0.8
SR28B	4.9	7.8	+2.9	7.0	+2.1
District 6					
SR21A	4.9	5.4	+0.5	4.6	-0.3
SR21B	<3.9	5.4	+1.5	4.6	+0.7
SR231A w/o GO	4.9	4.4	-0.5	4.4	-0.5
SR231A w/ GO	4.9	6.4	+1.5	5.4	+0.5
SR231B	4.9	7.1	-2.2	5.9	+1.0

<sup>1</sup>From Table 5.24 and comparisons of  $D_0$ , AP and subgrade elastic modulus.

<sup>2</sup>Based on an Asphalt Institute factor of 0.50 for the confined crushed rock layer.

<sup>3</sup>Based on an Asphalt Institute factor of 0.25 for the confined crushed rock layer.

The Asphalt Institute equivalent thicknesses given in Table 5.28 came from two different calculations. The first equivalent thicknesses were based on the assumption that the crushed rock layer had an Equivalency Factor of 2. The second equivalency thickness was based upon the assumption that the crushed rock layer had an AC equivalency of 4. When the crushed rock has an equivalency of 4, it is approximately equal to the granular base used in the AASHTO Road Test (AASHTO [1]).

Based on this simple analysis, about one-half of the test sections work best with either equivalency factor.

### **5.9 VARIABLE CRUSHED ROCK THICKNESS**

SR17 was a unique road in this study because the thickness of the crushed rock layer in the granular overlay varied considerably within the test section. These variations were created to compensate for weak areas in the pavement. Although the as-built showed 11 different sections with different thicknesses, these changes were probably more gradual. In any case, if the thickness of the granular layer had any effect on the stiffness of the pavement, this should have been reflected in the  $D_0$ . Figure 5.16 shows a comparison of  $D_0$  and the crushed rock thicknesses.

### **5.10 CHAPTER SUMMARY**

Granular overlays can make a pavement system stiffer, as seen in SR28A, or can be used to stiffen a weak section of pavement, as seen in SR231A. The crushed rock layer has an equivalent thickness equal to between 1/2 and 1/4 of an AC layer. If the pavement is in good condition then the equivalency factor tends to be higher.

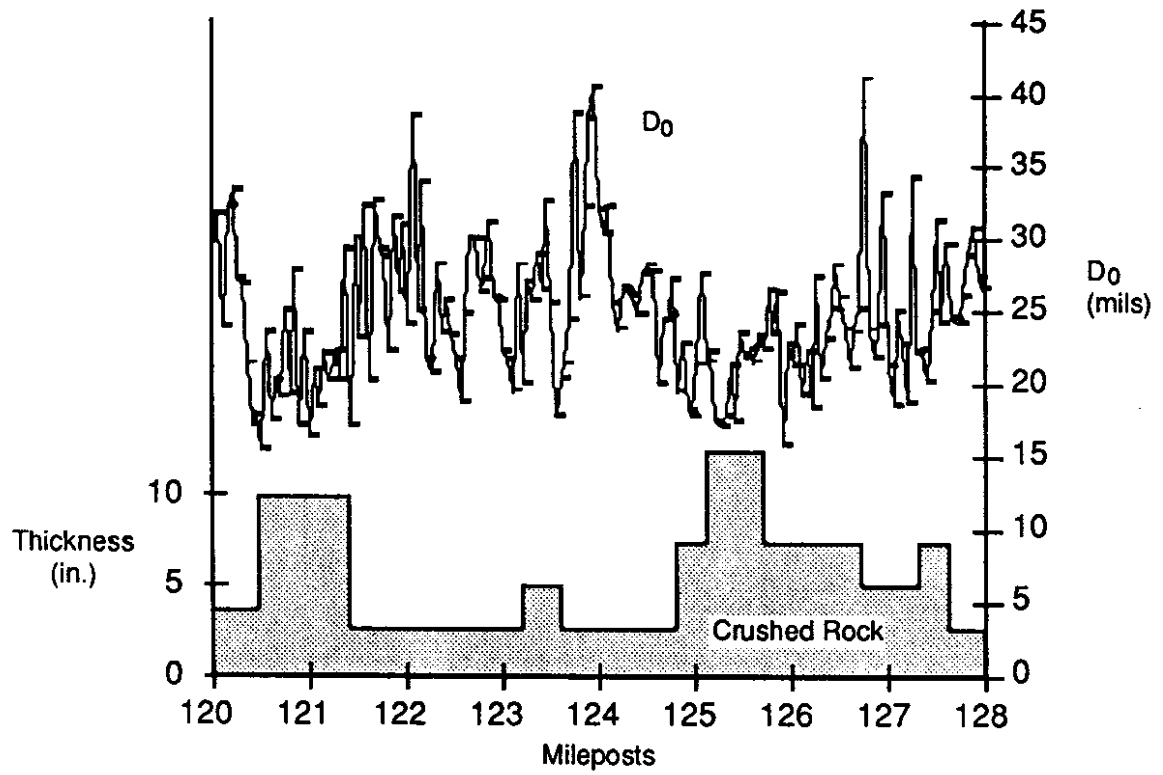


Figure 5.16. Plot of SR 17 Showing the Variation in  $D_0$  with the Thickness of the Crushed Rock Layer in the Granular Overlay



## CHAPTER 6

### ELASTIC LAYER ANALYSIS

#### 6.1 INTRODUCTION

In addition to the analyses described in Chapter 5, an elastic layer analysis was performed on the FWD data. As shown in Figure 5.1, the deflection measured by each sensor is the result of stresses on continually deeper layers. Whereas the deflection under the first layer is the result of stress on all layers, deflections under consecutive sensors are less affected by the top layers. The shape and magnitude of the deflection basin is therefore a product of the specific properties of each of the pavement layers.

One method of analyzing this system is to use elastic layer theory. In this method, all layers are assumed to be isotropic, homogeneous and infinite in the horizontal plane. Each layer is defined by its thickness, modulus of elasticity and Poisson's ratio. By combining this information with the size and magnitude of the force on the surface, a deflection basin can be calculated. Although the pavement system does not meet all of these assumptions, the analysis process can produce useful results.

Elastic layer analysis works well when the layers closely match these assumptions, but it does not when the layers do not. A pavement or subgrade layer that is not level or contains discontinuities produce a deflection basin that cannot be analyzed with these assumptions.

Another notable problem is the effect of stress stiffening on the crushed rock layer in the granular overlay. As the radial distance from the load increases, the stress on the granular layer decreases and thus so does the modulus of elasticity. This means that the modulus of elasticity of the crushed rock layer varies with the radius from the load. This was one of the many reasons that accurately calculating the moduli for the layers in the road with granular overlays was difficult.

## **6.2 EVERCALC**

The elastic layer program used in this study was EVERCALC Version 3.0. It is based on CHEVNL (Section 3.3).

The program requires the layer thickness and the Poisson's ratio for each layer and allows the modulus of elasticity for each layer to be either fixed or calculated. The program accepts up to five layers in the pavement system but its speed is significantly reduced with a greater number of layers. Although there is no lower limit on the thickness of the layers, layers that are less than 1 in. (25 mm) thick results in unrealistic moduli.

### **6.2.1 Layer Thicknesses**

The layer thicknesses were obtained from WSPMS and were checked by two sources. WSPMS was used as the primary reference because of the breadth of information that it contained (Section 4.2). This information included a list of all contracts performed on each section of road and the layer thicknesses as reported in the as-builts. The data in WSPMS have been entered over a 20 year period and contain some errors. Therefore, the thicknesses of the granular overlays were verified by examining the as-builts for the projects and by drilling the pavement surfaces. However, only a 3/4 in. drill was available so the pavement layers were difficult to identify.

In general, these sources agreed well. In every case the data from WSPMS agreed with the as-builts (as should be the case). In most cases, where accurate measurements could be taken of the pavement surface thickness, these measurements agreed with the thicknesses in WSPMS. One notable exception was SR21A, which had a measured surface thickness only one half of the plan thickness. The effect of this variation is discussed later. In all other cases the measured thicknesses were within 20 percent of the plan thicknesses (Table 5.2).

A problem with the WSPMS thicknesses is that they include only contract projects. A problem with this was discovered in District 6. In that District, the maintenance crews sometimes applied a layer of prelevel or level-up AC before a pavement was resurfaced.



The prelevel layer served to fill in the ruts and level off the surface. Since this was done only on the parts of the road where it was required, the prelevel thickness varied from 0 to 3 in. (0 to 75 mm) and was recorded in WSPMS. The level-up course was observed on SR21B as well as sections of SR231 that were not tested. With no means of verifying the layer thicknesses, accurate layer thicknesses for these roads could not be determined. Estimates were made of the layer thicknesses for District 6, but no reasonable results were obtained.

### **6.2.2 Poisson's Ratio**

The Poisson's ratio was kept constant for each type of material throughout the project. The following ratios were always used:

Asphalt concrete	0.35
Bituminous Surface Treatment	0.40
Crushed Rock	0.40
Subgrade	0.45

### **6.2.3 Modeling**

Since the pavement cross sections are complex and could contain 10 layers of surfacing built over a period of 60 years, layers had to be grouped together. The program was prohibitively slow in analyzing pavements that had five layers, so four was kept as the maximum. Since the granular overlay was the object of this study, the surface and the crushed rock layer had to be kept separate. Therefore all of the old pavement surfacing layers were grouped into one layer and the base course was grouped with the subgrade in another layer. Analysis done with the base course separate from the subgrade confirmed that the two often had similar stiffnesses. Also, attempts at distinguishing between the different layers of old pavement were unsuccessful.

### **6.2.4 Outputs**

The program is set up to analyze the data that come from WSDOT's FWD. Therefore, it analyzed each of the four drops separately, then compared the results. For

each drop it attempted to calculate a basin within 1 percent of the root mean square error (RMS) of the measured basin. RMS is defined as the square root of the sum of squared relative differences (Equation 6.1).

$$\text{RMS} = \sqrt{\frac{1}{n_d} \left[ \sum \left( \frac{D_c - D_m}{D_m} \right)^2 \right]} \quad (\text{Equation 6.1})$$

where:

- RMS = root mean squared error,
- $n_d$  = number of deflection sensors,
- $D_c$  = calculated deflection, and
- $D_m$  = measured deflection.

Once the program had analyzed all four drops, it compared the four drops and calculated the  $K_1$  and  $K_2$  for each layer on the basis of Equation 3.1. The program then determined the moduli for each layer under a 9.0 kip (40 KN) load and estimated the stresses in the middle of each layer. It also calculated the modulus of elasticity for the surface layer for a temperature of 77° F (25° C). These results, along with the errors in each back calculation were then saved and the next section was analyzed.

### **6.3 ANALYSIS**

Because of the complexities of the pavement system and the inaccuracies of the layer thickness data, most of the backcalculation analyses of the test sections contained unacceptably large convergence errors. Out of the eight test sections analyzed, only two had a significant number of tests with reasonable results. Reasonable results were defined as results that had RMS errors less than 1.5 percent and moduli within an acceptable range of the expected moduli for the material. The acceptable range of moduli for the crushed rock layer was 20 to 130 ksi (138 to 896 MPa). The lower limit of 20 ksi (138 MPa) was the typical stiffness of an unconfined crushed rock layer. Test sections that had fewer than 10 percent of the results within the acceptable range were considered unacceptable.

### **6.3.1 Sections with Poor Results**

SR24 was analyzed using three basic modes: all layers having unfixed moduli, the old pavement (prior surfacings) fixed at 100 ksi (689 MPa) and with the BST surface fixed at values ranging from 140 to 700 ksi (964.6 to 4823 MPa). Unfortunately, less than 10 percent of the test sections had RMS errors of less than 1.5 percent.

SR28B was analyzed with all layers unfixed, the BST surface fixed at values ranging from 30 to 300 ksi (206.7 to 2067 MPa), the old AC layer fixed at 200 and 400 ksi (1378 to 2756 MPa). Each time less than 10 percent of the sections had RMS errors lower than 2.5 percent and very few of these had reasonable results. When the BST surface was fixed at 200 ksi (1378 MPa), the average moduli for the crushed rock layer in all sections with RMS errors of less than 1.5 percent was over 400 ksi (2756 MPa).

SR21A was analyzed with all layers unfixed and the old pavement layers fixed at 50, 100 and 300 ksi (344.5, 689, and 2067 MPa). In the analysis, the moduli of the surface averaged 5.0 ksi (34.45 MPa) and the crushed rock 10 ksi (68.9 MPa). When the section was analyzed using the measured thickness for the surface as opposed to the thickness listed in WSPMS, less than 5 percent of the sections had RMS errors of less than 1.5 percent and these had surface moduli of around 20.0 ksi (138 MPa) and crushed rock moduli of about 5 ksi (34 MPa).

SR21B was analyzed with no layers fixed. The test results alternated between having unrealistically high values for the pavement layers and low values for the crushed rock layer and high values for the crushed rock layer and low values for the pavement layers. In the next analysis, the old pavement was fixed at 300 ksi (2067 MPa) and the moduli for the crushed rock layer averaged 3.0 ksi (21 MPa).

SR231A was analyzed in two parts. The first was the section without the granular overlay. Analysis of this section resulted in moduli for the pavement, base and subgrade of 280, 6.0 and 16 ksi (1930, 41, and 110), respectively. The moduli for the subgrade was close to the values calculated in Chapter 4 of 18 ksi (124 MPa) and 13 ksi (90 MPa) for the

north and south lanes. The section with the overlay was not as easy to analyze. Analyses were conducted with all layers unfixed and the old pavement fixed at 50 and 100 ksi (344 and 689 MPa), but few results were reasonable. Less than 10 percent of the sections had errors of less than 2.5 percent and the average modulus for the crushed rock layer was 3 ksi (21 MPa).

SR231B was analyzed with no fixed layers and with the old pavement layer fixed at 100 ksi (689 MPa). Both times less than 10 percent of the sections had RMS errors of less than 2.5 percent. Of the results, the average surface moduli was 1,000 ksi (6890 MPa) and the crushed rock layer was 20 ksi (138 MPa).

### **6.3.2 Backcalculation Results for SR28B**

The best results came from the analysis of SR28A. This section had an AC surface course and included a mile section of road without a granular layer (Section 5.3.2). The test section is located in an open, level area with no visible rock. The road was well elevated and there was no signs of water.

Initially, the section of road without the overlay was analyzed. For the purpose of this analysis the pavement was divided into three layers: the surface, base course and subgrade. The results of this analysis are shown in Table 6.1.

Table 6.1. EVERCALC Results for SR28A without the Granular Overlay  
(Included are only the results with RMS errors of less than 1.5 percent — total of 17 deflection locations.)

Direction of Travel	AC	Base Course				Subgrade			
	E adj. (ksi)	E (ksi)	$\theta$ (psi)	K <sub>1</sub>	K <sub>2</sub>	E (ksi)	$\theta$ (psi)	K <sub>1</sub>	K <sub>2</sub>
North									
Mean	312	39.1	14.6	1.9E4	0.35	22.7	6.10	2.6E4	0.08
S D	92.3	15.4	1.7	1.8E4	0.14	3.5	0.58	4.5E3	0.03
South									
Mean	323	22.2	14.0	5.9E3	0.52	21.5	5.58	2.4E4	0.07
S D	45	5.3	0.52	1.6E3	0.10	1.8	0.21	2.3E3	0.02

The results of this analysis for the surface and subgrade were consistent, in that the standard deviations were low and the correspondence between the lanes was good. Additionally, the mean value for the subgrade from this analysis was close to the value of 25 ksi (172 MPa) and 22 ksi (152 MPa), as calculated in Section 5.5.1. The only result that did vary widely was K1 for the granular layer. This was the case in every analysis. On the basis of this analysis, it was assumed that the base course and the subgrade had very close moduli and could be considered one layer. Also, since the pavement layer in this model is the same as the old pavement layer for the pavement with the granular overlay, the old pavement should have had a modulus of elasticity no lower than 300 ksi (2067 MPa).

An attempt was then made to analyze the granular overlay section. This was modeled as a four-layer section with the granular overlay as two layers, the old pavement layers as a third and the base and subgrade combined into a fourth. The first analysis was conducted without any fixed layers. This yielded widely varying results. Next the old pavement layer was fixed. The modulus of this layer was fixed at 500 ksi (3445 MPa). A value slightly higher than 300 ksi (2067 MPa) was chosen to reflect the protection that would be offered by the granular overlay. The results of this analysis are shown in Table 6.2.

Table 6.2. EVERCALC Results for SR28A with the Granular Overlay  
(Included are only the results with RMS errors of less than 1.5 percent and reasonable values for the moduli, as defined earlier.)

Direction of Travel	AC	Crushed Rock Layer				Old AC	Count
	E adj.	E (ksi)	$\theta$ (psi)	K <sub>1</sub>	K <sub>2</sub>	E (ksi)	(total)
North							
Mean	959	75.9	104	4.8E3	0.74	500	14
S D	457	40.0	13.4	9.4E3	0.15		(49)
South							
Mean	817	74.2	94.0	3.7E3	0.76	500	12
S D	435	53.0	16.0	4.8E3	0.12		(48)

Although these results represented only 25 percent of the sections, the results that had RMS errors of less than 2.5 percent and represented 75 percent of the data were quite similar. Additional analyses varied the modulus of elasticity of the old pavement from 300 ksi (2067 MPa) to 800 ksi (5512 MPa), but this only changed the moduli for the granular overlay layers by approximately 20 percent.

### **6.3.3 Backcalculation Results for SR17**

A second road that produced good results was SR17. This was the same road with multiple layer thicknesses that was analyzed in Section 5.10. The results of this analysis are shown in Table 6.3. The values for the modulus of elasticity of the granular layer corresponded closely with those of SR28A (Table 6.2). One difference in the data is that the bulk stress for SR17 is approximately half of that of SR28A. SR17 has a BST surface while SR28A has an AC surface. Since the BST surface on SR17 is thinner and less stiff than the AC surface on SR28A, it is reasonable that the BST surface would exert less confining pressure than the AC and this is why the confining pressure is different.

To analyze the effect of the thickness on the calculated moduli, the tests with good results were overlaid on a plot of the layer thicknesses (Figure 6.1). Although the layer thickness changes are shown as abrupt jumps, in fact, they taper. If the modulus of elasticity of the granular layer declined as the thickness of the granular layer increased, then

Table 6.3. EVERCALC Results for SR17 with the Granular Overlay  
(Included are only the results with RMS errors less than 1.5 percent and reasonable values for the moduli.)

Direction of Travel	BST	Crushed Rock Layer				Old BST	Count
	E fixed (ksi)	E (ksi)	$\theta$ (psi)	$K_1$	$K_2$	E (ksi)	(total)
East							
Mean	500	85.1	51.0	2.4 E4	0.12	113	19
SD		19.0	34.2	3.4 E4	0.86	177	(81)
West							
Mean	500	82.3	49.0	5.4 E4	0.22	101.8	13
SD		27.4	33.9	8.2 E4	0.38	124	83

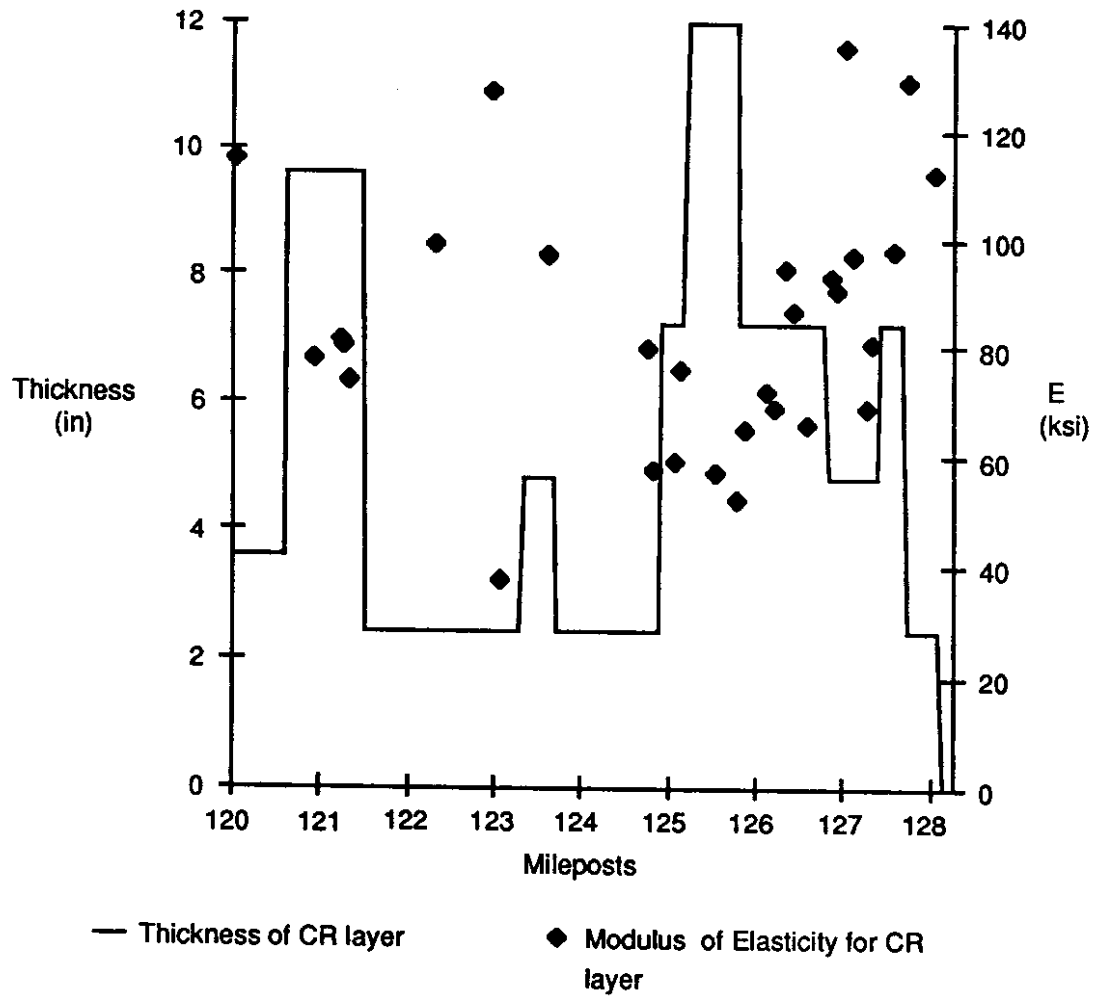


Figure 6.1. Plot of the Thickness of the Crushed Rock Layer in the Granular Overlay on SR17 against Backcalculated Moduli for this Layer

thicker layers would be less stiff than thinner layers. This trend is evident in the groupings of the data points.

The EVERCALC program assumes that the modulus of elasticity is constant for each pavement layer. To check this assumption, the cross-section of SR17 (recall Figure 5.4) and the layer properties shown in Table 6.3 were entered in ELSYM5 and the stresses at a variety of points were calculated. The results of this analysis are shown in Figure 6.2. The crushed rock layer extended from a depth of 1.2 in. to 3.6 in.

Since the modulus of elasticity of the crushed rock layer is largely dependent upon the bulk stress, a drop in the bulk stress will cause a drop in the modulus of elasticity. Figure 6.2 shows that the bulk stress varies considerably with the radial distance, hence the modulus varies as well.

The issue of shear stress was then examined. The shear stresses from the same ELSYM analysis were calculated. Figure 6.3 shows the results of the calculations. The peak shear is at 6 in., slightly beyond the edge of the loading plate. At this point the bulk stress is at half of its original value. This indicates that a problem of shear could occur at the edge of a load.

#### **6.4 CHAPTER SUMMARY**

Based on the analyses of SR28A and SR17, the modulus of elasticity for the crushed rock layer of the granular overlay was approximately 80 ksi (551.2 MPa) under a 9.0 kip load. The South African studies showed elastic moduli ranging from 29.0 to 75.4 (and higher) as shown in Table 6.4 (discussed in Section 3.2.3). One of the reasons for the higher modulus of elasticity is that the bulk stress in the crushed rock layer in the granular overlay was higher than in the inverted pavement.



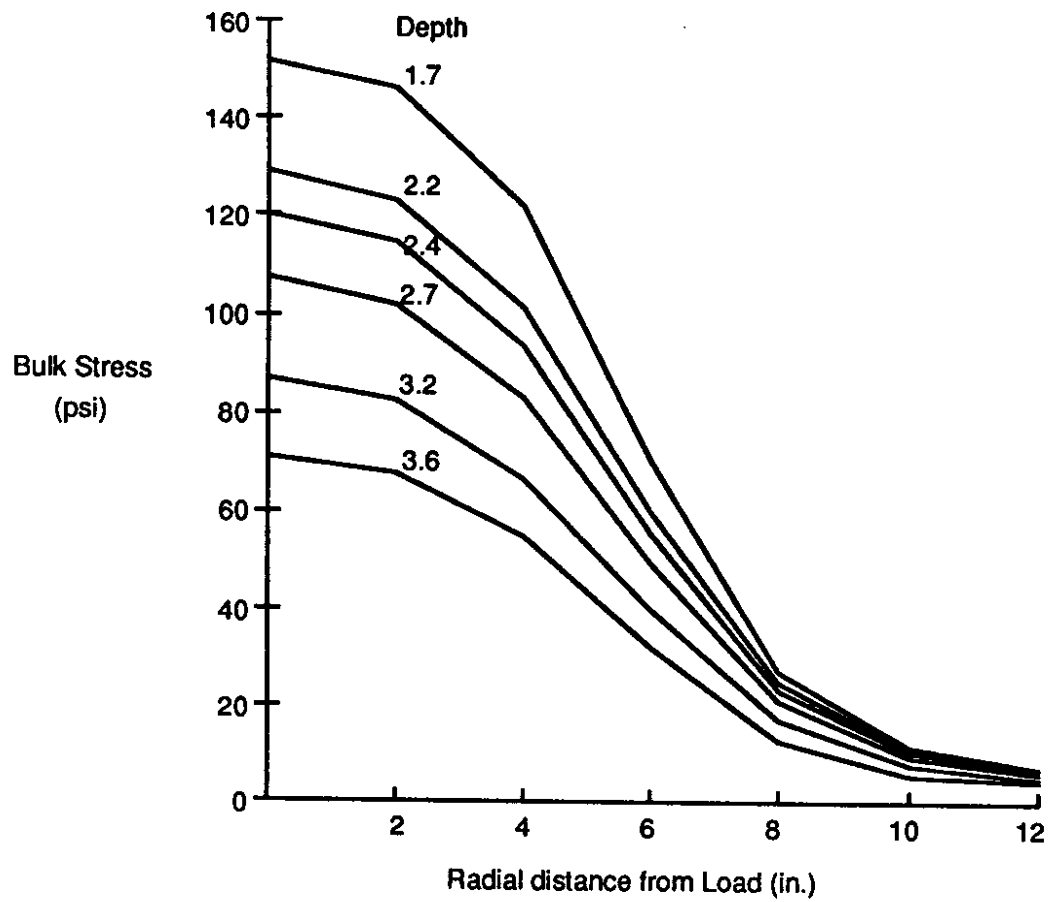


Figure 6.2. Bulk Stress for the Crushed Rock Layer in SR17  
Assuming that the Modulus of Elasticity is Constant

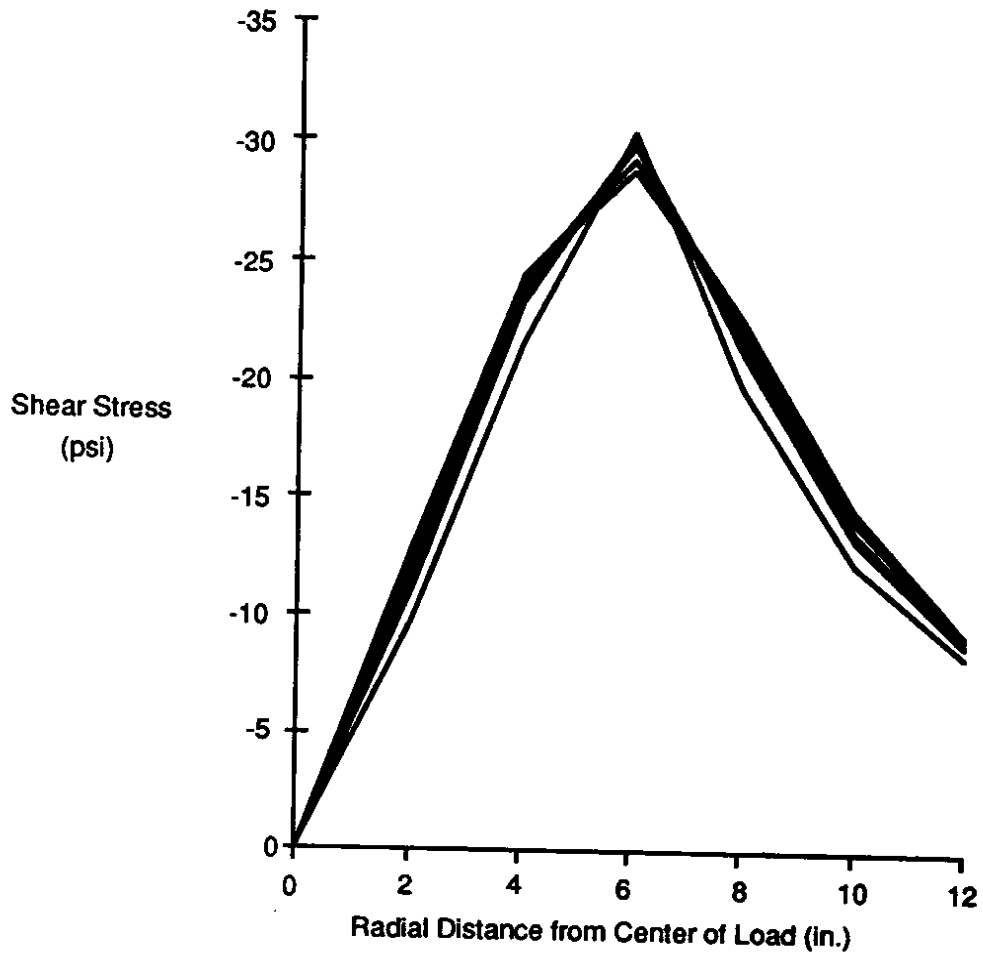


Figure 6.3. Shear Stress for the Crushed Rock Layer in SR17 Assuming that the Modulus of Elasticity is Constant

**Table 6.4. Typical Elastic Moduli and Bulk Stresses from Inverted Pavements (Maree et al. [16])**

Road	Thickness (in.)	Load (ksi)	Elastic Modulus (ksi)	$\theta$ (psi)
P157/1	7.0	9.0	29.0	48.9
		15.7	43.5	58.4
P157/2	5.5	9.0	48.9	53.7
		15.7	75.4	89.6



## **CHAPTER 7**

### **SUMMARY AND CONCLUSIONS**

#### **7.1 INTRODUCTION**

Although granular overlays have been used in a variety of countries around the world, their behavior has not been well documented. This study examined granular overlays from several perspectives and drew initial conclusions as to how to design and build the overlays.

#### **7.2 BACKGROUND INFORMATION**

In Chapter 3 some of the various advantages and limitations of granular overlays were discussed. Granular overlays were found to be useful in reducing reflection cracking, insulating the old pavement surface against extremes in temperature, and improving the road geometry. It was also mentioned that the added thickness of the granular overlay can preclude its use in areas where the road geometry is limited.

In designing granular overlays the importance of protecting the crushed rock layer was stressed. Several South African studies were cited that showed a reduction in stress-stiffening in inverted pavements when the crushed rock layer became saturated. In light of this, the authors of this report suggest that the old pavement surface be sealed and that the new surface layer be made as impermeable as possible to maximize the performance of the granular overlay.

The affect of the rock quality and the compaction of the crushed rock layer was reviewed. In all of the South African studies, the inverted pavements with crushed rock that was more densely compacted and contained particles with a higher percentage of fractured faces was more resistant to deformation and to the reduction of the stress-stiffening caused by moisture infiltration. In one study (Horak et al. [6]), it was found that by tightening the specifications for the crushed rock, it was possible to obtain densities in

the crushed rock layer in excess of 100 percent of modified AASHTO. Therefore, by using a crushed rock with a dense gradation and a high percentage of fractured faces and by compacting it the maximum possible amount, the granular overlay will have a higher durability. The actual costs and benefits of tightening these specifications were not determined.

BST and AC overlays were examined as to their suitability as surfacings for granular overlays and BSTs were chosen as the more advantageous. BSTs have the advantages of being more flexible and thus better able to withstand the flexural stress applied to granular layer surfaces. BSTs are less expensive and easier to construct; however, they do not last as long as AC surfaces.

The thickness of the crushed rock layer was examined and was found to have a maximum recommended value of about 6 in. (150 mm). This recommendation came primarily from a South African study (Maree et al. [17]) which found that thicknesses beyond 6 in. (150 mm) did not significantly increase the pavements resistance to deformation. Additionally, in a paper on the use of granular overlays in Zimbabwe (Mitchell, [19]), the problems with compacting crushed rock layers thicker than 6.0 in. were cited as the reason that thicker layers are not used there. Mitchell [19] also mentioned that thinner layers were difficult to compact, but this has not been the experience with WSDOT where crushed rock layers as thin as 3.0 in. (75 mm) are regularly built (WSPMS, 1990).

The study conducted by Sibal [26] was discussed in some detail. His work studied the comparison of the number of 18 kip (80 kN) ESALs that both AC and granular overlain pavements can withstand. He examined both rutting and fatigue failure and calculated the thickness of crushed rock in a granular overlay that would provide the same life as an AC overlay. These equivalency factors ranged from 1.6 to 5.8 with most being around 2.0. Mitchell [19] also mentioned that the author had found that the AC equivalency factor was 2.0 for the confined crushed rock layer.

Cost data from Means [18] and WSDOT were examined to determine the cost effectiveness of granular overlays. Although the available data was limited, it was found that granular overlays designed with an equivalency factor of 2.0 are about 10 percent less expensive than AC overlays.

### **7.3 SURVIVAL LIFE CALCULATIONS**

The survival lives of BST, AC, and granular overlays were then examined. Although the study revealed that most WSDOT pavements were badly distressed at the time that they were overlain with granular overlays, their useable life was still at least as long as those which did not receive the granular overlay. The difference was largest when a BST surface was placed over the crushed rock layer, the predicted performance period of the pavement was increased by 20 percent. In the case of AC surfaced pavements, the increase caused by the crushed rock layer was not significant. The additional useable life offered by the granular overlay was small in part due to the type of roads that were overlain by the different techniques. Granular overlays were generally only used on roads that had significant cracking. In Section 5.3.2 it was pointed out that on SR17 between Mileposts 120 and 128, a BST was applied which lasted less than 3 years. After the BST failed, a granular overlay was applied and this overlay had already lasted 6 years (at the time this report was prepared) with only slight deterioration. Therefore, if granular overlays were applied to roads in conditions comparable to roads which received the BST and AC resurfacings, the useable life of granular overlays would probably be longer. To reinforce this, a review of the performance of not only SR17 but also SR21A, SR21B and SR231A and SR231B suggest that the granular overlays out perform plain BSTs by factors ranging from a low of two to a high of ten times better (as measured in years to comparable PCR levels). Further, the initial performance of granular overlays is even better yet when compared to plain BSTs (15 to 30 times better) which is only suggesting that the quick

failures of BSTs placed on pavements in poor condition is precluded by use of the granular overlays.

#### **7.4 NONDESTRUCTIVE TESTING**

Eight pavements with granular overlays were tested with a FWD and the results from these tests were examined in Chapters 5 and 6. Chapter 5 concentrated on using different techniques to directly analyze the output from the testing while Chapter 6 discussed the attempts made to back calculate the layer moduli from the deflection data.

The results of the direct analysis of the data showed that the pavements with the granular overlays were generally stiffer than those without the overlay. An exception to this was SR231A where the section with the granular overlay was approximately equal to the section without it. A reason given was that the PCR of the section without the granular overlay was much higher at the time of overlay than the section with the granular overlay. Therefore, the pavement under the granular overlay was probably weaker than that under the section without the overlay.

A comparison was also made between the calculated Asphalt Institute equivalent AC thickness and the thickness of a typical pavement which would have the same  $D_0$  and Area Parameter. In most cases, the crushed rock layer was found to be equal to an AC layer that was about 50 percent thicker.

#### **7.5 ELASTIC LAYER ANALYSIS**

When the results of the tests were used in a back calculation program, most of the test sections could not be analyzed. Reasons stated for these problems included inaccurate layer thicknesses, non-level or non-uniform pavement layers or subgrade, and the complexity of the pavement structure. The two sections that were successfully back calculated were in good condition and had crushed rock layer moduli around 80 ksi (550 MPa) under a 9.0 ksi (40 kN) load. In order to more successfully calculate the moduli for these roads, the true layer thicknesses would need to be determined.



## **7.6 SUMMARY**

In general, granular overlays are an effective method of rehabilitation for pavements where the thickness of the pavement structure needs to be increased or if there are problems with reflection cracking.

Granular overlays can also be a less expensive alternative to AC overlays in situations where the traffic loadings are appropriate. This is especially true for rural areas where haul distances are long since AC is more difficult to transport than crushed rock.

The design of a granular overlay should concentrate on making the crushed rock layer as dense as possible and protecting it from moisture infiltration. A properly designed and constructed confined crushed rock layer will provide the same stiffness as an AC layer that is twice as thick (Equivalency Factor = 2.0).

A limitation on the use of granular overlays that was not studied was the maximum traffic or ESAL count. Although the South African studies commonly cited 18 kip (80 kN) ESAL counts of over 20 million for inverted pavements, WSDOT experience has shown that this is much higher than can be expected for granular overlays as currently designed and constructed. Although an attempt was made to study the ESAL count on the test roads that were evaluated during this study, the ESAL count made was not considered to be accurate. The recommended maximum ADT for BSTs of 2000 to 5000 with 15% trucks is the best estimate of the maximum traffic.

## **7.7 CONCLUSIONS**

The following conclusions are listed based on the entire study of granular overlays:

1. Granular overlays are effective at reducing reflection cracking, insulating the old pavement surface against extremes in temperature, and improving the road geometry.
2. In order to protect the granular layer, the old pavement surface should be sealed and the new surface layer be made as impermeable as possible.

3. **BSTs are more appropriate surfacings for granular overlays than are AC overlays given the costs and expected range of traffic.**
4. **By using a crushed rock with a dense gradation and a high percentage of fractured faces and by compacting it the maximum possible amount, the granular overlay will have a higher durability.**
5. **The crushed rock layer should have a maximum recommended thickness of 6 in. (150 mm) (based on structural considerations only) and a minimum value of 3.0 in. (75 mm).**
6. **The AC equivalency factor for the confined crushed rock layer that is properly constructed and well protected is 2.0.**
7. **When designed with an equivalency factor of 2.0, granular overlays are slightly less expensive than AC overlays.**
8. **The "typical" survival lives for different overlays are shown in Table 7.1.**
9. **The "typical" moduli for confined crushed rock layers are shown in Table 7.2.**
10. **The recommended maximum ADT for BSTs of 2000 to 5000 with 15 percent trucks is the best estimate of the maximum traffic count that granular overlain roads can withstand as currently designed and constructed.**
11. **Consideration should be given by WSDOT to using Crushed Surfacing Base Course (maximum aggregate size = 1-1/4 in.) for the crushed rock portion of the granular overlay on some projects and evaluating its performance. The gradation is similar (but not the same) to the South African G1 material specification.**
12. **WSDOT should consider building an "inverted" pavement section on an appropriate rehabilitation project in the "dryer" part of the state Districts 2,5 or 6). The existing section could be scarified, treated with cement (CTB), crushed rock placed over the CTB plus surfacing. In this manner, the**

section could be evaluated for performance. Granted, this is not a "classic" granular overlay but it is an extension of the concept and, in theory, accommodates modest to high ESAL levels.

Table 7.1. Survival Times and Predicted Performance Periods for the Overlays

Type of Resurfacing	Actual Survival Life	Predicted Performance Period		
		PCR 40	PCR 20	PCR 0
BST Only	9.2	7.0	8.2	9.3
G O w/BST surface	—	7.5	8.3	11.0
AC Only	9.7	10.2	11.3	12.1
G O w/AC surface	—	9.5	11.3	11.8

Table 7.2. Moduli Calculated for Confined Crushed Rock Layers in Granular Overlays (WSDOT) and Inverted Pavements (South Africa)

Road	Crushed Rock Thickness (in.)	Load (kips)	Modulus of Elasticity (ksi)	Bulk Stress (psi)
WSDOT				
SR28A	3.0	9.0	75	99
SR17	2.4-12	9.0	84	50
South African				
P157/1	7.0	9.0	29	48.9
		15.7	43.5	58.4
P157/2	5.5	9.0	48.9	53.7
		15.7	75.4	89.6



## ACKNOWLEDGMENTS

The authors wish to express their appreciation to Mr. John Livingston and Ms. Linda Pierce for their technical support, Mr. Duane Wright, and Ms. Mary Marrah for their help with the graphics, Ms. Amy O'Brien for her editing. Further, the review comments provided by Mr. Keith Anderson assisted the authors in improving the report. We thank you all.



## REFERENCES

1. AASHTO. The AASHTO Guide for the Design of Pavement Structures. AASHTO; Washington, D. C., 1986.
2. AASHTO. Standard Specifications for Transportation Materials and Methods of Sampling and Testing. AASHTO, Washington, D. C., 1986.
3. Deoja, B. B. A Comparison of Cushion Course and Asphalt Concrete Overlays on Flexible Pavements. Thesis for the University of Washington, Seattle, 1986.
4. Freeme, C. R., Maree, J. H. and Viljoen, A. W. "Mechanistic Design of Asphalt Pavements and Verification Using the Heavy Vehicle Simulator," The Fifth International Conference on the Structural Design of Asphalt Pavements. Proceedings. The University of Michigan, 1982.
5. Hoffman, M. ed. The World Almanac and Book of Facts, 1989. Scripps Howard, Co. New York, 1988.
6. Horak, E; du Pisani, J. C.; and van der Merwe, C. J. "Rehabilitation Alternatives for Typical 'Orange Free State' Rural Roads," Proceedings of the Annual Transportation Convention. National Institute for Transport and Road Research, Perth, 1986.
7. Horak, E; de Villiers, E. M. and Wright, D "Improved Performance of a Deep Granular Base Pavement with Improved Material and Control Specifications," 1987.
8. Irick, P. ed. Roadway Design in Seasonal Frost Areas. National Cooperative Highway Research Program Syntheses of Highway Practice, Report No. 26. Transportation Research Board, Washington, D. C., 1974.
9. Kingham, I. R. and Jester, N. R. Deflection Method for Designing Asphalt Concrete Overlays for Asphalt Pavements. Research Report No 83-1. The Asphalt Institute, Collage Park MD, 1983.
10. Jackson, D. C.; Jackson, N. C. and Mahoney, J. P. "Washington State Chip Seal Study," Transportation Research Record No. 1259, TRB; Washington, D. C., 1990.
11. Jackson, S. ed. Atlas Climatologique de L'Afrique. South African Government Publications, Pretoria, 1961.
12. Mahoney, J. P. "Comparison of Laboratory Resilient Moduli of Recompacted Samples—Revised," Letter to WSDOT, Seattle, 1990.
13. Mahoney, J. P.; Hicks, R. G. and Jackson, N. C. Flexible Pavement Design and Rehabilitation. Course Notes, Federal Highway Administration, 1988.

14. Mahoney, J. P. and Jackson, N. C. An Advanced Course in Pavement Management Systems. Federal Highway Administration, 1990.
15. Mahoney, J. P. "State-of-the-Art Asphalt Concrete Overlay Design Procedures," EHWA Proceedings; Salt Lake City, 1984.
16. Maree, J. H.; van Zyl, N. J. W. and Freeme, C. R., "Effective Moduli and Stress Dependence of Pavement Materials as Measured in Some Heavy-Vehicle Simulator Tests," Transportation Research Record No. 852. Washington, D. C., 1982.
17. Maree, J. H.; Freeme, C. R.; van Zyl, N. J. W. and Savage, P. F. "The Permanent Deformation of Pavements with Untreated Crushed-Stone Bases as Measured in Heavy Vehicle Simulator Tests," Proceedings of the 11th Australian Road Research Board Conference. Melbourne, 1982.
18. Means. Mean's Heavy and Highway Construction Data, 1990. 4th Annual edition, R. S. Means Co. Inc., Kingston, Ma, 1989.
19. Mitchell, R. L. "The Economics of Overlay Design and Road Rehabilitation," Highway Investment in Developing Countries. The Institute of Civil Engineers, London, 1983.
20. Monismith, C. L. and Finn, F. N. "Overlay Design—A Synthesis of Methods," Asphalt Concrete Overlays: Theory and Practice. National Cooperative Highway Research Program Syntheses of Highway Practice, Report No. 26. Transportation Research Board, Washington, D. C., 1984.
21. Murray, B., Project Manager-WSDOT, "Telephone Interview," Wenatchee, Washington, 1990.
22. Newcomb, D. Development and Evaluation of a Regression Method to Interpret Dynamic Pavement Deflections. Ph. D. Dissertation, University of Washington, Seattle, 1986.
23. Otte, E and Monismith, C. L. "Some Aspects of Upside-Down Pavement Design," The Eighth Australian Road Research Board Conference, Volume 8. Perth, 1976
24. Reister, S., Project Manager-WSDOT, "Telephone Interview," Wenatchee, Washington, 1990.
25. Rutherford, M. S; Mahoney, J. P.; Hicks, R. G. and Rwebangira, T. Guidelines for Spring Highway Use Restriction. Washington State Department of Transportation, Olympia, WA 1985.
26. Sibal, V. Cushion Course Overlays—An Alternative to Asphalt Concrete Overlays. Research Paper, University of Washington, Seattle, 1988.
27. Sherman, G. Minimizing Reflection Cracking of Pavement Overlays. National Cooperative Highway Research Program, Synthesis of



- Practice Report No. 92, Transportation Research Board, Washington, D. C. 1982.
28. Sowers, G. Introductory Soil Mechanics and Foundations: Geotechnical Engineering. MacMillan Publishing Co., Inc., New York, 1979.
  29. Stokes, B., Project Manager-WSDOT, "Telephone Interview," Wenatchee, Washington, 1990.
  30. Viljoen, A. W.; Freeme, C. R.; Servas, V. P. and Rust, F. C. "Heavy Vehicle Simulator Aided Evaluation of Overlays on Pavements with Active Cracks," The Sixth International Conference on the Structural Design of Asphalt Pavements. Proceedings. The University of Michigan, 1987.
  31. Washington State Department of Transportation. 1991 Standard Specifications for Road, Bridge and Municipal Construction. Washington State Department of Transportation; Olympia, Washington, 1991.
  32. Washington State Department of Transportation. Washington State Pavement Management System. 1990.
  33. van Zyl, N. J. and Maree, J. H. "The Behavior of High-Standard Crushed-Stone Base Pavement during a Heavy Vehicle Simulator Test," The Civil Engineer in South Africa. Pretoria, 1983.
  34. Bowles, J. E., Foundation Analysis and Design, McGraw - Hill, New York, 1968.
  35. Terzaghi, K. and Peck, R. B., Soil Mechanics in Engineering Practice, John Wiley and Sons, New York, 1967.
  36. The Asphalt Institute, Asphalt Overlays for Highway and Street Rehabilitation, Manual Series No. 17, The Asphalt Institute, June 1983 Edition.